คุณลักษณะและสมบัติในการเร่งปฏิกิริยาของตัวเร่งปฏิกิริยาโคบอลต์บนเซอร์โคเนียที่เตรียมโดยวิธีไกลโคเทอร์มอลในปฏิกิริยาไฮโดรจิเนชันของคาร์บอนมอนอกไซด์

นางสาวณัฐกานต์ เต้าชัยภูมิ

วิทยานิพนธ์นี้เป็นส่วนหนึ่งของการศึกษาตามหลักสูตรปริญญาวิศวกรรมศาสตรมหาบัณฑิต
สาขาวิชาวิศวกรรมเคมี ภาควิชาวิศวกรรมเคมี
คณะวิศวกรรมศาสตร์ จุฬาลงกรณ์มหาวิทยาลัย
ปีการศึกษา 2547

ISBN: 974-53-1760-8

CHARACTERISTICS AND CATALYTIC PROPERTIES OF GLYCOTHERMAL-DERIVED ZIRCONIA SUPPORTED COBALT CATALYSTS IN CARBONMONOXIDE HYDROGENATION

Miss Nuttakarn Taochaiyaphum

A Thesis Submitted in Partial Fulfillment of the Requirements
for the Degree of Master of Engineering in Chemical Engineering
Department of Chemical Engineering
Faculty of Engineering
Chulalongkorn University
Academic Year 2004

ISBN: 974-53-1760-8

Thesis Title	CHARACTERISTICS AND CATALYTIC PROPERTIES OF GLYCOTHERMAL-DERIVED ZIRCONIA SUPPORTED COBALT CATALYSTS IN CARBONMONOXIDE HYDROGENATION
By	Miss Nuttakarn Taochaiyaphum
Field of Study	Chemical Engineering
Thesis Advisor	Joongjai Panpranot, Ph.D.
Thesis Co-advisor	Professor Piyasan Praserthdam, Dr.Ing.

Accepted by the Faculty of Engineering, Chulalongkorn University in Partial Fulfillment of the Requirements for the Master's Degree

…..……..…… Dean of the Faculty of Engineering
(Professor Direk Lavansiri, Ph.D.)

THESIS COMMITTEE

…… Chairman
(Associate Professor Suttichai Assabumrungrat, Ph.D.)

……. Thesis Advisor
(Joongjai Panpranot, Ph.D.)

……. Thesis Co-advisor
(Professor Piyasan Praserthdam, Dr.Ing.)

……. Member
(Assistant Professor Seerong Prichanont, Ph.D.)

……. Member
(Akawat Sirisuk, Ph.D.)

ณัฐกานต์ เต้าชัยภูมิ: คุณลักษณะและสมบัติในการเร่งปฏิกิริยาของตัวเร่งปฏิกิริยาโคบอลต์บนเซอร์โคเนียที่เตรียมโดยวิธีไกลโคเทอร์มอลในปฏิกิริยาไฮโดรจิเนชันของคาร์บอนมอนอกไซด์ (CHARACTERISTICS AND CATALYTIC PROPERTIES OF GLYCOTHERMAL-DERIVED ZIRCONIA SUPPORTED COBALT CATALYSTS IN CARBONMONOXIDE HYDROGENATION) อ. ที่ปรึกษา: ดร. จูงใจ ปั้นประณต, อ. ที่ปรึกษาร่วม: ศ. ดร. ปิยะสาร ประเสริฐธรรม, 125 หน้า. ISBN : 974-53-1760-8.

วิทยานิพนธ์นี้ศึกษาคุณลักษณะและสมบัติในการเร่งปฏิกิริยาของตัวเร่งปฏิกิริยาโคบอลต์บนเซอร์โคเนียที่เตรียมโดยวิธีไกลโคเทอร์มอลในปฏิกิริยาไฮโดรจิเนชันของคาร์บอนมอนอกไซด์ โดยใช้สารละลายไกลคอลที่แตกต่างกัน 2 ชนิด คือ 1,4-บิวเทนไดออล และ 1,5-เพนเทนไดออล และใช้สารละลายเซอร์โคเนียม เอ็น-โพรพอกไซด์ที่มีความเข้มข้นของเซอร์โคเนีย 20.5 และ 29.5% พบว่าเซอร์โคเนียที่เตรียมโดยวิธีไกลโคเทอร์มอล จะมีพื้นที่ผิวสูงและมีผลึกขนาด 3-4 นาโนเมตร ตัวเร่งปฏิกิริยาที่มีปริมาณการดูดซับไฮโดรเจนและมีความว่องไวเริ่มต้นในปฏิกิริยาไฮโดรจิเนชันของคาร์บอนมอนอกไซด์สูงที่สุด คือ ตัวเร่งปฏิกิริยาโคบอลต์ บนตัวรองรับเซอร์โคเนียที่เตรียมจากสารละลาย 1,4-บิวเทนไดออล และสารละลายเซอร์โคเนียม เอ็น-โพรพอกไซด์ ที่มีความเข้มข้นของเซอร์โคเนีย 20.5% ทั้งนี้เนื่องมาจากกลไกการตกผลึกของเซอร์โคเนียในสารละลาย 2 ชนิด ต่างกัน ผลึกเซอร์โคเนียที่เตรียมจากสารละลาย 1,4-บิวเทนไดออล มีแรงกระทำระหว่างโลหะโคบอลต์และตัวรองรับต่ำ เมื่อเทียบกับผลึกเซอร์โคเนียที่เตรียมใน 1,5-เพนเทนไดออล ดังแสดงโดยอุณหภูมิรีดิวซ์ที่ต่ำกว่าในการทำรีดักชันแบบโปรแกรมอุณหภูมิ อย่างไรก็ตามอัตราการเกิดปฏิกิริยาของตัวเร่งปฏิกิริยาดังกล่าวลดลงอย่างรวดเร็ว ทำให้อัตราการเกิดปฏิกิริยาที่สภาวะคงที่ต่ำกว่าของตัวเร่งปฏิกิริยาเซอร์โคเนียที่เตรียมใน 1,5-เพนเทนไดออล เมื่อเติมซิลิกาปริมาณเล็กน้อยในขั้นตอนการเตรียมเซอร์โคเนียในสารละลาย 1,4-บิวเทนไดออล อัตราการเกิดปฏิกิริยาที่สภาวะคงที่มีค่าเพิ่มขึ้น นอกจากนี้เมื่อเปรียบเทียบผลของเซอร์โคเนียทางการค้าที่มีขนาดอนุภาคในระดับนาโนเมตรและไมโครเมตร กับเซอร์โคเนียที่เตรียมโดยวิธีไกลโคเทอร์มอลในการใช้เป็นตัวรองรับตัวเร่งปฏิกิริยาโคบอลต์ พบว่าเซอร์โคเนียทางการค้าที่มีขนาดนาโนเมตร มีความว่องไวในปฏิกิริยาไฮโดรจิเนชันของคาร์บอนมอนอกไซด์สูงกว่าเซอร์โคเนียทางการค้าที่มีขนาดไมโครเมตร อย่างไรก็ตามเซอร์โคเนียที่เตรียมโดยวิธีไกลโคเทอร์มอลมีความว่องไวในปฏิกิริยาไฮโดรจิเนชันของคาร์บอนมอนอกไซด์สูงที่สุด ดังนั้นมีความเป็นไปได้ในการพัฒนาเซอร์โคเนียที่เตรียมโดยวิธีไกลโคเทอร์มอลสำหรับใช้เป็นตัวรองรับของตัวเร่งปฏิกิริยาโคบอลต์โดยเลือกชนิดของไกลคอลและความเข้มข้นของสารละลายเซอร์โคเนียมที่เหมาะสม

ภาควิชา .....วิศวกรรมเคมี..... ลายมือชื่อนิสิต.....
สาขาวิชา .....วิศวกรรมเคมี..... ลายมือชื่ออาจารย์ที่ปรึกษา.....
ปีการศึกษา .....2547..... ลายมือชื่ออาจารย์ที่ปรึกษาร่วม .....

#4670295021 : MAJOR CHEMICAL ENGINEERING
KEY WORD : NANOCRYSTALLINE ZIRCONIA/ GLYCOTHERMAL METHOD/ ZIRCONIA SUPPORTED COBALT

NUTTAKARN TAOCHAIYAPHUM: CHARACTERISTICS AND CATALYTIC PROPERTIES OF GLYCOTHERMAL-DERIVED ZIRCONIA SUPPORTED COBALT CATALYSTS IN CARBONMONOXIDE HYDROGENATION. THESIS ADVISOR: JOONGJAI PANPRANOT, Ph.D., THESIS COADVISOR: PROFESSOR PIYASAN PRASERTHDAM, Dr.Ing., 125 pp. ISBN : 974-53-1760-8.

Nanocrystalline ZrO_2 have been prepared by the glycothermal method with two different glycols [1,4-butanediol (BG) and 1,5-pentanediol (PeG)] with various Zr concentrations of zirconium *n*-propoxide (ZNP) solution (20.5 and 29.5 %) in the starting materials. Large surface area zirconias with crystallite sizes of 3-4 nm were obtained. Use of zirconia prepared in 1,4-butanediol with lower amount of Zr content as a support for cobalt catalyst resulted in the highest H_2 chemisorption and initial CO hydrogenation activities. Due to the different crystallization mechanism of ZrO_2 in the two glycols, the metal-support interaction for the zirconia prepared in 1,4-BG was lower than the ones prepared in 1,5-PeG as shown by lower reduction temperature in the TPR profiles. However, activity of such catalyst decreased sharply resulting in lower steady-state reaction rates than those of 1,5-PeG supported onces. Addition of small amount of Si during ZrO_2 synthesis was found to enhance steady-state rates of the cobalt catalysts supported on ZrO_2 prepared in 1,4-BG. Commercial zirconia in micron and nano-size were obtained from Aldrich for comparison purposes. The cobalt catalysts supported on commercial nano-size ZrO_2 exhibited higher CO hydrogenation activity than that the ones supported on micron-size ZrO_2. However, cobalt catalysts supported on ZrO_2 prepared by the glycothermal method exhibited the highest activities. There is a possibility to develop the glycothermal derived ZrO_2 as cobalt catalyst supports for CO hydrogenation, however, the type of the glycol and Zr concentration must be carefully chosen in order to prepare high activity Co/ZrO_2 catalysts.

Department …Chemical Engineering…..	Student's signature……..……...
Field of study…Chemical Engineering…	Advisor's signature……..……..
Academic year…..2004……...	Co-advisor's signature……...…….

ACKNOWLEDGEMENTS

The author would like to express her sincere gratitude and appreciation to her advisor, Dr. Joongjai Panpranot, for her invaluable suggestions, stimulating, useful discussions throughout this research and devotion to revise this thesis otherwise it can not be completed in a short time. Without the comments from her co-advisor, Professor Piyasan Praserthdam, this work would never have been achieved. The authors also would like to thank Dr. Nobuhiro Iwasa of Graduate School of Engineering, Hokkaido University for BET measurement of the catalysts. In addition, the author would also be grateful to Associate Professor Suttichai Assabumrungrat, as the chairman, and Dr. Seeroong Prichanont and Dr.Akawat Sirisuk, as the members of the thesis committee. The financial supports from TRF, TJTTP-JBIC and Graduate School of Chulalongkorn University are also gratefully acknowledged.

Most of all, the author would like to express her highest gratitude to her parents who always pay attention to her all the times for suggestions and have provided her support and encouragement. The most success of graduation is devoted to her parents.

Finally, the author wishes to thank the members of the Center of Excellence on Catalysis and Catalytic Reaction Engineering, Department of Chemical Engineering, Faculty of Engineering, Chulalongkorn University for their assistance especially Miss Patta Soisuvan.

CONTENTS

Page

CHAPTER

Page

CHAPTER

Page

LIST OF TABLES

LIST OF FIGURES

FIGURE **Page**

CHAPTER I

INTRODUCTION

Fischer Tropsch synthesis (FTS) is a catalytic reaction with a 75-year history. It is a method for production of hydrocarbons from synthetic gases ($CO+H_2$) which could be derived from coal or natural gas. Recently, FTS has again received much attention in both catalysis and chemical engineering fields because there are (1) abundant of coal and natural gas reserves in many remote areas around the world to supply as FTS feedstocks (Jess *et al.*, 1999), (2) more stringent environmental regulations for transportation fuels, and (3) uncertain price for crude oil. Moreover, high quality FTS products has been proven to be environmentally friendly compared with those from petroleum-based fuels.

Cobalt-based catalysts are commercially attractive for FTS based on natural gas-derived synthetic gases because of their high activity and selectivity for making long chain paraffins, low water-gas shift activity, and relatively low price compared to noble metal such as Ru (Reuel and Bartholomew, 1984; Backman *et al.*, 1998; Haddad *et al.*, 1995). As is generally true in hydrogenation reactions, the active phase of cobalt for FTS is metallic cobalt. Having the cobalt well-dispersed and reduced is required for a catalyst to have high activity. The metal surface areas can be increased by dispersing the cobalt precursor on high surface area supports such as silica and alumina. Several methods can be used to deposit the metal on the surface of the support. These include precipitation, ion exchange, and impregnation. Due to its simplicity, the most frequently used method in laboratories is incipient wetness impregnation, in which a metal salt dissolved in a solvent, usually water, is added to the support in an amount equal to the pore volume of the support. Subsequently, the solvent is removed and the precursor is reduced to obtain the active metal catalyst. A calcination step may be introduced after drying the precursor material. The activity of supported Co catalysts is proportional to the number of exposed cobalt atoms. A requirement for highly active Co catalyst is therefore a high dispersion of cobalt metal.

During recent years zirconia has attracted much attention from researchers in the field of heterogeneous catalysis as a support material as well as a catalyst. Generally, the interest in zirconia as a support materials can be ascribed to at least one of the following properties: (i) as a carrier, it gives rise to a unique kind of interaction between the active phase and support, this being manifested in both the catalytic activity and the selectivity pattern of the system (Prokhorenko *et al*., 1988 and Fujii *et al*., 1987); (ii) it can be more chemically inert than the classical supports (e.g., γ-alumina or silica) (Gavalas *et al*., 1984); and (iii) it is the only single-metal oxide which may possess four chemical properties, namely acidity or basicity as well as reducing or oxidizing ability (Tanabe, 1985). Zirconia as a catalyst support has shown promising results in many environmental catalysis reactions such as CO_2 hydrogenation (Bitter *et al*., 1997), CO oxidation (Dow and Huang, 1994), and Fischer-Tropsch reaction (Chuah, 1999 and Bruce and Mathews, 1982). Zirconia can also function as a catalyst by itself. For examples, it catalyses the hydrogenation of CO (He and Ekerdt, 1984), olefin (Domen *et al*., 1992) and dienes (Nakano *et al*., 1983). However, compared to common supports like silica and alumina which posses surface areas of 100-600 m^2/g, commercially available zirconia has surface area typically less than 50 m^2/g. Moreover, silica and alumina maintain their high surface area up to temperature around 1000^oC while the surface area of zirconia decreases rapidly when the material is heated above 500^oC (Chuah *et al*., 1998). One of the reasons cited for the instability of zirconia materials is the polymorphism, which gives rise to phase transitions. It was reported that stability of tetragonal phase of zirconia is important for applications as a catalyst or catalyst support.

Recently, Inoue et al. (Inoue *et al*.,1993 and Inoue *et al*.,2000) found that thermal treatment of zirconium alkoxides in organic solvents like glycols (i.e., glycothermal method) directly yielded tetragonal zirconia having a large surface area and a fairly high thermal stability. In addition, the glycothermal reaction does not require any precaution for handling alkoxides, and reproducible results are obtained even without the purification of the starting materials. Thus, it is interesting to study the synthesis of zirconia using the glycothermal method and their application as cobalt catalyst supports for Fischer-Tropsch synthesis.

The objectives of this research are

1. to investigate the effects of glycol source and Zr concentration in ZNP solution used in ZrO_2 preparation on the physicochemical properties of ZrO_2 prepared by glycothermal method.
2. to investigate the effect of Si addition during ZrO_2 preparation on the physicochemical properties of ZrO_2 prepared by glycothermal method.
3. to investigate the characteristics and the catalytic properties of the different glycothermal-derived ZrO_2 and Si-modified ZrO_2 supported cobalt catalyst in CO-hydrogenation reaction.

CHAPTER II

THEORY

2.1 Fischer-Tropsch synthesis (FTS)

Fischer-Tropsch synthesis (FTS) or CO hydrogenation reaction, the production of liquid hydrocarbons from synthesis gases (CO and H_2) is a promising, developing route for environmentally sound production of chemicals and fuels from coal and natural gas. During the past decades, FTS has been developed continuously by many researchers, although the rise and fall in research intensity on this process has been highly related to the demands for liquid fuels and relative economics. This synthesis is basically the reductive polymerization (oligomerization) of carbon monoxide by hydrogen to form organic products containing mainly hydrocarbons and some oxygenated products in lesser amounts. The main reactions of FTS are:

$$CO + 3H_2 \rightarrow CH_4 + H_2O \quad (1)$$

$$CO + 2H_2 \rightarrow (\frac{1}{n})(C_nH_{2n}) + H_2O \quad (2)$$

$$CO + H_2O \rightarrow CO_2 + H_2 \quad (3)$$

$$2CO \rightarrow C + CO_2 \quad (4)$$

Equations (1) is the formation of methane, the equation (2) is the synthesis of hydrocarbons higher than methane, the equation (3) is the water-gas shift reaction, and the equation (4) is the Boudouard reaction resulting in which results in deposition of carbon.

The reaction mechanism of methanation can be described by the following set of mechanism:

(1) $CO + * = CO*$

(2) $CO* + * = C* + O*$

(3) $H_2 + 2* = 2H*$

(4) $C* + H* = CH* + *$

(5) $CH* + H* = CH_2* + *$

(6) $CH_2* + H* = CH_3* + *$

(7) $CH_3* + H* = CH_4(g) + 2*$

(8) $O* + H* = OH* + *$

(9) $OH* + H* = H_2O(g) + 2*$

Normally, catalysts used for FTS are group VIII metals. By nature, the hydrogenation activity increases in order of Fe < Co < Ni < Ru. Ru is the most active. Ni forms predominantly methane, while Co yields much higher ratios of paraffins to olefins and much less oxygenated products such as alcohols and aldehydes than Fe does.

Commercially, Entrained bed reactors or slurry bubble column reactors are used in FTS since they can remove heat from this exothermic synthesis, allowing better temperature control.

The current main goal in FTS is to obtain high molecular weight, straight chain hydrocarbons. However, methane and other light hydrocarbons are always present as less desirable products from the synthesis. According to the Anderson-Schulz-Flory (ASF) product distribution, typically 10 to 20% of products from the synthesis are usually light hydrocarbon (C_1-C_4). These light alkanes have low boiling points and exist in the gas phase at room temperature, which is inconvenient for transportation. Many attempts have been made to minimize these by-products and increase the yield of long chain liquid hydrocarbons by improving chain growth probability. It would be more efficient to be able to convert these less desirable products into more useful forms, rather than re-reforming them into syngas and recycling them (Farrauto and Bartholomew, 1997). Depending upon the type of catalyst used, promoters, reaction conditions (pressure, temperature and H_2/CO

ratios), and type of reactors, the distribution of the molecular weight of the hydrocarbon products can be noticeably varied.

2.2 Cobalt (Young, 1960; Othmer, 1991)

2.2.1 General

Cobalt, a transition series metallic element having atomic number 27, is similar to silver in appearance.

Cobalt and cobalt compounds have expended from use colorants in glasses and ground coat frits for pottery to drying agents in paints and lacquers, animal and human nutrients, electroplating materials, high temperature alloys, hard facing alloys, high speed tools, magnetic alloys, alloys used for prosthetics, and used in radiology. Cobalt is also as a catalyst for hydrocarbon refining from crude oil for the synthesis of heating fuel.

2.2.2 Physical Properties

The electronic structure of cobalt is [Ar] $3d^7 4s^2$. At room temperature the crystalline structure of the α (or ε) form, is close-packed hexagonal (cph) and lattice parameters are a = 0.2501 nm and c = 0.4066 nm. Above approximately 417^{o}C, a face-centered cubic (fcc) allotrope, the γ (or β) form, having a lattice parameter a = 0.3544 nm, becomes the stable crystalline form. Physical properties of cobalt are listed in Table 3.1.

The scale formed on unalloyed cobalt during exposure to air or oxygen at high temperature is double-layered. In the range of 300 to 900^{o}C, the scale consists of a thin layer of mixed cobalt oxide, Co_3O_4, on the outside and cobalt (II) oxide, CoO, layer next to metal. Cobalt (III) oxide, Co_2O_3, may be formed at temperatures below 300 ^{o}C. Above 900^{o}C, Co_3O_4 decomposes and both layers, although of different appearance, are composed of CoO only. Scales formed below 600^{o}C and above

750^{o}C appear to be stable to cracking on cooling, whereas those produced at 600-750^{o}C crack and flake off the surface.

Cobalt forms numerous compounds and complexes of industrial importance. Cobalt, atomic weight 58.933, is one of the three members of the first transition series of Group 9 (VIIIB). There are thirteen know isotopes, but only three are significant: ^{59}Co is the only stable and naturally occurring isotope; ^{60}Co has a half-life of 5.3 years and is a common source of γ-radioactivity; and ^{57}Co has a 270-d half-life and provides the γ-source for Mössbauer spectroscopy.

Cobalt exists in the +2 or +3 valance states for the major of its compounds and complexes. A multitude of complexes of the cobalt (III) ion exists, but few stable simple salt are known. Octahedral stereochemistries are the most common for cobalt (II) ion as well as for cobalt (III). Cobalt (II) forms numerous simple compounds and complexes, most of which are octahedral or tetrahedral in nature; cobalt (II) forms more tetrahedral complex than other transition-metal ions. Because of the small stability difference between octahedral and tetrahedral complexes of cobalt (II), both can be found equilibrium for a number of complexes. Typically, octahedral cobalt (II) salts and complexes are pink to brownish red; most of the tetrahedral Co (II) species are blue.

Table 2.1 Physical Properties of Cobalt (Othmer, 1991)

Property	Value
atomic number	27
atomic weight	58.93
transformation temperature, ^{o}C	417
heat of transformation, J/g[a]	251
melting point, ^{o}C	1493
latent heat of fusion, ΔH_{fus} J/g[a]	395
boiling point, , ^{o}C	3100
latent heat of vaporization at bp, ΔH_{vap} kJ/g[a]	6276
specific heat, J/(g·^{o}C)[a]	
15-100^{o}C	0.442
molten metal	0.560
coefficient of thermalexpansion, $^{o}C^{-1}$	
cph at room temperature	12.5
fcc at 417^{o}C	14.2
thermal conductivity at 25 ^{o}C, W/(m·K)	69.16
thermal neutron absorption, Bohr atom	34.8
resistivity, at 20 ^{o}C[b], $10^{-8}\Omega$·m	6.24
Curie temperature, ^{o}C	1121
saturation induction, $4\pi I_s$, T[c]	1.870
permeability, μ	
initial	68
max	245
residual induction, T[c]	0.490
coercive force, A/m	708
Young's modulus, Gpac	211
Poisson's ratio	0.32

Table 2.1 Physical Properties of Cobalt (cont.)

Property	Value		
Hardness[f], diamond pyramid, of %Co	99.9	99.98[e]	
At 20 °C	225	253	
At 300 °C	141	145	
At 600 °C	62	43	
At 900 °C	22	17	
strength of 99.99 %cobalt, MPa[g]	as cast	annealed	sintered
tensile	237	588	679
tensile yield	138	193	302
compressive	841	808	
compressive yield	291	387	

[a] To convert J to cal, divided by 4.184.

[b] conductivity = 27.6 % of International Annealed Copper Standard.

[c] To convert T to gauss, multiply by 10^4.

[d] To convert GPa to psi , multiply by 145,000.

[e] Zone refined.

[f] Vickers.

[g] To convert MPa to psi , multiply by 145.

2.2.3 Cobalt Oxides

Cobalt has three well-known oxides:

Cobalt (II) oxide, CoO, is an olive green, cubic crystalline material. Cobalt (II) oxide is the final product formed when the carbonate or the other oxides are calcined to a sufficiently high temperature, preferably in a neutral or slightly reducing atmosphere. Pure cobalt (II) oxide is a difficult substance to prepare, since it readily takes up oxygen even at room temperature to re-form a higher oxide. Above about 850^{o}C, cobalt (II) oxide form is the stable oxide. The product of commerce is usually dark gray and contains 75-78 wt % cobalt. Cobalt (II) oxide is soluble in water, ammonia solution, and organic solvents, but dissolves in strong mineral acids. It is used in glass decorating and coloring and is a precursor for the production of cobalt chemical.

Cobalt (III) oxide, Co_2O_3, is form when cobalt compounds are heated at a low temperature in the presence of an excess of air. Some authorities told that cobalt (III) oxide exists only in the hydrate form. The lower hydrate may be made as a black power by oxidizing neutral cobalt solutions with substances like sodium hypochlorite. H_2O is completely converted to Co_3O_4 at temperatures above 265^{o}C. Co_3O_4 will absorb oxygen in a sufficient quantity to correspond to the higher oxide Co_2O_3.

Cobalt oxide, Co_3O_4, is formed when cobalt compounds, such as the cabonate or the hydrated sesquioxide, are heated in air at temperatures above approximately 265^{o}C and not exceeding 800^{o}C.

2.3 Co-based Catalysts

Supported cobalt (Co) catalysts are the preferred catalysts for the synthesis of heavy hydrocarbons from natural gas based syngas (CO and H_2) because of their high Fischer-Tropsch activity, high selectivity for linear hydrocarbons and low activity for the water-gas shift reaction. It is known that reduced cobalt metal, rather than its oxides or carbides, is the most active phase for CO hydrogenation in such catalysts. Investigations have been done to determine the nature of cobalt species on various supports such as alumina, silica, titania, magnesia, carbon, and zeolites. The influence of various types of cobalt precursors used was also investigated. It was found that the used of organic precursors such as Co (III) acetyl acetate resulting in an increase of CO conversion compared to that of cobalt nitrate.

2.4 Cobalt-Support Compound Formation (Co-SCF)

Compound formation between cobalt metal and the support can occur under pretreatment and/or reaction conditions, leading to catalyst deactivation. The compound formation of cobalt metal with support materials, however, is difficult to predict because of the lack of sufficient thermodynamic data. Co-support compound formation can be detected evidentially.

2.5 General Feature of Zirconia

Zirconia exhibits three polymorphs, the monoclinic, tetragonal, and cubic phases. Figure 2.1 shows the typical systems: cubic, tetragonal and monoclinic onses. Crystal structure of cubic, tetragonal and monoclinic zirconia are shown in Figure 2.2 The monoclinic is stable up to ~1170^{o}C, at which temperature it transforms into the tetragonal phase, which is stable up to 2370^{o}C (Cormak and Parker, 1990). The stabilization of the tetragonal phase below 1100^{o}C is important in the use of zirconia as a catalyst in some reaction. Above 2370^{o}C, the cubic phase is stable and it exists up to the melting point of 2680^{o}C. Due to the martensitic nature of the transformations, neither the high temperature tetragonal nor cubic phase can be quenched in rapid cooling to room temperature. However, at low temperature, a metastable tetragonal zirconia phase is usually observed when zirconia is prepared by certain methods, for example by precipitation from aqueous salt solution or by thermal decomposition of zirconium salts. This is not the expected behavior according to the phase diagram of zirconia (i.e., monoclinic phase is the stable phase at low temperatures). The presence of the tetragonal phase at low temperatures can be attributed to several factors such as chemical effects, (the presence of anionic impurities) (Srinivasan *et al*., 1990 and Tani *et al*., 1982) structural similarities between the tetragonal phase and the precursor amorphous phase (Osendi *et al*., 1985; Tani, 1982 and Livage, 1968) as well as particle size effects based on the lower surface energy in the tetragonal phase compared to the monoclinic phase (Garvie, 1978; Osendi *et al*., 1985 and Tani 1982). The transformation of the metastable tetragonal form into the monoclinic form is generally complete by 650-700 ^{o}C.

Crystal system	Unit cell shape
Cubic	$a = b = c, \alpha = \beta = \gamma = 90^o$
Tetragonal	$a = b \neq c, \alpha = \beta = \gamma = 90^o$
Monoclinic	$a \neq b \neq c, \alpha = \gamma = 90^o, \beta \neq 90^o$

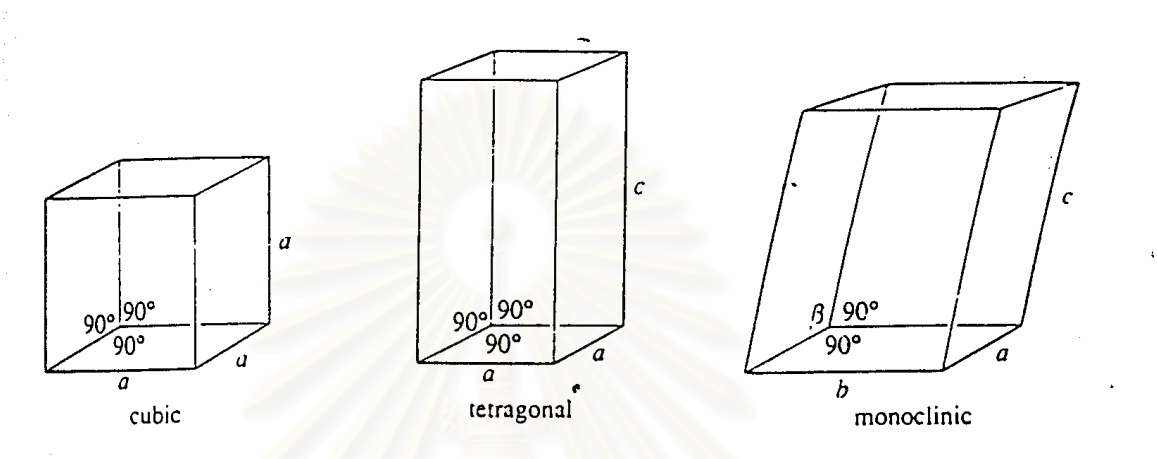

Figure 2.1 The unit cells of the crystal systems. (West, 1997)

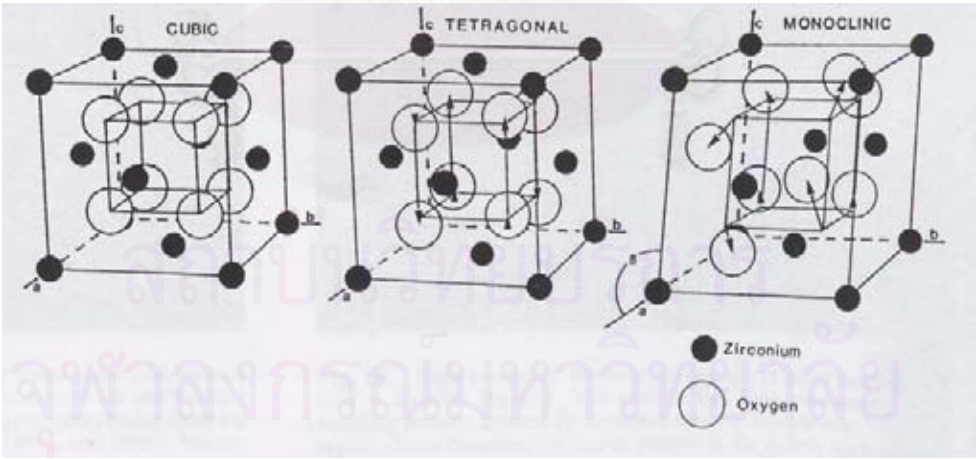

Figure 2.2 Crystal structure of cubic, tetragonal and monoclinic zirconia. (Heuer, 1987)

2.6 Preparation of Zirconia

The main conventional synthesis for multicomponent ceramic powders is a solid-state reaction between oxide and/or carbonate powder precursors. Thus, repeated cycle of milling and calcination at high temperatures are required to achieve the solid-state reaction. Disadvantages of this method are large grain sizes due to the high firing temperatures and poor chemical homogeneity. In addition, undesirable phase can form. Therefore, chemical routes are attracting much attention because they allow production of powders in an unaggregated form. This route also uses lower reaction temperatures for producing the required crystalline phases. In addition, chemical routes have the potential for achieving improved chemical homogeneity on the molecular scale. Major chemical routes, which are under intensive worldwide investigation for powder preparation, are described below.

2.6.1 Precipitation Method

It is possible to control precipitation reactions to such a degree that the concentration of the solute exceeds that for nucleation for only a brief period. This is achieved by bringing the solution into supersaturation, either by changing the temperature, the salt concentration, the pH, or by exploiting the slow release of some hydrolysis products in a water solution.

Zirconia was prepared by adding a solution of zirconium chloride to the well-stirred precipitating solution (e.g. NH_4OH, KOH, or NaOH) at room temperature. The pH of the solution was controlled. The resulting precipitate was removed, and then washed with ammonium nitrate solution. When no more chloride was detected in the washings (silver nitrate test), the precipitate was rinsed with deionized water. The obtained sample was then dried overnight at 100^{o}C. The obtained product was amorphous hydrous oxide and the crystalline material was obtained after calcination at 500^{o}C. The resulting zirconia was predominantly monoclinic, 84%. After heat treatment at 500^{o}C for 1 h, the surface area was only 65 m^2/g and decreased further to 40 m^2/g when calcined for 12 h. (Chuah *et al*., 1998)

2.6.2 Sol-gel Method

To prepare a solid using the sol-gel method, a sol is first prepared form a suitable reactants in a suitable liquid. Sol preparation can either be simply the dispersal of an insoluble solid or addition of a precursor which reacts with the solvent to form a colloid product. A typical example of the first is the dispersal of oxides or hydroxides in water with the pH adjusted so that the solid particles remain in suspension rather than precipitate out. A typical example of the second method is the addition of metal alkoxides to water. The alkoxides are hydrolysed giving the oxide as a colloidal product. The sol is then either treated or simple left to form a gel. To obtain a final product, the gel is heated. This heating serves several purposes: it removes the solvent, it decomposes anions such as alkoxides or carbonates to give oxides, it allows rearrangement of the structure of the solid and it allows crystallization to occur.

Zirconia was obtained from hydrolysis of zirconium *n*-propoxide with ethanol in an argon atmosphere to avoid precipitation. The mixture was kept at 50^{o}C for 1 h under constant agitation. Gellation was induced by adding distilled water dropwise. The fresh gel was amorphous and tetragonal zirconia was crystallized between 300^{o}C to 500^{o}C (Aguilar, 2001).

2.6.3 Hydrothermal Method

The hydrothermal reaction is suitable for the preparation of powders; from nano-particles to single crystals. High temperature, high-pressure aqueous solution, vapors and/or fluids in hydrothermal processing can act on materials as (a) transfer medium of pressure, temperature, and mechanical energy, (b) adsorbate, which plays a role of catalyzer or reaction accelerator, (c) solvent which dissolves or reprecipitates the solid materials, (d) reagent which forms hydroxides, oxides, oxyhydroxides and/or salts. The substances which act as (b) and/or (c) are called mineralizer. The mineralizer can be distilled water or ions such as F^- or OH^-. This synthesis system can assure the homogeneity of the particles in molecular or atomic scale when the process was ideally controlled. (Yoshimura and Somiya, 1999) Wet gel hydrous zirconia obtained from the precipitation method described above was washed and then

encapsulated in an autoclave filled with distilled water or mineralizer solution. The wet gel was subjected to hydrothermal treatment as the autoclave was heated. Pressure inside the autoclave was not controlled.

2.6.4 Glycothermal and Solvothermal Method

Glycothermal method and solvothermal method have been developed for synthesis of metal oxide and binary metal oxide by using glycol and organic solvent as the reaction medium, respectively. The use of glycol or solvent other than water in the hydrothermal method produced the different form of intermediate phase. The preparation method is described in the experimental section, Chapter 4.

2.7 The formation of zirconia in glycol solvents (Kongwudthiti, 2002)

2.7.1 Chemical properties

Zirconium tetra n-propoxide $Zr(OC_3H_7)_4$, molecular weight of 327.6, is a yellow-brown liquid; density = 1.05 g/ml; solidification point below -70^oC; flammable, flash point below 21^oC; soluble in hydrocarbons. Usually, zirconium alkoxides hydrolyze in moist air.

Table 2.2 The physical properties of glycols (Lide, 2000-2001)

glycol	chemical formula	boiling point(^oC)	density (g/ml)
ethylene glycol	$HO(CH_2)_2OH$	197	1.113
1,3-propanediol	$HO(CH_2)_3OH$	215	1.053
1,4-butanediol	$HO(CH_2)_4OH$	235	1.016
1,5-pentanediol	$HO(CH_2)_5OH$	239	0.994
1,6-hexanediol	$HO(CH_2)_6OH$	243-250	0.995

2.7.2 Mechanism of zirconia in glycol solvents

When ethylene glycol (EG) was used as the reaction medium, the crystalline product was not obtained even at reaction temperature of 300°C. This can be attributed to the difficulty in cleavage of C-O bonds of ethylene glycol moieties due to electron withdrawing effect of intramolecular hydroxyl group. Such effect caused the formation of relatively unstable carbocation, therefore the C-O bond is difficult to be broken down. The use of 1,3-propanediol (1,3-PG) resulted in the formation of unidentitied phase and zirconia was not formed even by the reaction at 300°C. As demonstrated later, unidentified phase has glycol moieties in crystal lattice. Similar to the reaction in ethylene glycol, the inability of 1,3-propanediol (1,3-PG) for the formation of crystalline zirconia can also be attributed to the difficulty in heterolytic cleavage of C-O bond in unidentified phase because electron-withdrawing effect of the intramolecular hydroxyl group disturbs the bond breaking of C-O bonds. Based on the inductive effect (i.e., electron withdrawing effect) of the hydroxyl group, the cleavage of C-O bond is expected to proceed more easily with increasing carbon number of glycol because the relatively stable carbocation was formed when the carbon number of glycol increased. When 1,4-butanediol (1,4-BG) was used, pure tetragonal zirconia was obtained at 300°C for 2 h. For the reaction in 1,4-butanediol, the cleavage of the C-O bond was also accelerated by the participation of the intramolecular group forming tetrahydrofuran, which was actually detected by a gas chromatographic analysis of the supernatant after the reaction in 1,4-BG (Inoue, M.; Kominami, H.; and Inui, T., 1993). The reaction in 1,6-hexanediol (1,6-HG) also yielded tetragonal zirconia but the use of 1,5-pentanediol (1,5-PeG) resulted in the formation of a mixture of tetragonal and monoclinic phases.

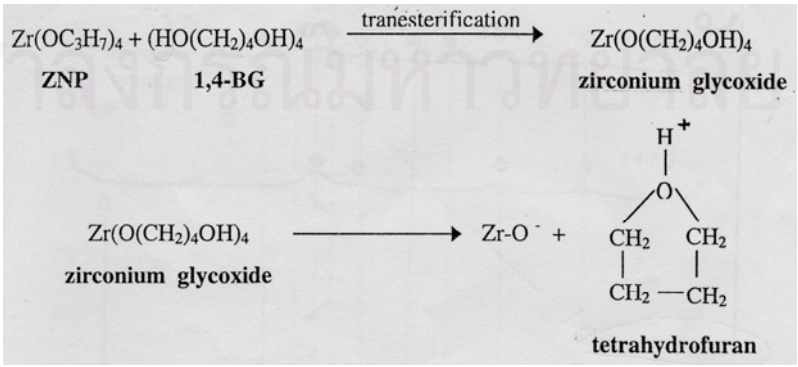

Figure 2.3 Mechanism of glycothermal-derived ZrO_2

CHAPTER III

LITERATURE REVIEWS

3.1 Application of ZrO_2 in FTS

There have been a number of researchers studying the effect of ZrO_2 as a promoter, a support modifier, and a catalyst support in the Fischer-Tropsch synthesis. Most studies show significant improvement in activities and selectivities of the cobalt catalysts. Followings are some recent studies in application of ZrO_2 in the Fischer-Tropsch synthesis.

3.1.1 As a Promoter

S. Ali *et al*. (1995) investigated the influence of Zr promotion of 20 wt% Co/SiO_2 on Fischer-Tropsch synthesis using catalysts prepared in different ways and having different loadings of Zr (up to 8.5 wt%). The catalysts were investigated using FTS ($H_2/CO=2$), H_2-D_2 exchange, and CO dissociation to provide insight into how Zr modifies the Co properties. The Zr-promoted exhibited higher overall rates of FTS compared to unpromoted Co/SiO_2. The sequentially impregnated $Co/Zr/SiO_2$ catalysts appeared to be the most active. However, the co-impregnation method of preparation appeared to result in higher cobalt dispersion. While Zr promotion did not appear to promote or inhibit H_2 activation, hydrogen spillover may have been partly responsible for enhancing the activity of the sequentially impregnated $Zr/Co/SiO_2$ catalysts. Zr also possibly created an active interface with Co that increased catalyst activity by facilitating Co dissociation. Although high levels of promotion tended to increase the selectivity for higher hydrocarbon, Zr appears to be primarily an excellent rate promoter for Co/SiO_2.

A. Feller *et al*. (1999) studied the addition of zirconium oxide chloride to the catalyst formulation of Co/SiO_2. It leads to a higher reducibility of cobalt, due to the formation of a cobalt zirconium species, which can be reduced at lower temperatures than cobalt silicate. Furthermore, the metal particle size of cobalt is increased, but the

size of cobalt clusters is reduced. The Co–Zr/SiO_2 catalysts were tested for their activity in the Fischer–Tropsch synthesis. The steady-state activity increased with increasing zirconium loading, which was attributed to the resistance against reoxidation of the larger cobalt particles and thus to the larger amount of surface cobalt metal present at steady-state in the zirconium promote catalysts. Based on the assumption that the intrinsic activity of cobalt in these catalysts remains unchanged, the observed changes in selectivity could be explained on the basis of secondary reactions in the Fischer–Tropsch system. With increasing zirconium content the number of surface metal atoms at steady-state conditions increases, leading to a higher extent of secondary reactions, but the size of the cobalt clusters decreases, leading to a decrease in the extent of secondary reactions. With increasing zirconium content the extent of secondary hydrogenation of olefins (e.g., ethene) passes a minimum, and the C_{5+}-selectivity passes a maximum due to readsorption of small, reactive organic product compounds, which can be incorporated in larger product compounds. Double bond isomerization increases with increasing zirconium content. This might be attributed to the catalytic activity of zirconia.

R. Oukaci *et al*. (1999) studied the catalyst support in both promoted and non-promoted cobalt catalysts was found to play a major role in influencing the overall hydrocarbon production rate with little or no effect on catalyst selectivity (except for titania) in both the fixed-bed and the slurry bubble column reactor. Zr oxide had a similar effect on the activity of Co/silica. Addition of ZrO_2 to the support prior to the impregnation of cobalt probably serves somewhat to hinder the formation of cobalt silicates. ZrO_2 was found, thus, to be an excellent F–T synthesis rate promoter for SiO_2-supported Co catalysts without any effect, negative or positive, on catalyst selectivity. However, the long-term protecting effect of the zirconia remains to be determined. It is also important to note the differences observed in the two reaction systems, i.e. fixed-bed versus slurry bubble column reactors.

G.R. Moradi *et al*. (2003) studied the effect of zirconia addition at various loading ratios on the performance of 10 wt% Co/SiO2 catalysts for the socalled reaction of Fischer–Tropsch synthesis. The catalysts were prepared through a new pesudo sol–gel method which permits a uniform distribution of the incorporated components and a low deviation from theoretical composition. By increasing zirconia,

Co–SiO2 interaction decreases and is replaced by Co–Zr interaction which favours reduction of the catalysts at lower temperatures. The activity and selectivity toward higher hydrocarbons of the promoted catalysts increase with increasing zirconium loading ratios. No appreciable decrease in activity was observed when all catalysts were employed under H_2/CO at 230 ^oC and 8 bar for 240 h.

3.1.2 As a Support Modifier

D.G. Yadav *et al.* (1999) reported zirconium oxide, or zirconia, when modified with anions such as sulfate ions forms a highly acidic or superacidic catalyst depending on the treatment conditions. This catalyst is found to be well suited for catalyzing reactions of industrial importance, e.g. Fischer–Tropsch reaction. The yield of C_3 was found to decrease with increase in the amount of S-ZrO_2, whereas the yields of C_1, C_2, C_5 and C_6 hydrocarbons were negligible. Also, the formation of isoalkanes was found to be substantially more than alkenes. All the above changes were attributed to secondary reactions of primary FTS products over the strongly acidic S-ZrO_2. These secondary reactions were found to involve oligomerization-cracking, skeletal isomerization, hydrogen transfer and coking. The calcination temperature of S-ZrO_2 had a strong effect on its activity for the secondary reactions.

F. Rohra *et al.* (2000) studied the effect of adding zirconia to the alumina support on supported cobalt Fischer–Tropsch catalysts. At 5 bar and H_2:CO ratio 9:1 zirconia addition to the support leads to a significant increase in both activity and selectivity to higher hydrocarbons as compared to the unmodified catalysts. Reducibility and cobalt dispersion on the other hand are not improved by the presence of zirconia compared to the unmodified catalysts. SSITKA measurements have been performed in order to determine the intrinsic activity per active site. At constant temperature, zirconia-modified and unmodified catalysts showed basically the same intrinsic activity. Similar results were obtained with a noble metal (Pt) promoted catalyst. The promoting effect appears to be mainly due to coverage effects rather than a change in the intrinsic activity of the active sites. The turnover frequencies were found to be independent of pressure but strongly temperature dependent. However, the increase in turnover frequency did not account for the entire increase in

reaction rate with temperature. This indicates that also the coverage of reactive intermediates increases with increasing temperature.

G. Jacobs *et al.* (2002) studied TPR and H_2 chemisorption with pulse reoxidation were carried out on cobalt Fischer–Tropsch catalysts prepared using different supports (e.g. Al_2O_3, TiO_2, SiO_2, ZrO_2 modified SiO_2, ZrO_2 modified Al_2O_3) employing a variety of promoters, including noble metals and metal cations. Addition of non-reducible metal oxides such as B, La, Zr, and K was found to cause the reduction temperature of Co species to shift to higher temperatures, resulting in a decrease in the percentage reduction. For both Al_2O_3 and SiO_2, modifying the support with Zr was found to enhance the dispersion. Increasing the cobalt loading, and therefore the average Co cluster size, resulted in improvements to the percentage reduction.

B. Jongsomjit *et al.* (2003) reported Zr modification of the alumina support had a significant impact on the properties of Co/γ-Al_2O_3 catalysts. The overall catalytic activity during FTS increased significantly (> 65%) upon Zr modification. SSITKA showed that the number of active reaction intermediates (N_M) increased with Zr modification while the intrinsic activity ($1/\tau M$) remained constant. Most of this increase appears to have been due to an increase in reducibility during standard reduction. The increase in reducibility appeared to have been caused by a decrease in the amount of Co-SCF, as seen by Raman spectroscopy. Zr modification may have caused (i) a stabilization of the alumina support by blocking its defect sites, thus blocking Co “aluminate” formation, and/or (ii) aminimization of the impact of water vapor in modifying the surface properties of alumina, thereby decreasing the ease of Co reaction with the alumina. Thus, in summary, Zr modification increased Co reducibility and, probably, the number of exposed Co sites active for CO hydrogenation. Considering the variation in TOFH but the lack of variation in $1/\tau M$ (a measure of intrinsic activity), it is likely that TOFH is in error due to errors in measuring accurately by H_2 chemisorption the number of reduced Co surface atoms.

3.1.3 As a Catalyst Support

M. Kraum *et al.* (1999) studied the dependence of the activity of cobalt-based catalysts for Fischer–Tropsch synthesis on the type of cobalt precursor and support material**.** All catalysts were characterised by XRD, XPS, TPR and CO pulse experiments. The catalytic performance of the catalysts was examined at a total pressure of 20 bar, a temperature of 200ºC, a space velocity (GHSV) of 1200 $h^{-1}$and using a syngas having a H_2 to CO ratio equal to 2.

For catalysts prepared by incipient wetness impregnation, titania, ceria and zirconia were additionally used as supports. The activity changed in the following order: $ZrO_2 < TiO_2 < CeO_2$.

K. Maruya *et al*. (2000) investigated the selective formation of isobutene from CO and H_2 over ZrO_2. ZrO_2 catalysts having different fraction of monoclinic phase were prepared by changing pH value in the mother solution at the precipitation of zirconium hydroxide. The rate of isobutene formation increased with an increase in the volumetric fraction of monoclinic phase in ZrO_2, while those of C_1, C_2, C_3, and C_5+ were independent of the fraction. The amounts of adsorbed methoxy and formate species during the reaction and also of the surface sites with strong basicity increased with an increase in the fraction of monoclinic phase. Chemical trapping experiment showed that the amount of surface methoxy species is comparable to that of site with the strong basicity. These findings were explained by both coordinate unsaturation and stronger basicity based on the configuration of ZrO_2 group in the monoclinic structure.

D.I. Enache *et al.* (2002) reported the thermal treatment, which leads to the best catalytic results, is the direct reduction of the nitrate precursor in the reactor. The effect of the pretreatment is higher in the case of zirconia supported catalyst. The direct reduction of nitrate precursors is even more effective when using a slow-temperature ramping protocol. This phenomenon is explained by the exothermicity of the nitrate reduction. The slower the temperature ramps, the better the heat evacuation, avoiding any increase in cobalt-support interactions or particle

agglomeration. The reduction of Co_3O_4 oxide is difficult and leads to an increase of the cubic crystallised cobalt at the expense of amorphous cobalt or hexagonal cobalt with stacking faults. The direct reduction of nitrate precursor increases the quantity of amorphous cobalt or hexagonal cobalt with crystallographic defects, which are active phases in this reaction. At the same time, the direct reduction leads to weaker metal-support interactions than does precalcination of catalysts. The nitrogen-flow calcination conducts to an intermediate situation. The quantity of crystallised Co_3O_4 is less important than in the case of airflow calcination and it is more reducible.

D.I. Enache *et al.* (2004) studied the activity and the selectivity of cobalt catalysts supported on a crystallised and on an amorphous zirconia were compared with cobalt supported on a γ-alumina catalyst. The catalysts supported on zirconium dioxide were found to present a better reducibility of the active phase and also to be capable of hydrogen adsorption via a spillover mechanism. It is proposed that these properties could account for a better catalytic activity and an increase of the chain growth probability (α). At the same time, the estimated quantity of crystallised Co_3O_4 obtained after airflow calcination (for the same total cobalt loading) is related with the surface area of the support.

M. Shinoda *et al.* (2004) investigated the Co/SiO_2 catalysts derived from silica bimodal supports in slurry phase FTS. The catalysts showed high activities and favorable selectivities due to high dispersion of supported cobalt crystalline by bimodal structure, as proved by XRD and TEM, and fastened diffusion efficiency inside catalyst pellet with bimodal structure. Furthermore, besides the spatial effect from bimodal structure as shown in silica–silica bimodal catalyst, significantly enhanced activity was realized using ZrO_2-silica bimodal support, as ZrO_2 inside the large pores of SiO_2 not only formed small pores but also intrinsically promoted FTS.

3.2 Synthesis of ZrO_2 and Si-modified ZrO_2 Using Glycothermal Method

There have been several studies on the glycothermal synthesis of zirconia. The glycothermal-derived zirconia have a large surfacr area and high thermal stability. The addition of small percentages of silica in the preparation of zirconia was found to play an important role in zirconia stabilization. However, have not been reported to used of glycothermal-derived zirconia as a support for cobalt on CO hydrogenation reaction.

M. Inoue *et al*. (2000) reported the formation of large surface area zirconia rare-earth oxide solid solution by the glycothermal method. The products maintained large surface area even after calcination at high temperature. When the RE content in the product was small, the product partly transformed into the monoclinic phase, but the products with large RE contenes maintained the tetragonal phase.

F.D. Monte *et al*. (2000) reported the addition of small percentages of silica in the preparation of zirconia was found to plays an important role in tetragonal zirconia stabilization; i.e., the tetragonal zirconia is stable for temperatures ranging from 600^{o}C to 1100^{o}C, a larger range of temperature than that observed for pure zirconia (the polymorphic transformation to the monoclinic phase begins at 500^{o}C in pure zirconia). For low silica percentage samples, the improvement of the tetragonal phase stability is due to the lattice deformation resulting from the chemical interactions at the silica-zirconia interface, e.g., the formation of Si-O-Zr bonds identified through FT-IR spectroscopy. The Si-O-Zr groups can be taken as chemical impurities, which are able to stabilize the zirconia tetragonal phase.

S. Kongwudthiti *et al.* (2002) reported silica-modified zirconia was directly obtained by the reaction of mixture of zirconium n-propoxide and tetraethyl orthosilicate in 1,4-butanediol at 300 ^{o}C. The products possessed large surface areas and maintained the tetragonal phase even after calcinations at high temperatures.

S. Kongwudthiti *et al*. (2003) investigated the influences of concentration of zirconium n-propoxide in the solution and drying condition on primary and secondary particle size, and pore system of the powders. Nanocrystalline zirconia powders have

been prepared by the reaction of zirconium n-propoxide in 1,4-butanediol and 1,5-pentanediol at 300 ^{o}C for 2 h. When 1,4 butanediol was used, increasing the concentration of zirconium n-propoxide increased the primary and secondary particle size and BET surface area while the physical properties of zirconia prepared in 1,5-pentanediol were not affected by such factors. To investigate the effect of drying method, glycol was removed from the autoclave at reaction temperature instead of by the conventional process in which the product is washed in methanol and air-dried. This change improved the pore system of powders prepared in 1,5-pentanediol, probably through the reduction of coagulation among the ultrafine particles during the drying process.

S. Kongwudthiti *et al.* (2003) reported SiO_2-modified ZrO_2 with Si/Zr ratios of 0.04–0.15, prepared by the reaction of zirconium n-propoxide and TEOS in 1,4-butanediol, exhibit Si–O–Zr bonds formed during the reaction. Powders produced show a high degree of silica and zirconia homogeneity. The presence of Si–O–Zr bonds in the powder retards the crystal growth of zirconia.

Q. Zhaoa *et al.* (2004) studied the effects of curing and Si doping were separated by curing ZrO_2 powders in a Teflon flask and doping with different amounts of TEOS solutions (0–10.9 wt.% Si in ZrO_2). Curing increased the pore volume and the pore size of ZrO_2 powders but had negligible effect on the surface area after 4 h of heat treatment at elevated temperatures. Si doping could significantly increase the surface area, delay the crystallization, stabilize the tetragon phase of ZrO_2, and retard the crystallite growth. The Si effects did not depend on the sequence of the Si addition. Significant SSA enhancement on Si-doped ZrO_2 was observed for cured samples. Additionally, the pore size and the pore volume could be controlled by varying the concentration of Si doping.

CHAPTER IV

EXPERIMENTAL

This chapter describes the experimental systems and procedures used in this study. The chapter is divided into three parts; (4.1) catalyst preparation (4.2) catalyst characterization and (4.3) reaction study. The first part (section 4.1) presents catalyst preparation including materials used, preparation of zirconia support, cobalt loading and catalyst nomenclature. The second part (section 4.2) shows the details of characterization techniques such as AAS, BET, XRD, TGA, TPR, H_2 chemisorption, SEM, and TEM. And the last part (section 4.3) illustrates the reaction study in CO hydrogenation.

4.1 Catalyst Preparation

The details of chemicals used in this experiment are follows

4.1.1 Chemicals

1. Cobalt (II) nitrate hexahydrate available from Aldrich.
2. Zirconium tetra-*n*-propoxide [$Zr(OC_3H_7)_4$, ZNP-30] 29.5% Zr available from Mitsuwa's pure Chemicals.
3. Zirconium *n*-propoxide [$Zr(OC_3H_7)_4$, ZNP-20] 20.5% ZrO_2 available from Strem Chemical.
4. Tetraethyl orthosiliocate [$(C_2H_5O)_4Si$, TEOS] available from Aldrich.
5. 1,4-butanediol (1,4-BG) available from Aldrich.
6. 1,5-pentanediol (1,5-PeG) available from Merck.
7. Zriconium oxide available from Aldrich.

The calculation of amount of regents required in the reaction is shown in Appendix A.

4.1.2 Equipment

The equipment for the synthesis of zirconia consisted of:

Autoclave Reactor

- Made from stainless steel
- Volume of 1000 cm^3 and 10 cm inside diameter
- The thermocouple is attached to the reagent in the autoclave and maximum temperature of 350^oC
- Pressure gauge in the range of 0-140 bar
- Test tube was used to contain the reagent and glycol

The autoclave reactor is shown in Figure 4.1

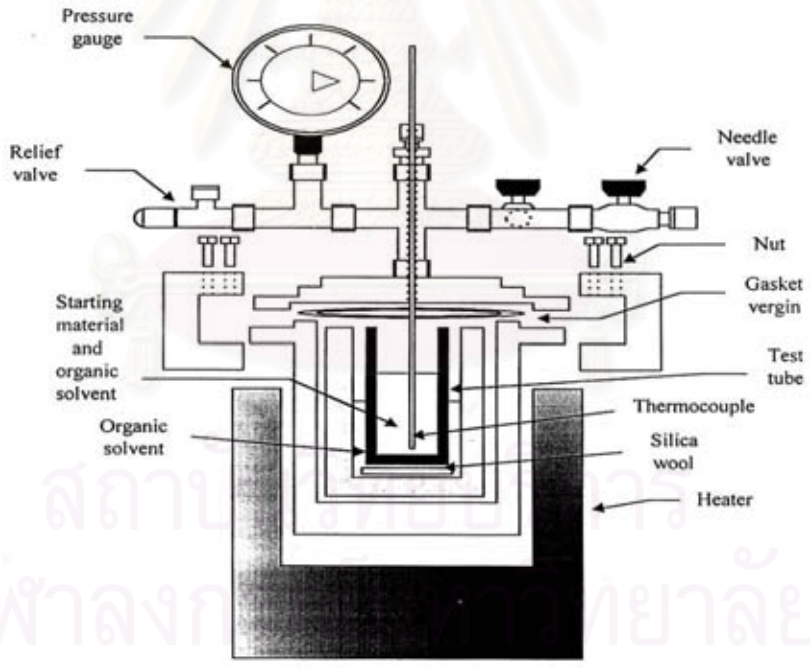

Figure 4.1 Autoclave reactor

The diagram of the reaction equipment for synthesis of zirconia is shown in Figure 4.2

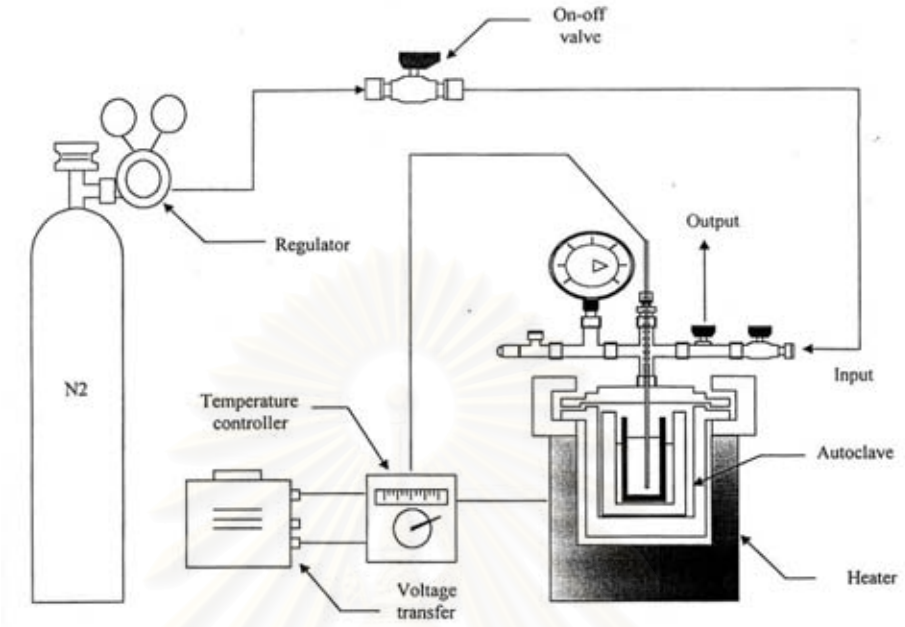

Figure 4.2 Diagram of the reaction equipment for the synthesis of zirconia

4.1.3 Preparation of ZrO_2 Support

Zirconia was prepared by using zirconium *n*-propoxide 15 g as a starting material. The starting materials were suspended in 100 ml of solvent (glycol) in the test tube, and then set up in 300 ml autoclave. In the gap between the test tube and autoclave wall, 30 ml of glycol was added. After the autoclave was completely purged with nitrogen, the autoclave was heated to 300°C at the rate of 2.5 °C/min and held at that temperature for 2 hours. Autogeneous pressure during the reaction gradually increased as the temperature was raised. After the reaction, the autoclave was cooled to room temperature. The resulting products were collected by repeatedly washed with methanol and centrifugation and then the products were dried in air.

4.1.4 Preparation of Si-modified ZrO_2 Support

For the synthesis of silica-modified zirconia, the method are the same with that to obtain pure zirconia whereas the mixture of zirconium *n*-propoxide 15 g and an amount of tetraethyl orthosilicate (TEOS) at Si/Zr ratio of 0.005, 0.01, and 0.02 was used as the starting material.

4.1.5 Cobalt Loading

The Co/ZrO_2 catalysts were prepared by the incipient wetness impregnation of the supports with aqueous solution of cobalt nitrate. Cobalt loading was approximately 8% by weight of catalyst. The samples were washed thoroughly and dried at 110°C for 1 day. The catalysts were calcined in air at 300 °C for 2 h.

4.1.6 Catalyst Nomenclature

The different zirconia are designated as ZrO_2-BG-20, ZrO_2-BG-30, ZrO_2-PeG-20, and ZrO_2-PeG-30, in which ZrO_2 refer to zirconia, BG and PeG refer to the glycol used (BG = 1,4-butanediol, PeG = 1,5-pentanediol) and the number 20 and 30 refer to the concentration of Zr in the ZNP solution used. Cobalt catalysts supported on different zirconia are designated as Co/ZrO_2-BG-20 for Co supported on ZrO_2-BG-20 and so on.

The catalyst are designated as ZrO_2-BG-20(0.005Si), ZrO_2-BG-20(0.02Si) and ZrO_2-PeG-20(0.01Si), in which the number 0.005, 0.01 and 0.02 refer to atomic ratio of Si/Zr.

4.2. Catalyst Characterization

4.2.1 Atomic Absorption Spectroscopy

The bulk composition of cobalt was determined by Varian Spectra A800 atomic absorption spectroscopy (AAS). The composition content of catalysts was collected using varian, Spectra A800 at the Department of Science Service Ministry of Science Technology and Environment.

4.2.2 N_2 Physisorption

BET apparatus for the single point method

The reaction apparatus of BET surface area measurement consisted of two feed lines for helium and nitrogen. The flow rate of the gas was adjusted by means of fine-metering valve on the gas chromatograph. The sample cell made from pyrex glass.

The mixture gases of helium and nitrogen flowed through the system at the nitrogen relative of 0.3. The catalyst sample (ca. 0.3 to 0.5 g) was placed in the sample cell, which was then heated up to 160 ^{o}C and held at this temperature for 2 h. After the catalyst sample was cooled down to room temperature, nitrogen uptakes were measure as follows.

Step (1) Adsorption step: The sample that set in the sample cell was dipped into liquid nitrogen. Nitrogen gas that flowed through the system was adsorbed on the surface of the sample until equilibrium was reached.

Step (2) Desorption step: The sample cell with nitrogen gas-adsorption catalyst sample dipped into the water at room temperature. The adsorbed nitrogen gas was deorbed from the surface of the sample. This step was completed when the indicator line was in the position of base line.

Step (3) Calibration step: 1 ml of nitrogen gas at atmospheric pressure was injected through the caribration port of the gas chromatograph and the area was measured. The area was the calibration peak.

BET apparatus for the multipoint method

The BET surface areas for the multipoint method were measured by N_2 physisorption using a Quantachrome Nova 1000 automated system. Each sample was degassed in the system at 150^{o}C for 2 h prior to N_2 physisorption.

4.2.3 X-ray Diffraction (XRD)

The X-ray diffraction (XRD) patterns of powder were performed by a X-ray diffractometer SIEMENS D5000 connected with a computer with Diffract ZT version 3.3 program for fully control of the XRD analyzer. The experiments were carried out by using Ni-filtered CuKα radiation. Scans were performed over the 2θ ranges from 10^{o} to 80^{o}. The crystallite size was estimated from line broadening according to the Scherrer equation and α-Al_2O_3 was used as standard.

4.2.4 Thermalgravimetric Analysis (TGA)

TGA was used to determine the weight loss pattern and the reducibility of catalysts by DIAMOND TG/DTA. The catalyst sample 10-20 mg used in the operation and temperature ramping from 35° C to 800° C at 10 °C/min. The carrier gas was N_2 UHP.

4.2.5 Temperature Programmed Reduction (TPR)

TPR was used to determine the reducibility of catalysts. The catalyst sample 100 mg used in the operation and temperature ramping from 35^{o}C to 800^{o}C at 10^{o}C/min. The carrier gas will be 5 % H_2 in Ar. During reduction, a cold trap will be placed to before the detector to remove water produced. A thermal conductivity detector (TCD) will be measure the amount of hydrogen consumption. The calibration of hydrogen consumption was performed with bulk cobalt oxide (Co_3O_4) at the same conditions.

4.2.6 Hydrogen Chemisorption

Static H_2 chemisorption at 100 ^oC on the reduce catalysts was used to determine the number of reduce surface cobalt metal atoms and overall cobalt dispersion. The total hydrogen chemisorption was calculated from the number of injection of a known volume. H_2 chemisorption was carried out following the procedure discribed by Reuel and Bartholomew (1984) using a Micrometritics Pulse Chemisorb 2700 instrument at the Analysis Center of Department of Chemical Engineering, Faculty of Engineering, Chulalongkorn University. Prior to chemisorption, the catalysts were reduced at 350 ^oC for 3 hours after ramping up at a rate of 1 ^oC/min.

4.2.7 Scanning Electron Microscopy (SEM)

Catalyst granule morphology of the samples were observed by JSM-5410LV scanning electron microscopy at the Scientific and Technological Research Equipment Center, Chulalongkorn University (STREC).

4.2.8 Transmission Electron Microscopy (TEM)

The cobalt oxide particle size and particle size distribution on ZrO_2 were observed using JEOL-JEM 1220 transmission electron microscope operate at 70 kV at Kasedsart University.

4.2.9 Infrared Spectroscopy (IR)

The functional group in the samples was determined by using Infrared spectroscopy Nicolet impact 400 at Petrochemical Engineering Laboratory, Chulalongkorn Unoversity. Before measurement, the sample was mixed with KBr and then was formed into a thin wafer.

4.3 Reaction Study in CO Hydrogenation

4.3.1 Materials

The reactant gas mixture used for the reaction study was composed of 9.73 vol% carbon monoxide in hydrogen and supplied by Thai Industrial Gas Limited (TIG). The total flow rate was 30 ml/min. Ultra high purity hydrogen and high purity argon manufactured by Thai Industrial Gas Limited (TIG) were used for reduction and balanced flowrate.

4.3.2 Equipment

The CO hydrogenation system is schematically shown in Figure 4.3. The system is consisted of a reactor, an automatic temperature controller, an electrical furnace and a gas controlling system.

4.3.2.1 Reactor

The reactor was made from a stainless steel tube (O.D. 3/8”). Two sampling points were provided above and below the catalyst bed. Catalyst was placed in the middle of the reactor and held by two quartz wool layers.

4.3.2.2 Automation Temperature Controller

This unit is consisted of a magnetic switch connected to a variable voltage transformer and a solid state relay temperature controller model no. SS2425DZ connected to a thermocouple. Reactor temperature was measured at the bottom of the catalyst bed in the reactor. The temperature control set point is adjustable within the range of 0-800^{o}C at the maximum voltage output of 220 volt.

4.3.2.3 Electrical Furnace

The electrical furnace was used to supply heat to the reactor for CO hydrogenation. The reactor could be operated from room temperature up to 800^{o}C at the maximum voltage of 220 volt.

4.3.2.4 Gas Controlling System

The flowrate of each gas used in this study was controlled by a gas controlling system which consisted of a pressure regulator, an on-off valve and the gas flow rates were adjusted by using metering valves.

4.3.2.5 Gas Chromatograph

The composition of hydrocarbons in the product stream was analyzed by a Shimadzu GC14B gas chromatograph equipped with a flame ionization detector. A Shimadzu GC8A (molecular sieve 5A) gas chromatograph equipped with a thermal conductivity detector was used to analyze CO and H_2 in the feed and product streams. The operating conditions for each instrument are shown in the Table 4.1.

4.3.3 CO Hydrogenation Procedure

CO hydrogenation was performed using 0.1 g of catalyst was packed in the middle of the stainless steel microrector, which located in the electrical furnace. The total flow rate was 60 ml/min with the H_2/CO ratio of 10/1. The catalyst sample was re-reduced *in situ* in flowing H_2 at 350^{o}C for 3 h prior to CO hydrogenation. CO hydrogenation was carried out at 220^{o}C and 1 atm total pressure. The streams were analyzed by gas chromatography technique.

Table 4.1 Operating Condition for Gas Chromatograph

Gas chromatograph	Shimadzu GC8A	Shimadzu GC14B
Detector	TCD	FID
Column	Molecular Sieve 5A	VZ10
Carrier gas	He (99.999%)	N_2 (99.999%)
Carrier gas flow	30 ml./min.	30 ml./min.
Column temperature		
- Initial	40^oC	70^oC
- Final	40^oC	70^oC
Detector temperature	100^oC	100^oC
Injector temperature	100^oC	150^oC
Analyzed gas	N_2, CO, O_2	Hydrocarbon C_1-C_4

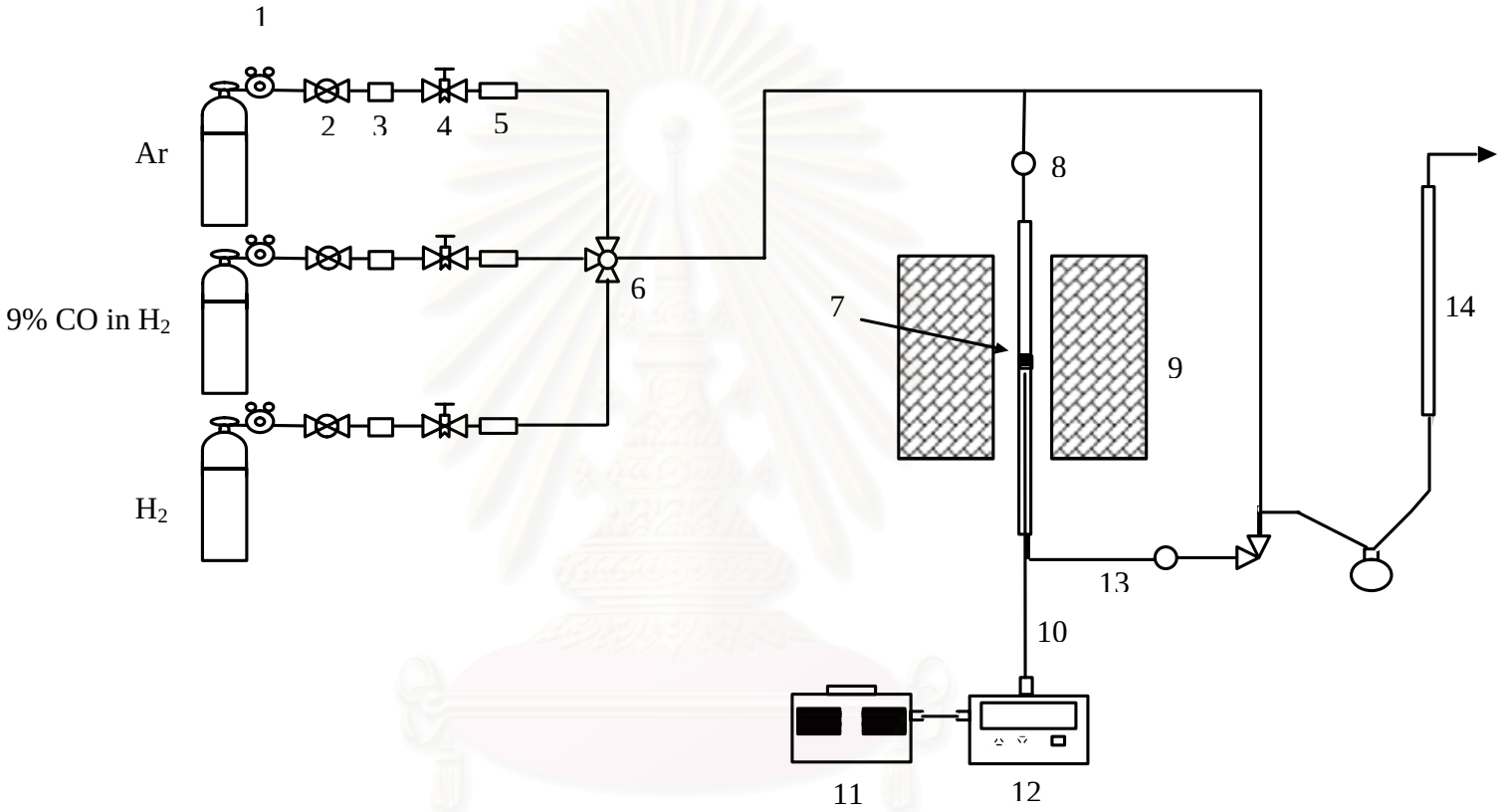

1. Pressure Regulator 2. On-Off Value 3. Gas Filter 4. Metering Valve
5. Back Pressure 6. 3-way Valve 7.Catalyst Bed 8. Sampling point
9. Furnace 10. Thermocouple 11. Variable Voltage Transformer 12. Temperature Controller
13. Heating Line 14. Bubble Flow Meter

Figure 4.3 Flow diagram of CO hydrogenation system

CHAPTER V

RESULTS AND DISCUSSION

The results and discussion in this chapter are divided into four sections. Section 5.1 explains the effects of glycol source and zirconium concentration in ZNP solution used in ZrO_2 preparation on the physicochemical properties of ZrO_2 prepared by glycothermal method. The characteristics and the catalytic properties of the glycothermal-derived ZrO_2 supported cobalt catalysts in CO hydrogenation reaction are explained in section 5.2. Section 5.3 explains the effect of Si addition during ZrO_2 preparation on the physicochemical properties of ZrO_2 prepared by glycothermal method and the characteristics and the catalytic properties of Si-modified ZrO_2 supported cobalt catalysts in CO hydrogenation reaction. Section 5.4 presents a comparative study of cobalt catalysts supported on micron-size ZrO_2 and nano-size ZrO_2 in CO hydrogenation reaction.

5.1 The Physicochemical Properties of ZrO_2 Prepared by Glycothermal Method

In this section, the effects of glycol source and zirconium concentration in ZNP solution used in ZrO_2 preparation on the physicochemical properties of ZrO_2 prepared by glycothermal method were investigated. Commercial zirconia from Aldrich was used for comparison purposes. 1,4-Butanediol (1,4-BG) and 1,5-pentanediol (1,5-PeG) were the glycols used as the reaction medium for the synthesis of ZrO_2 from zirconium *n*-proproxide (ZNP) solution with a concentration of about 20 or 30% Zr. The glycothermal-derived ZrO_2 particles were characterized by various analysis techniques such as SEM, XRD, N_2 physisorption, and TGA.

5.1.1 Scanning Electron Microscopy (SEM)

The zirconia obtained by glycothermal method are white powders. Typical SEM micrographs for ZrO_2 samples prepared in 1,4-BG, 1,5-PeG and commercial zirconia (micro-size) are shown in Figures 5.1. The samples prepared in 1,4-BG (Figure 5.1 a and b) had a spherical shape and a dense mass and seemed to be formed by aggregation of primary particles. The lower initial zirconium concentration in ZNP solution resulted in smaller size of ZrO_2 particles. The results were consistent with Kongwudthiti *et al*. (Kongwudthiti *et al*., 2003). They reported that increasing ZNP concentration increases mean microsphere diameter while reducing sharply the number of small microspheres. The average particle sizes of the secondary particles (appeared as separate spherical particles) were found to be 1.2 and 3.1 micron for ZrO_2 particles from ZNP solutions with Zr = 20 and 30%, respectively. The ZrO_2 particles prepared in 1,5-PeG did not form separate spherical particles. The particle sizes were slightly increased with increasing Zr concentration in the ZNP solution. Each particle prepared by this method is a single crystal grown from a nucleous (Inoue, 2000: 855). The crystallization pathway of zirconia in the two solvents (1,4-BG and 1,5-PeG) was reported to be completely different (Kongwudthiti *et al*., 2003). While the synthesis in 1,5-PeG a homogeneous solution (i.e., glycoxide) was formed after the mixture was heated to 250 ^{o}C and cooled down, the synthesis in 1,4-BG yielded a solid precipitate. The authors suggested that crystal growth of zirconia in 1,5-PeG proceeded by precipication and crystallization of the glycoxide while zirconia particles crystallized from solid-state transformation in 1,4-BG.

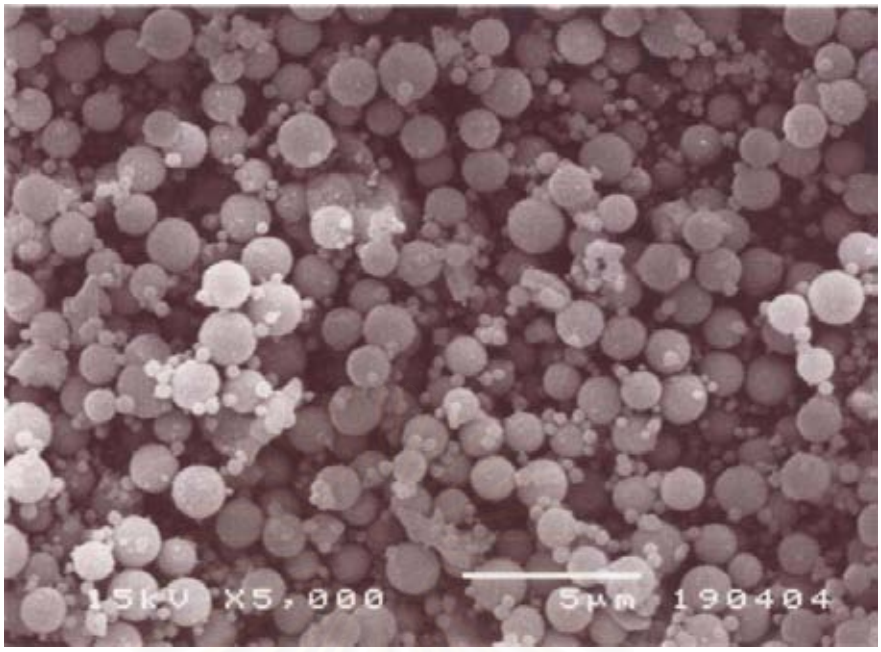

Figure 5.1 (a) SEM micrograph of ZrO_2-BG-20 catalyst granules

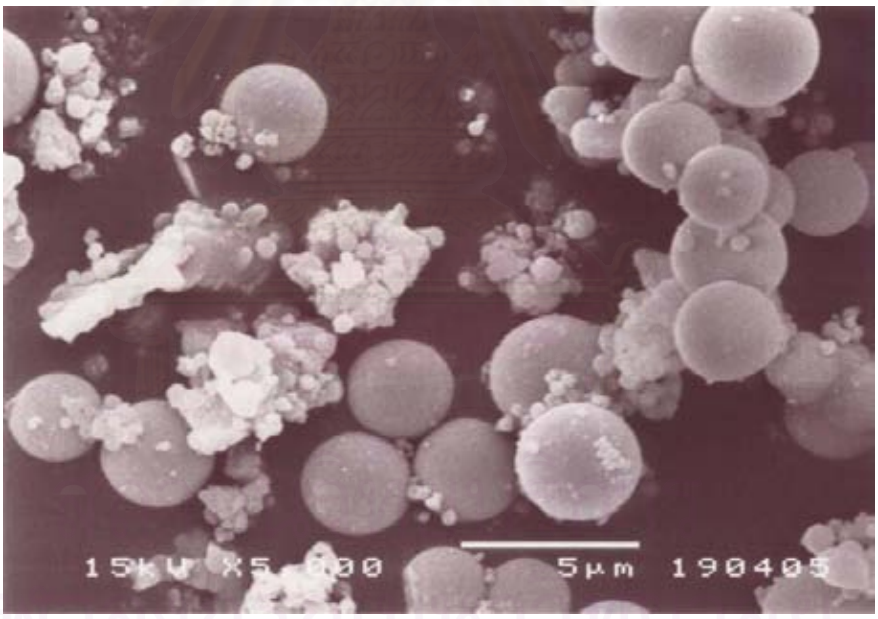

Figure 5.1 (b) SEM micrograph of ZrO_2-BG-30 catalyst granules

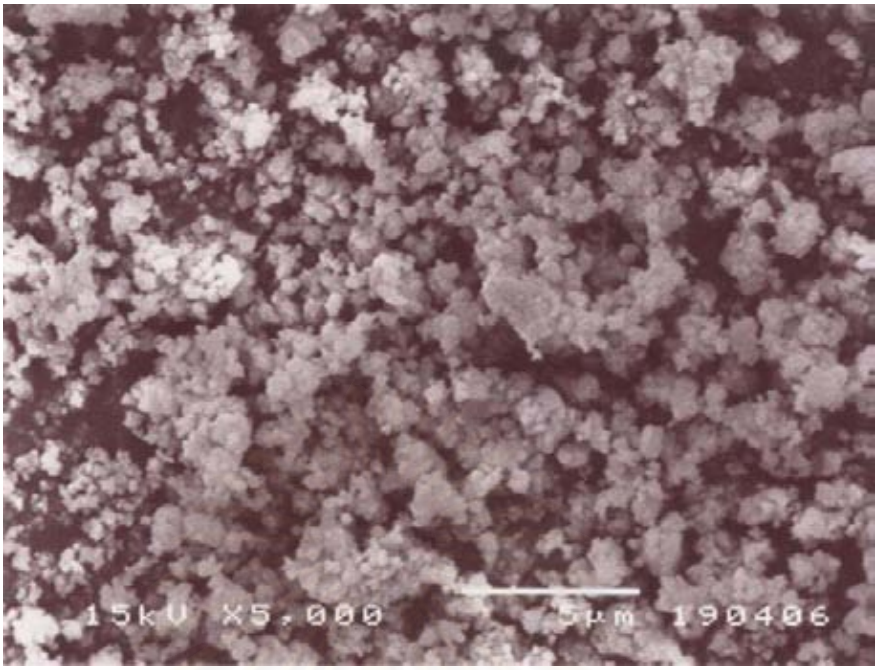

Figure 5.1 (c) SEM micrograph of ZrO_2-PeG-20 catalyst granules

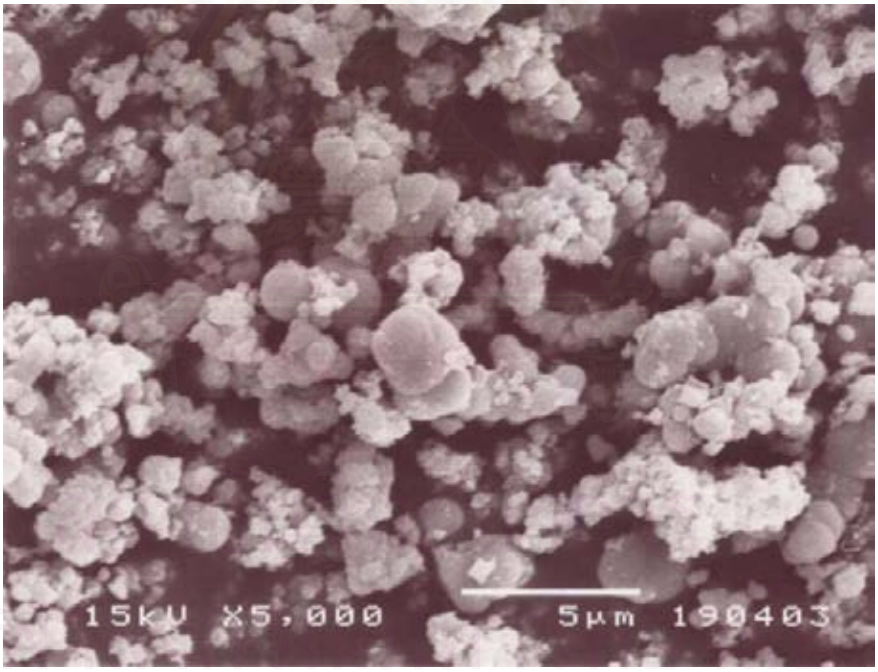

Figure 5.1 (d) SEM micrograph of ZrO_2-PeG-30 catalyst granules

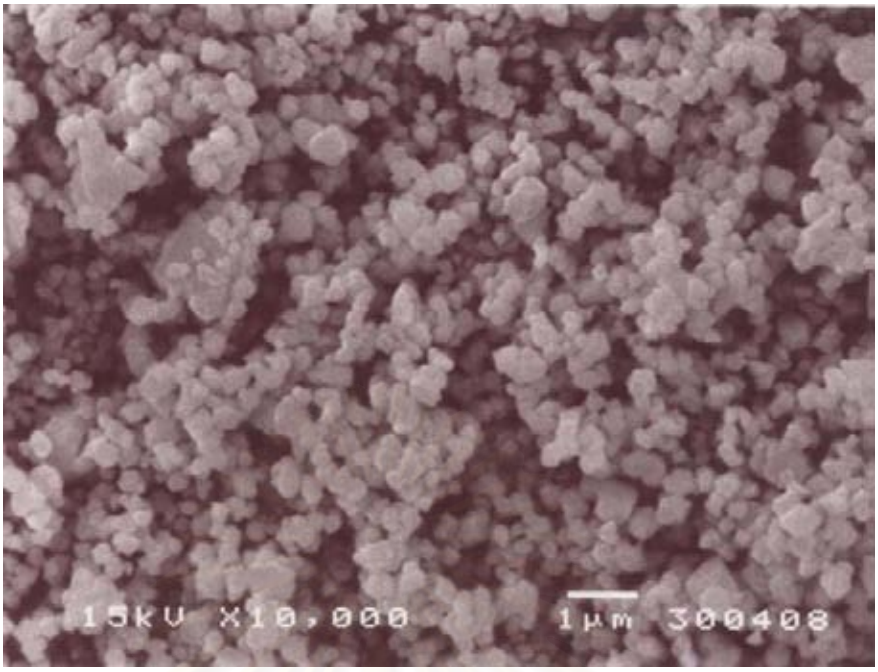

Figure 5.1 (e) SEM micrograph of ZrO_2-commercial catalyst granules

5.1.2 X-ray Diffraction (XRD)

The X-ray diffraction patterns of the different ZrO_2 samples prepared by glycothermal method and commercial ZrO_2 are shown in Figure 5.2. The ZrO_2 phase presenting in the samples and the average crystallite size of the ZrO_2 calculated using XRD line broadening and Scherrer's equation are given in Table 5.1. The XRD patterns of all the samples prepared in glycothermal method indicated tetragonal crystalline zirconia. No other crystal structures were observed. The average crystallite size of the ZrO_2 prepared by glycothermal method were determined to be ca. 3-4 nm. In contrast the XRD pattern of the commercial zirconia indicated both monoclinic and tetragonal crystalline phases. The crystallite size of commercial was found to be 9 nm.

Table 5.1 Phases Presented in the ZrO_2 Samples and the Average Crystallite Sizes

Catalyst	ZrO_2 Phase	Crystal Size (nm)[a]
ZrO_2-BG-20	T	4.0
ZrO_2-BG-30	T	3.0
ZrO_2-PeG-20	T	3.7
ZrO_2-PeG-30	T	3.6
ZrO_2-commercial	T ,M	10.5

[a] Based on XRD line broadening.

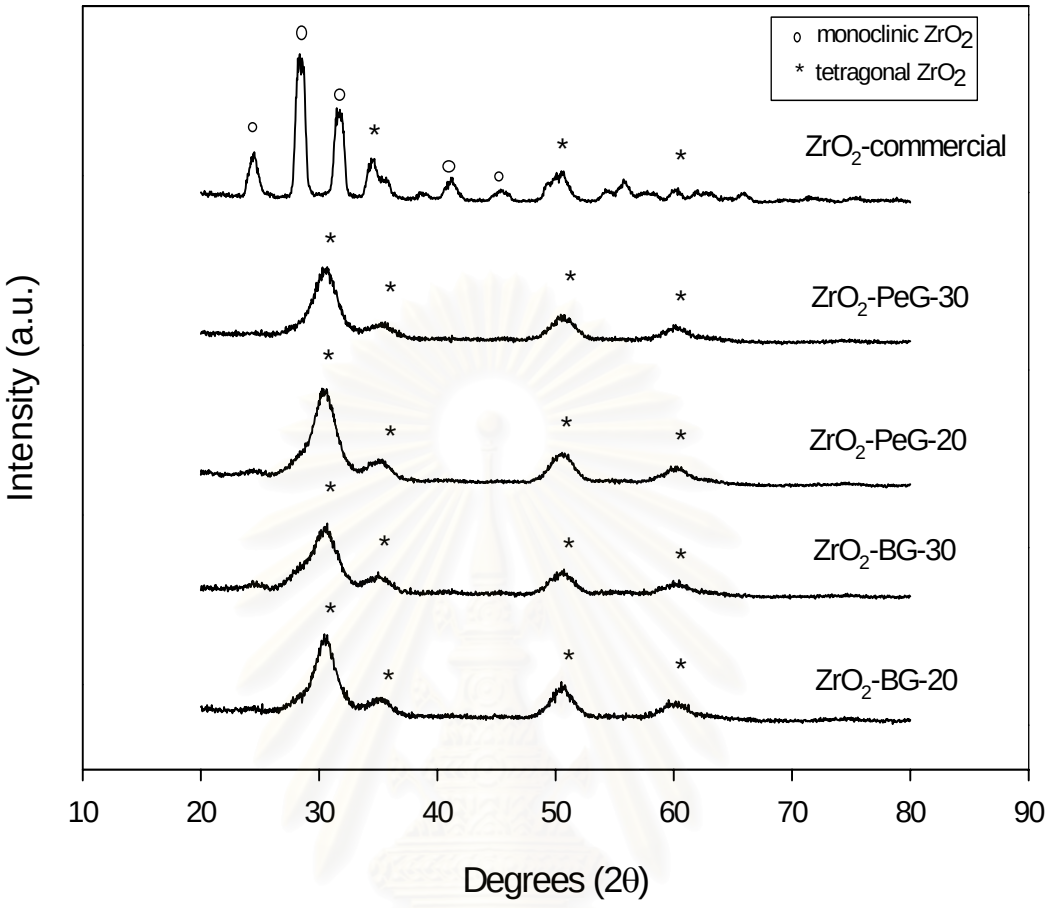

Figure 5.2 XRD patterns of the glycothermal-derived ZrO_2 and the commercial ZrO_2

5.1.3 N_2 Physisorption

The BET surface area of zirconia samples prepared by glycothermal method and commercial zirconia were determined by adsorption and condensation of N_2 at liquid N_2 temperature using static vacuum procedure. This technique is so-called "BET method" according to the inventors'name (Bruanaure, Emmett, and Teller). The results are given in Table 5.2. The BET surface areas of the glycothermal-derived zirconia were found to be much higher (97-209 m^2/g) than that of commercial zirconia. The BET surface area of zirconia obtained in 1,4-BG increased slightly with decreasing Zr concentration in ZNP solution whereas the BET surface area of zirconia prepared in 1,5-PeG was independent of Zr concentration.

Table 5.2 N_2 Physisorption Results

Catalysts	BET S.A. [a] (m^2/g)
ZrO_2-BG-20	206
ZrO_2-BG-30	195
ZrO_2-PeG-20	220
ZrO_2-PeG-30	207
ZrO_2-commercial	50[b]

[a] Using N_2 physisorption at 77 K. Error of measurement = +/- 10%.

[b] From single point BET in our laboratory

5.1.4 Thermo Gravimetric Analysis (TGA)

Thermogravimetric analysis (TGA) experiments were performed with pure zirconia prepared by glycothermal method in order to examine the decomposition of zirconia during high temperature treatment. Figure 5.3 and 5.4 show the thermal analysis of zirconia prepared by glycothermal method from the ZNP solutions with Zr = 20% in 1,4-BG and 1,5-PeG,respectively. The weight was slightly decreased probably due to the desorption of physisorbed species such as methanol and water. Thus, the glycothermal-derived zirconia are stable under the calcination conditions used in this study.

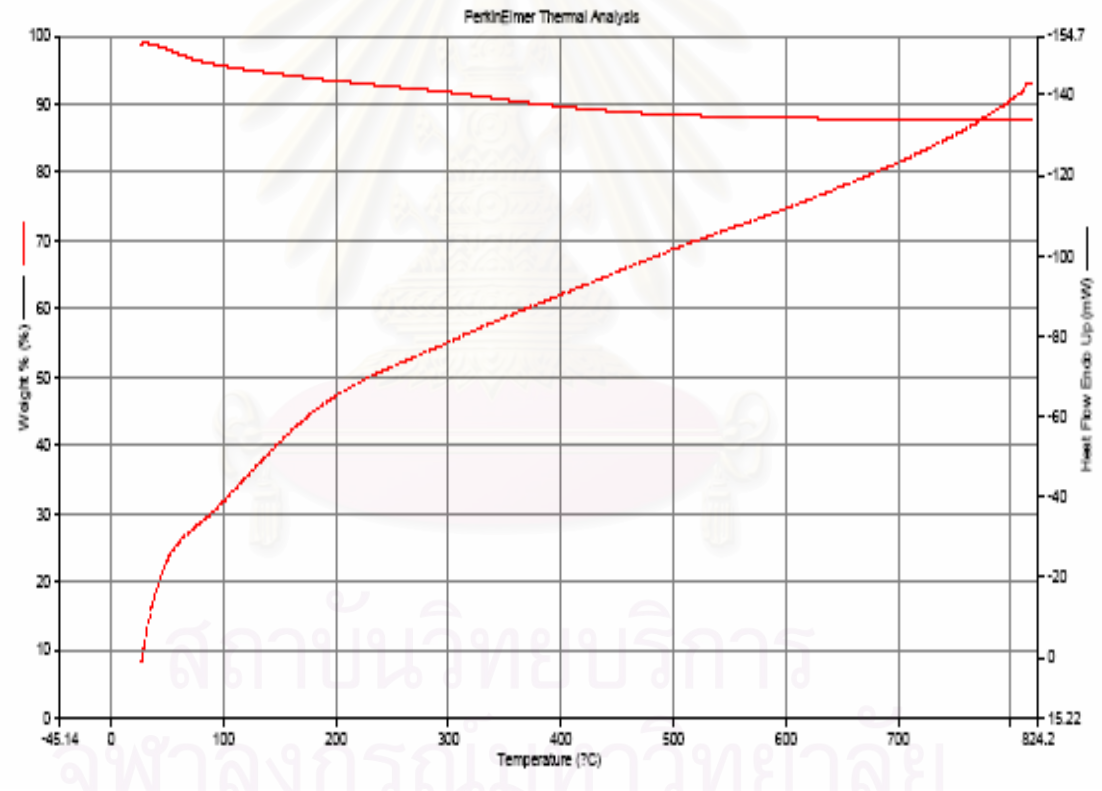

Figure 5.3 Thermogravimetric analysis (TGA) experiments for zirconia prepared by glycothermal method of zirconium n-propoxide in 1,4-butanediol.

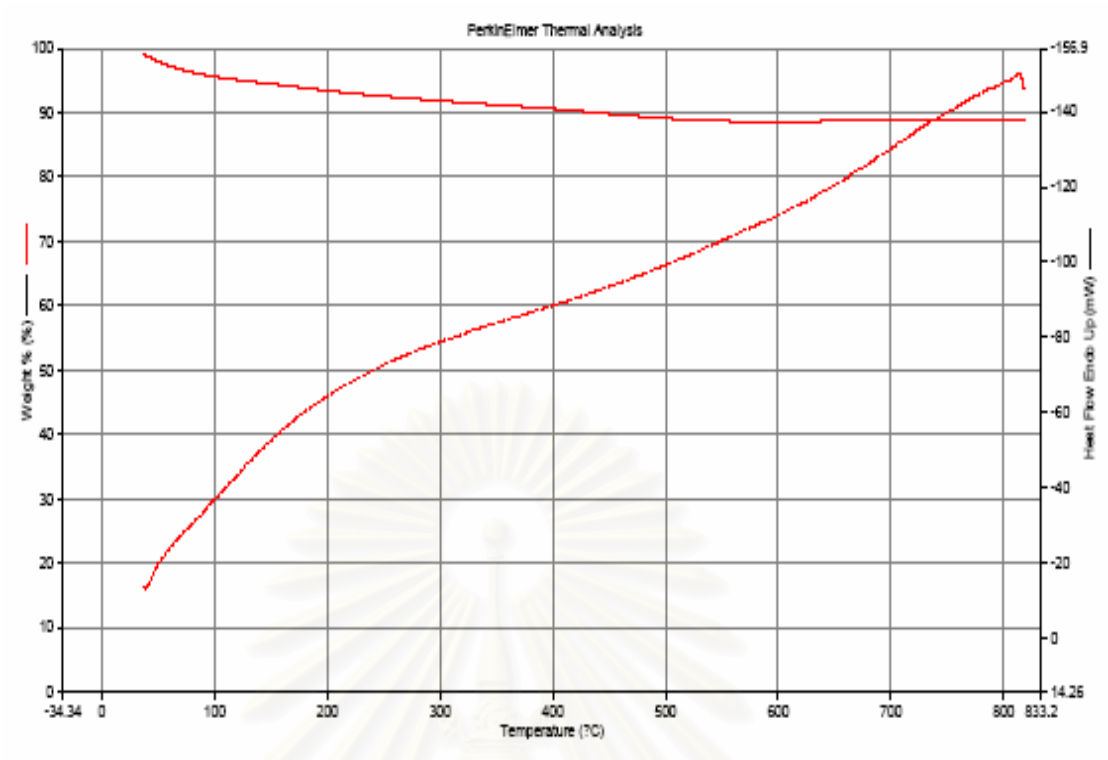

Figure 5.4 Thermogravimetric analysis (TGA) experiments for zirconia prepared by glycothermal method of zirconium n-propoxide in 1,5-pentanediol.

5.2 The Characteristics and Catalytic Properties of Glycothermal-derived ZrO_2 Supported Cobalt Catalysts

5.2.1 Catalyst Characterization

5.2.1.1 Atomic Absorption Spectroscopy (AAS)

The AAS was performed to determine the actual amounts of cobalt loading on the catalyst samples. The results are given in Table 5.3. In this study, cobalt loading on the catalyst samples was approximately 7-8 wt% in order to make it close to that required for a commercial Fischer-Tropsch catalyst.

Table 5.3 Atomic Absorption Results.

Catalysts	Co (Wt%)
Co/ZrO_2-BG-20	8.4
Co/ZrO_2-BG-30	8.4
Co/ZrO_2-PeG-20	7.3
Co/ZrO_2-PeG-30	8.2
Co/ZrO_2-commercial	7.9

5.2.1.2 N_2 Physisorption

The BET surface areas of cobalt supported on zirconia are shown in Table 5.4. The BET surface areas of the cobalt catalysts supported on different glycothermal derived ZrO_2 were found to be in the range of 160-180 m^2/g. The surface area of glycothermal-derived zirconia were found to be much higher than that of commercial zirconia. The BET surface areas of cobalt supported on zirconia were lower than the BET surface area of the unsupported zirconia. The significant decrease in surface area of the original support material suggests that cobalt was deposited significantly in the pores of ZrO_2.

Table 5.4 N_2 Physisorption Results

Catalysts	BET S.A. [a] (m^2/g)
Co/ZrO_2-BG-20	170
Co/ZrO_2-BG-30	160
Co/ZrO_2-PeG-20	173
Co/ZrO_2-PeG-30	180
Co/ZrO_2-commercial	46[b]

[a] Using N_2 physisorption at 77 K. Error of measurement = +/- 10%.

[b] From single point BET in our laboratory

5.2.1.3 X-ray Diffraction (XRD)

The X-ray diffraction patterns of the ZrO_2-supported cobalt catalysts are shown in Figure 5.5. After impregnation of 8 wt% cobalt and calcination at 300°C, no XRD peak for Co_3O_4 was observed for all the ZrO_2-supported cobalt catalysts except for the Co/ZrO_2-commercial catalyst. The results suggested that the crystallite sizes of cobalt oxide formed on the glycothermal-derived zirconia were probably smaller than the detectability limit of XRD. It is also possible that on glycothermal-derived zirconia, Co did not form Co_3O_4 crystallites but may have formed an amorphous cobalt oxide similar to what has been found for cobalt catalysts supported on TiO_2 prepared by sol-gel technique (Kraum, Baerns, 1999). The crystal sizes and zirconia phase of supported cobalt catalysts are given in Table 5.5. The crystal sizes of ZrO_2 in the zirconia-supported cobalt catalysts were found to be 3-4 nm. They were not significantly changed after impregnation of cobalt.

Table 5.5 Phases Present in the Samples and the Average Crystallite Size of Co/ZrO_2

Catalysts	ZrO_2 Phase	Crystal size of ZrO_2 [a] (nm)
Co/ZrO_2-BG-20	T	3.6
Co/ZrO_2-BG-30	T	3.4
Co/ZrO_2-PeG-20	T	3.2
Co/ZrO_2-PeG-30	T	3.5
Co/ZrO_2-commercial	T ,M	8.8

[a] Base on XRD line broadening.

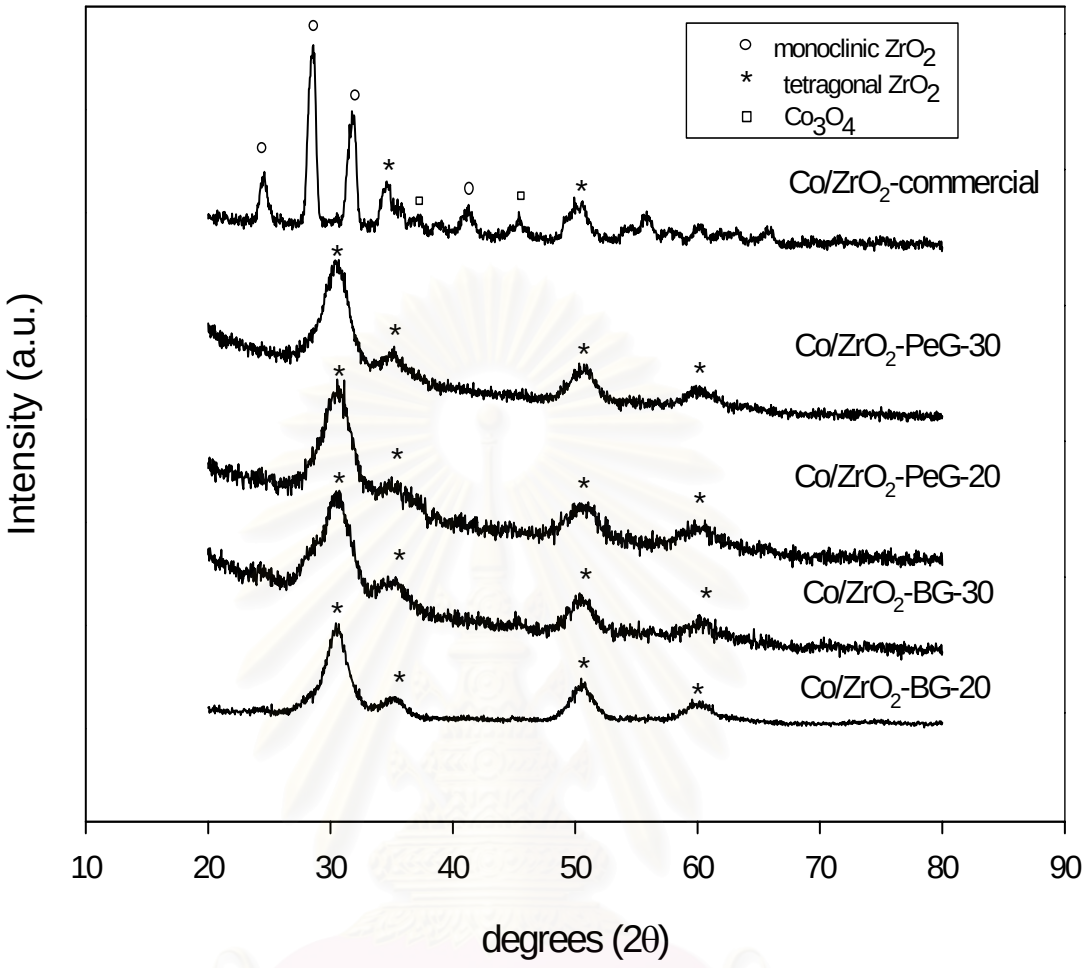

Figure 5.5 XRD patterns of the glycothermal-derived ZrO_2 and the commercial ZrO_2 supported cobalt catalysts.

5.2.1.4 Scanning Electron Microscopy (SEM)

The morphologies of the catalyst samples were determined by SEM technique. The typical morphology of the catalyst granules of various ZrO_2 supported cobalt catalysts are shown in Figure 5.6. It was found that the morphologies of the ZrO_2 after cobalt impregnation were not significant changed.

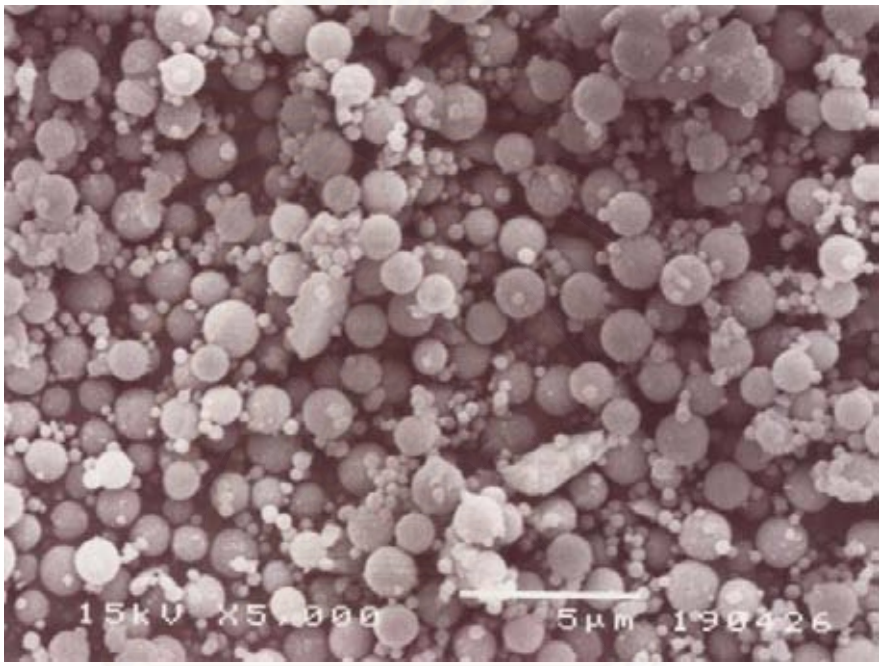

Figure 5.6 (a) SEM micrograph of Co/ZrO_2-BG-20 catalyst granules

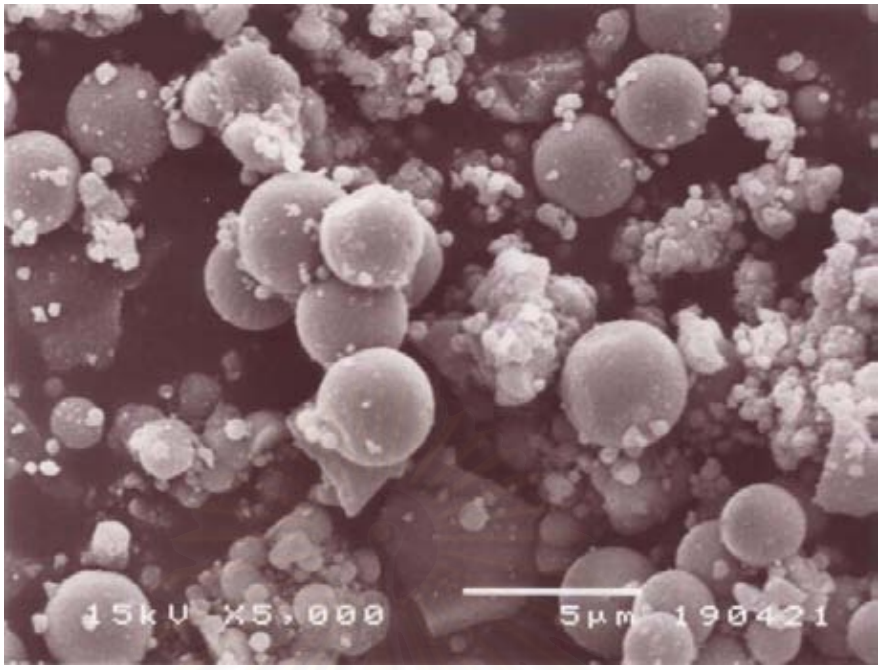

Figure 5.6 (b) SEM micrograph of Co/ZrO_2-BG-30 catalyst granules

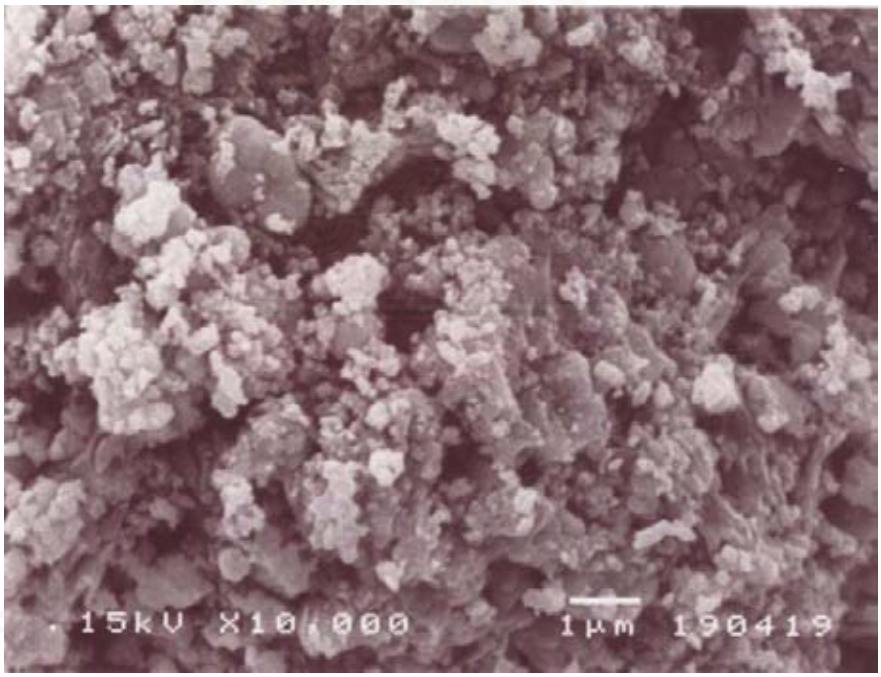

Figure 5.6 (c) SEM micrograph of Co/ZrO_2-PeG-20 catalyst granules

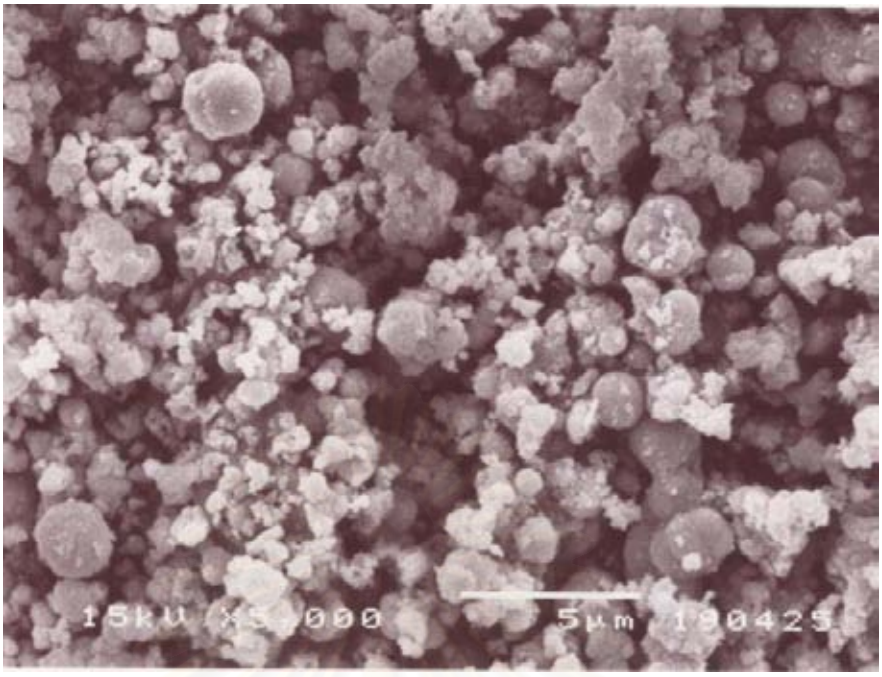

Figure 5.6 (d) SEM micrograph of Co/ZrO_2-PeG-30 catalyst granules

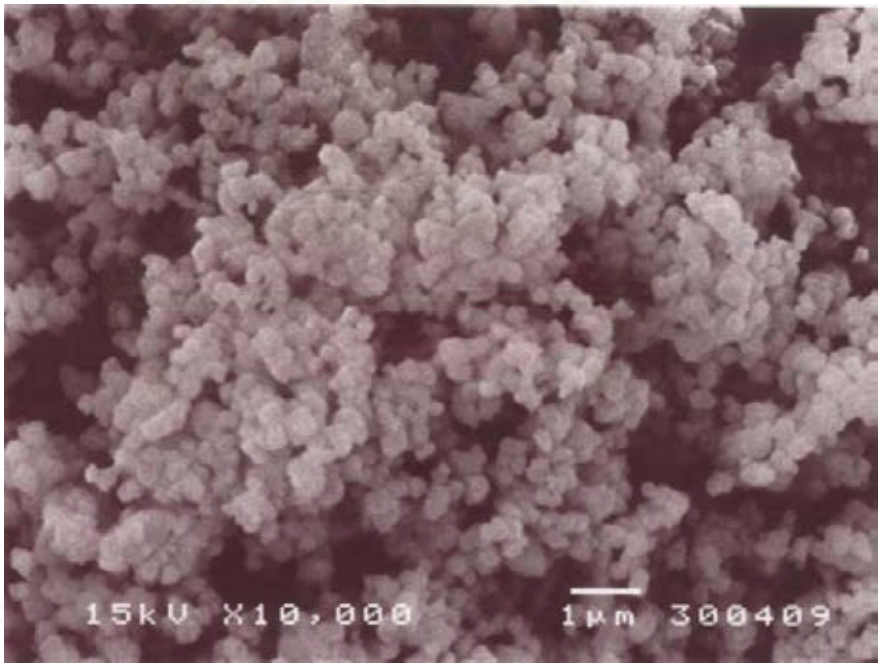

Figure 5.6 (e) SEM micrograph of Co/ZrO_2-Commercial catalyst granules

5.2.1.5 Transmission Electron Microscopy (TEM)

TEM micrographs were taken for all the catalysts in order to physically measure the size of cobalt oxide particles and/or cobalt clusters. The TEM micrographs of various ZrO_2 supported cobalt catalysts are shown in Figure 5.7. The average cobalt particle/cluster sizes from TEM are given in Table 5.6. It was found that the average cobalt particle/cluster sizes of Co/ZrO_2-BG catalysts (5-6 nm) were smaller than that of Co/ZrO_2-PeG catalysts (12-13 nm) and Co/ZrO_2-commercial (16.2 nm).

Figure 5.7 (a) TEM micrograph of Co/ZrO_2-BG-20

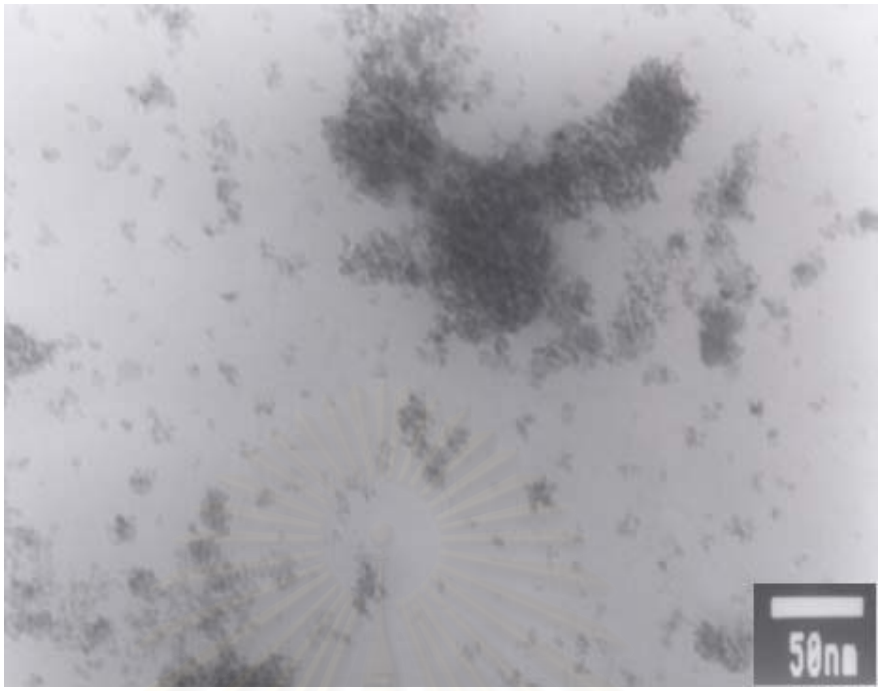

Figure 5.7 (b) TEM micrograph of Co/ZrO_2-BG-30

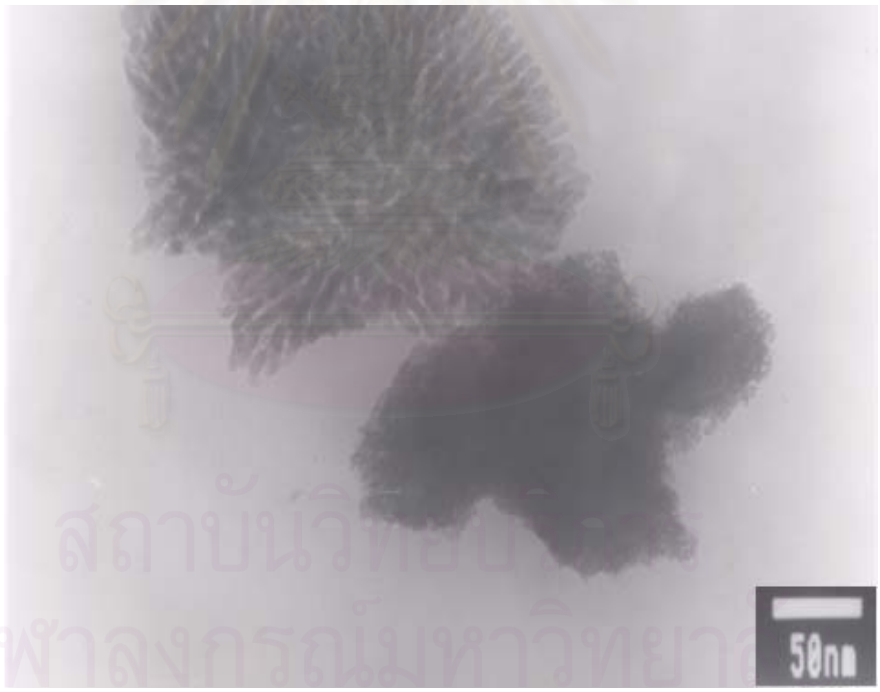

Figure 5.7 (c) TEM micrograph of Co/ZrO_2-PeG-20

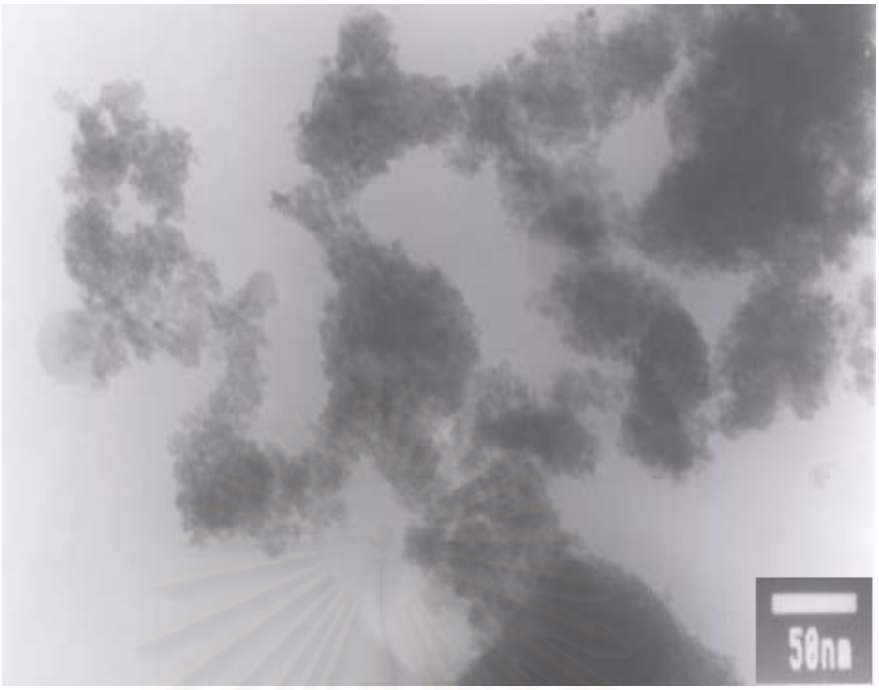

Figure 5.7 (d) TEM micrograph of Co/ZrO_2-PeG-30

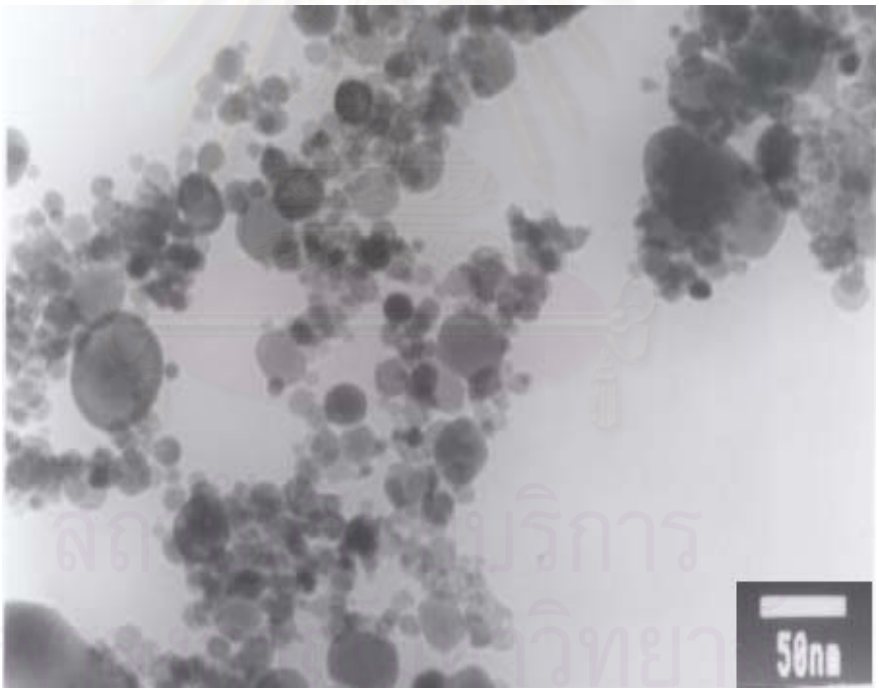

Figure 5.7 (e) TEM micrograph of Co/Commercial

Table 5.6 The Average Diameters of Cobalt Metal Sizes from TEM

Catalysts	dp Co_3O_4 (nm)
Co/ZrO_2-BG-20	5.7
Co/ZrO_2-BG-30	6.1
Co/ZrO_2-PeG-20	12.5
Co/ZrO_2-PeG-30	13.1
Co/ZrO_2-commercial	16.2

5.2.1.6 Hydrogen Chemisorption

The relative amounts of active cobalt metals on the catalyst samples were calculated from H_2 chemisorption experiments at 100^{o}C according to Bartholomew *et al.* (Bartholomew *et al.*, 1984). It is known that only surface Co metal atoms are active for CO hydrogenation not its oxide or carbide (Anderson, 1984). Hydrogen chemisorption technique provides the information on the number of cobalt active sites, % Co dispersion and mean diameter size of cobalt metal. The results are shown in Table 5.7. It was found that Co/ZrO_2-BG-20 exhibited the highest amount of H_2 chemisorption and CO hydrogenation activity. It should be noted that differences in the amount of H_2 chemisorption and the catalytic activities among the catalysts in this study were not due to difference in the BET surfaces areas or the crystallite sizes of zirconia because within experimental error the BET surface areas of all the catalysts and the crystal sizes of zirconia were quite similar. The crystallization mechanism of ZrO_2 in the two glycols probably yielded the final zirconia particles with different amount of crystal defects. Since crystal defects were frequently created especially when crystal growth proceeded rapidly, zirconia prepared in 1,4-BG which was found to form via solid-state reaction would contain more crystal defects compared to the ones prepared in 1,5-PeG which crystallized via precipitation of alkoxide solution. These defects in the zirconia particles may play a role in cobalt-support interaction during preparation of supported cobalt catalysts since the more defects in zirconia, the higher amount of H_2 chemisorption and CO hydrogenation activities were obtained.

The cobalt metal size and % cobalt dispersion were found to be in accordance with the results form XRD and SEM that high cobalt dispersion and small crystallite size of were obtained on the glycothermal-derived ZrO_2.

Table 5.7 Results from H_2 Chemisorption

Catalysts	Amount H_2 x10^{19} (atom/g Co)[a]	% Co dispersion[b]	dp Co^o (nm)[c]
Co/Zr-BG-20	15.3	49.7	1.9
Co/Zr-BG-30	8.0	22.3	4.3
Co/Zr-PeG-20	8.1	30.9	3.1
Co/Zr-PeG-30	7.1	30.2	3.1
Co/Zr-commercial	3.1	17.0	5.6

[a] Error of measurement = +/- 5%.

[b] Base on total number of Co atoms in the sample x fraction reduced

[c] dp Co^0 = 96 / (%D) (Moradi *et al*., 2003)

5.2.1.7 Temperature Programed Reduction (TPR)

Temperature programmed reduction is a powerful tool to study reduction behavior of a metal oxide. %Reducibility of a catalyst can be calculated from the area under the TPR peak. The percentage of reducibility of a catalyst is important since it directly relates to the amount of active Co^0 available for catalyzing hydrogenation reaction. Figure 5.8 shows the temperature program reduction (TPR) profiles of various zirconia supported cobalt catalysts. Reduction of cobalt in the oxide form, Co_3O_4 or Co_2O_3, to Co^0 involves a two-step reduction: first reduction of Co_3O_4 to CoO and then the subsequent reduction of CoO to Co^0 (Schanke *et al*., 1995, Zhang *et al*., 1999). The two reduction steps may not always be observed as separate peaks in TPR profile, as seen in Figure 5.8 for the reduction of bulk Co_3O_4 powder (Lapidus *et al*., 1999). However, a separation of the two reduction steps has often been found for supported cobalt catalysts due to interactions between cobalt and support materials (Panpranot *et al*., 2002, Hilmen *et al*., 1996). A wide range of variables such as metal particle size and metal-support interaction have an influence on the reduction behavior of cobalt catalysts resulting in the observation of different locations of the TPR peaks. Since the catalysts were pre-calcined at 300^{o}C, the nitrate precursor has been completely thermally decomposed below 300^{o}C (Lapidus *et al*., 1991). Therefore, the hydrogen consumption observed during TPR study cannot be ascribed to residual nitrates. As shown by higher reduction peaks in the TPR profiles, cobalt species on zirconia prepared in 1,5-PeG and commercial zirconia were more difficult to reduce than cobalt species on zirconia prepared in 1,4-BG indicating a stronger metal-support interaction. The dotted line in the graph represents the standard reduction temperature used to reduce the catalysts prior to reaction (350^{o}C), it was found that on the zirconia prepared in 1,5-PeG and commercial zirconia, a portion of cobalt oxide species could not be reduced at this temperature hence lower amount of active cobalt metals were available for H_2 chemisorption.

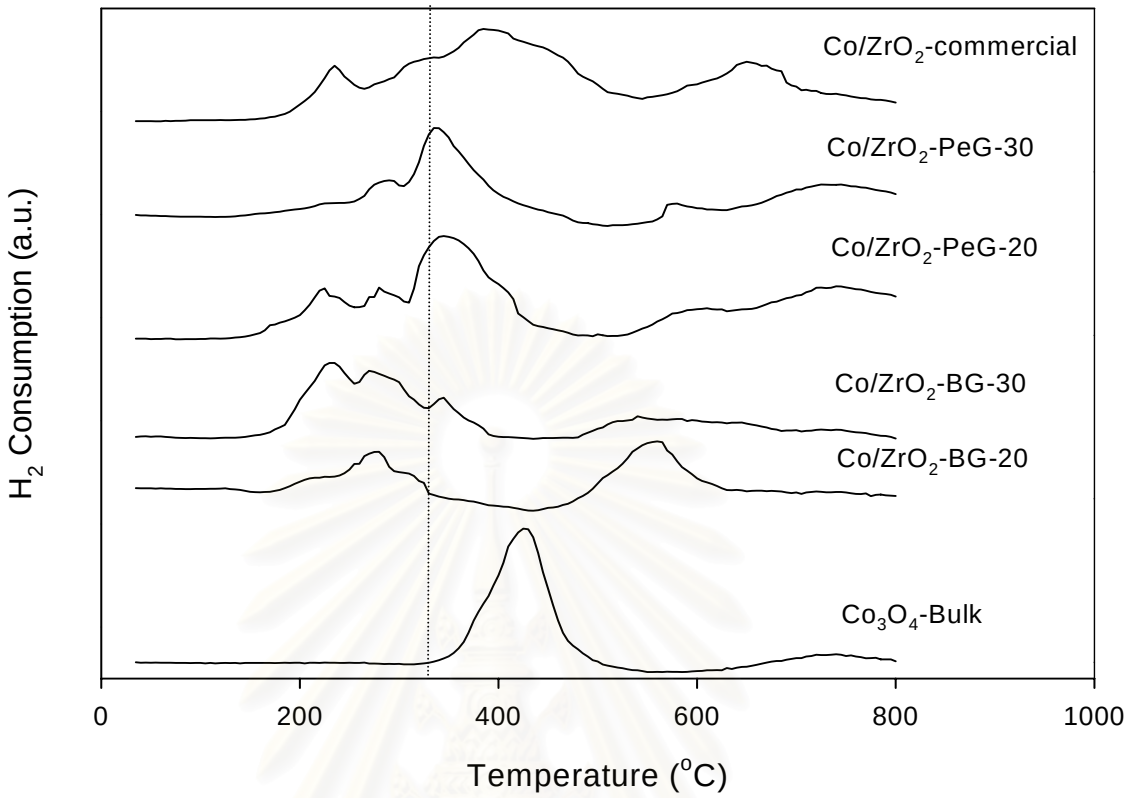

Figure 5.8 TPR profiles of cobalt supported on different ZrO_2 catalysts

Table 5.8 Results from TPR

Catalysts	% Reducibility during TPR[a] (30 - 350 ^{o}C)
Co/ZrO_2-BG-20	35.9
Co/ZrO_2-BG-30	41.1
Co/ZrO_2-PeG-20	35.5
Co/ZrO_2-PeG-30	27.9
Co/ZrO_2-commercial	22.3

[a] From TPR experiments. Correlates to percentage of metal reduce during standard reduction procedure (ramp 1 ^{o}C/min to 350 ^{o}C).

5.2.2 CO Hydrogenation Activity over Co/ZrO_2 Catalysts

Normally, after calcination at 300°C for 2 h. Cobalt is in the form of cobalt oxide phase (Co_3O_4 or Co_2O_3). Cobalt oxide has to be reduced to cobalt metal (Co^0) prior to reaction since cobalt metal is known to be the most active phase for CO hydrogenation, not its oxides. Before reaction, the catalyst was reduced in-situ in H_2 flow 50 cc/min at 350°C for 3 h in order to obtain metallic phase cobalt.

The CO hydrogenation reactions were carried out at 220°C, 1 atm, and H_2/CO ratio = 10 for all the catalyst samples. A relatively high H_2/CO ratio was used in order to minimize catalyst deactivation due to carbon deposition during reaction. Table 5.9 presents CO hydrogenation rates, selectivities, and TOF of these catalysts. It was found that at the reaction conditions used, Co/ZrO_2-BG-20 exhibited a much higher CO hydrogenation rate than all other catalysts in this study.

Table 5.9 Results CO Hydrogenation Reaction at Methanation Conditions[a].

Catalysts	CO hydrogenation rate ($gCH_2/gCo.h$)		Selectivity			TOF (s^{-1})
	Initial	Steady-state	C_1	C_2-C_3	C_4+	
Co/BG-20	14.5	1.6	29.5	11.4	59.1	1.1
Co/BG-30	12.0	1.7	53.6	11.7	34.8	1.7
Co/PeG-20	7.7	4.1	70.7	4.2	25.1	1.1
Co/PeG-30	6.4	3.3	73.4	7.5	19.1	1.1
Co/Commercial	1.7	1.4	57.8	27.8	14.4	0.7

[a] Reaction condition were 220 °C, 1 atm, and H_2/CO=10 (H_2/CO/Ar = 40/4/16 cc/min).

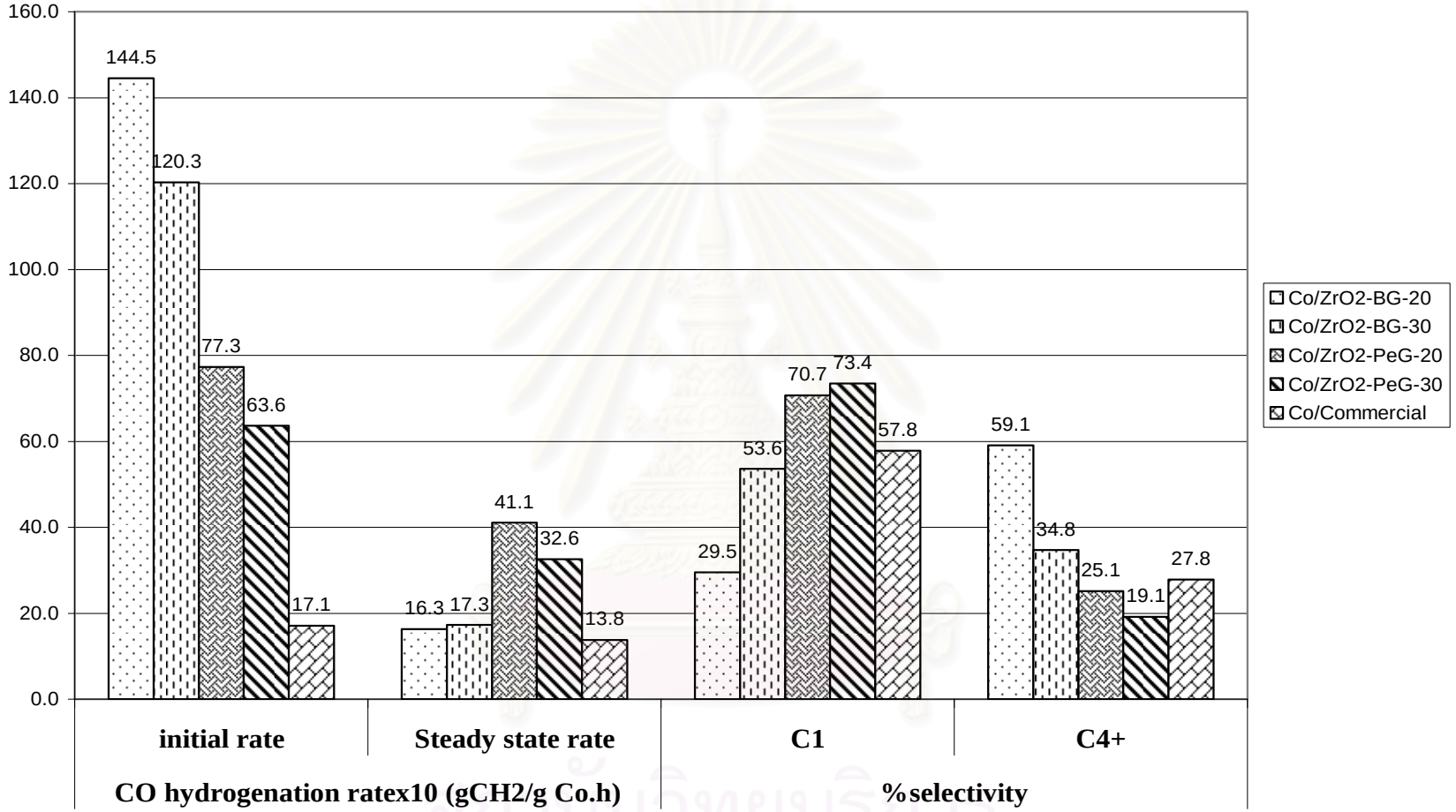

Figure 5.9 (a) Results of CO hydrogenation reaction for Co supported on ZrO_2.

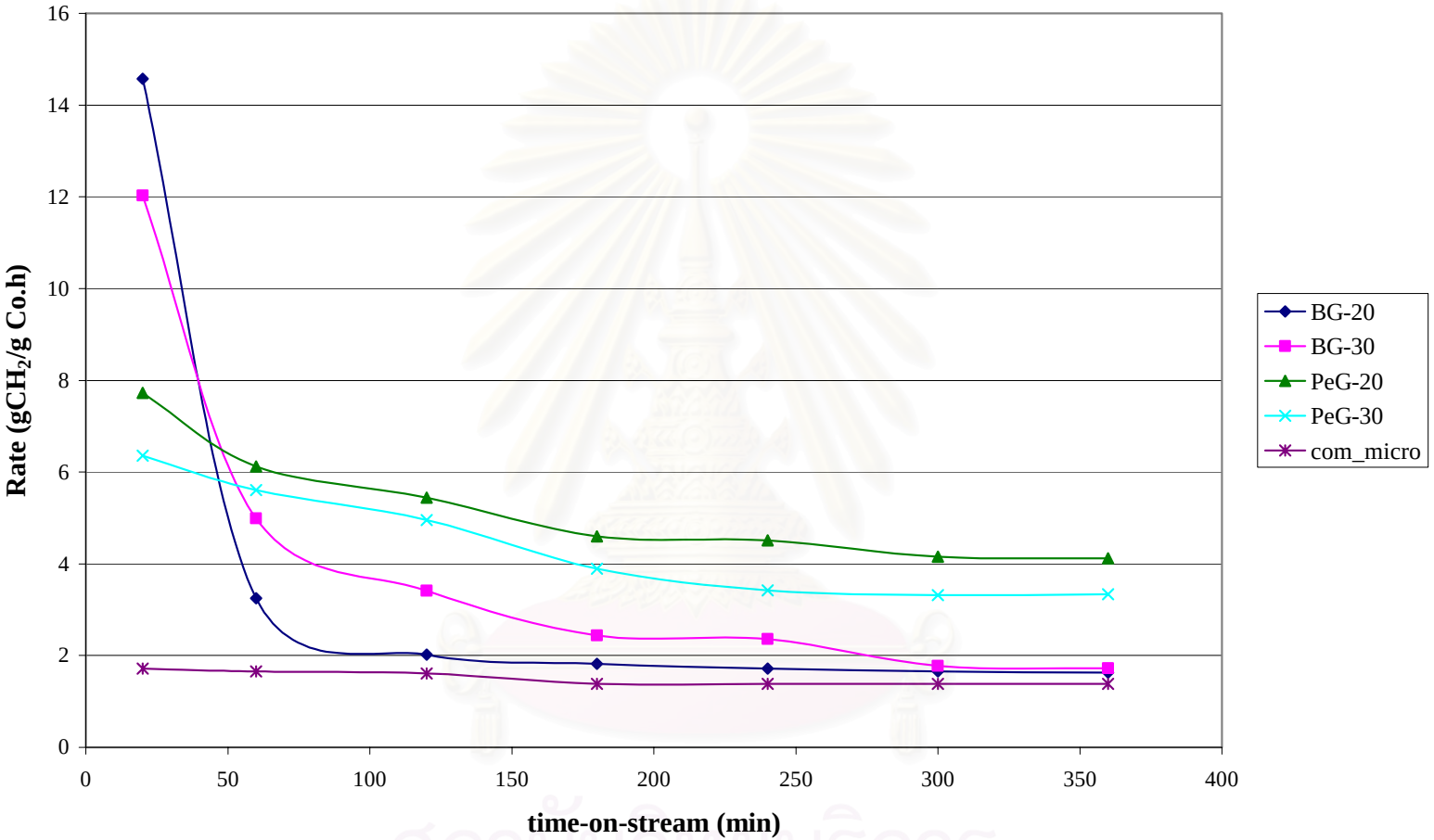

Figure 5.9 (b) CO hydrogenation rates vs time-on-stream.

5.2.3 Catalysts Characterization after CO Hydrogenation

After CO hydrogenation reaction, the characteristics of the catalysts were investigated in order to observe the catalyst deactivation. During CO hydrogenation, deactivation of supported cobalt catalysts is typically due to (1) blocking of pore and active surface by metal sintering and/or support collapse and/or condensation of hydrocarbon products (coking), and (2) oxidation of cobalt

Strong literature support exists in favor of cobalt catalyst oxidation during Fischer-Tropsch synthesis. Iglessia (Iglessia *et al*., 1992) concluded that rapid catalyst deactivation, as a result of cobalt oxidation, is to be anticipated in the case of supported cobalt catalysts with high cobalt dispersion (>15%).

In the present study, we focused only the deactivation by pore blocking due to metal sintering and/or support collapse and cobalt support compound formation because under the reaction conditions used, a relatively high H_2/CO ratio produce minimal carbon deposits and only high purity grade reaction gases were used, therefore, no sulphur was presented.

5.2.3.1 X-ray Diffraction (XRD)

The XRD results of Co/ZrO_2 after reduction and reaction without re-calcination treatment state are displayed in Figure 5.10 and 5.11, respectively. It was found that the XRD patterns of cobalt supported on zirconia prepare in 1,4-BG were not significant changed while the cobalt supported on zirconia prepare in 1,5-PeG exhibited diffraction peaks at 36.8° 2θ, the major peak of Co_3O_4 spinal. After reduction and reaction, the spent Co/ZrO_2-PeG catalysts exhibited diffraction peaks at 2θ of ca. 44.5° indicating the formation of Co metal. For the Co/ZrO_2-commercial catalyst ZrO_2 was partly transformed to a tetragonal phase after CO hydrogenation reduction.

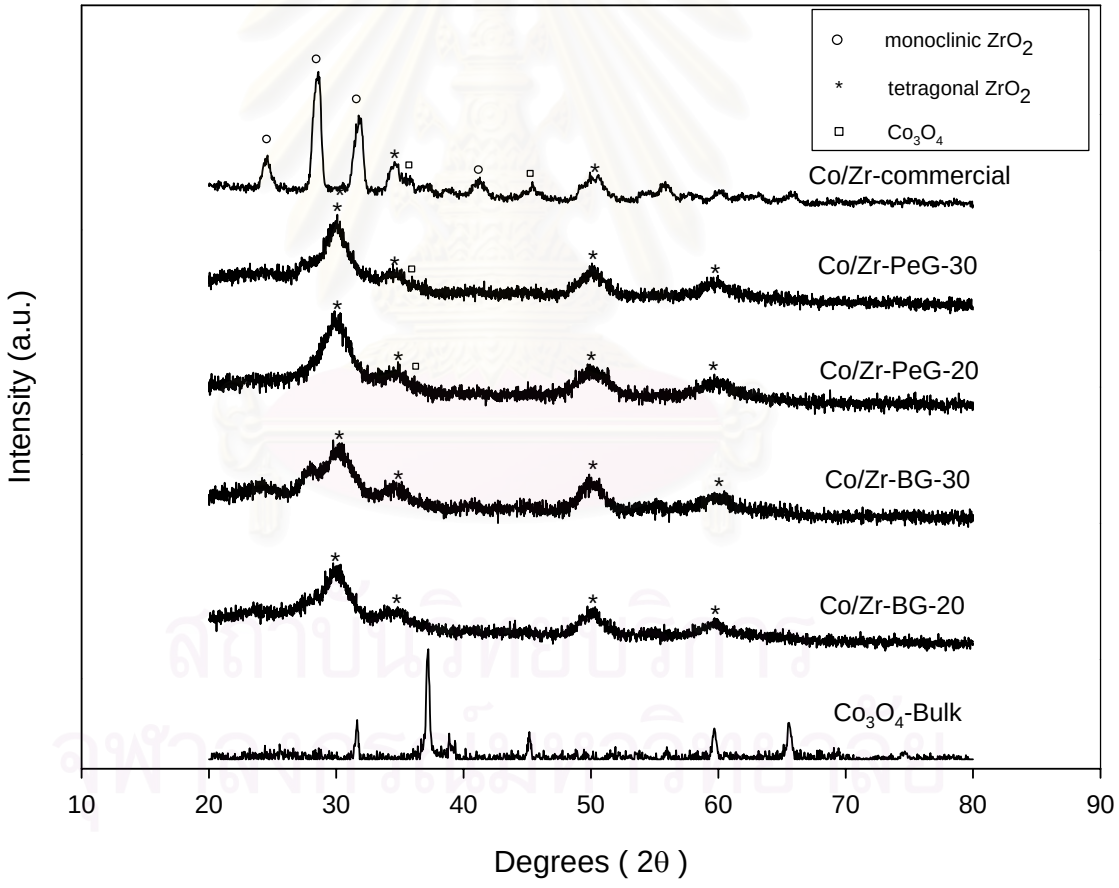

Figure 5.10 XRD patterns of ZrO_2 supported Co catalysts after reduction.

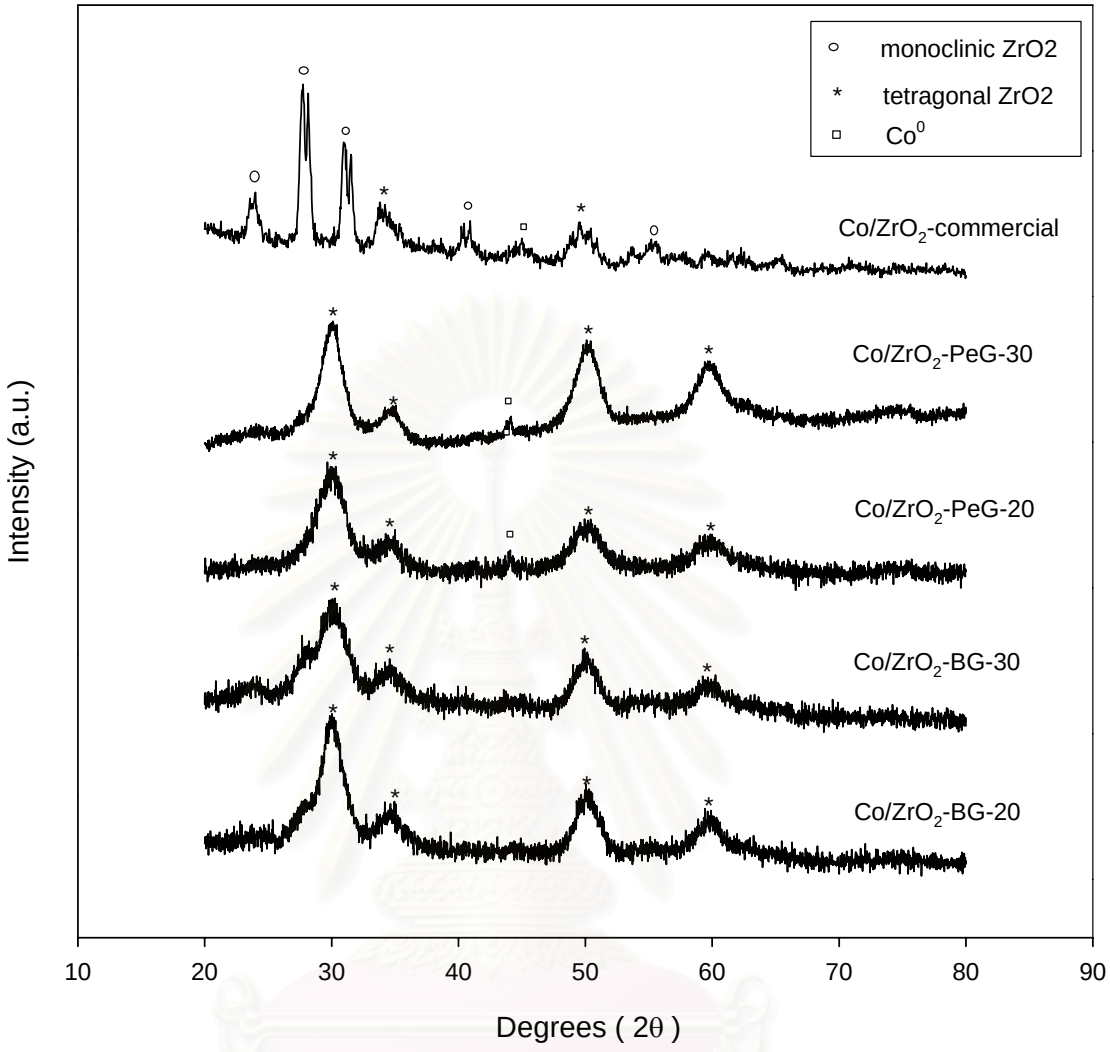

Figure 5.11 XRD patterns of spent ZrO_2 supported Co catalysts after reduction and reaction.

5.2.3.2 Scaning Electron Microscopy (SEM)

Typical SEM micrographs for the spent catalysts after CO hydrogenation reaction are shown in Figure 5.12. It was found that the spent Co/ZrO_2-BG catalysts were more dense mass spherical particle than that the fresh catalysts. In contrast the SEM micrographs for the spent catalysts after CO hydrogenation reaction of Co/ZrO_2-PeG and Co/ZrO_2-commercial catalysts were not significant changed.

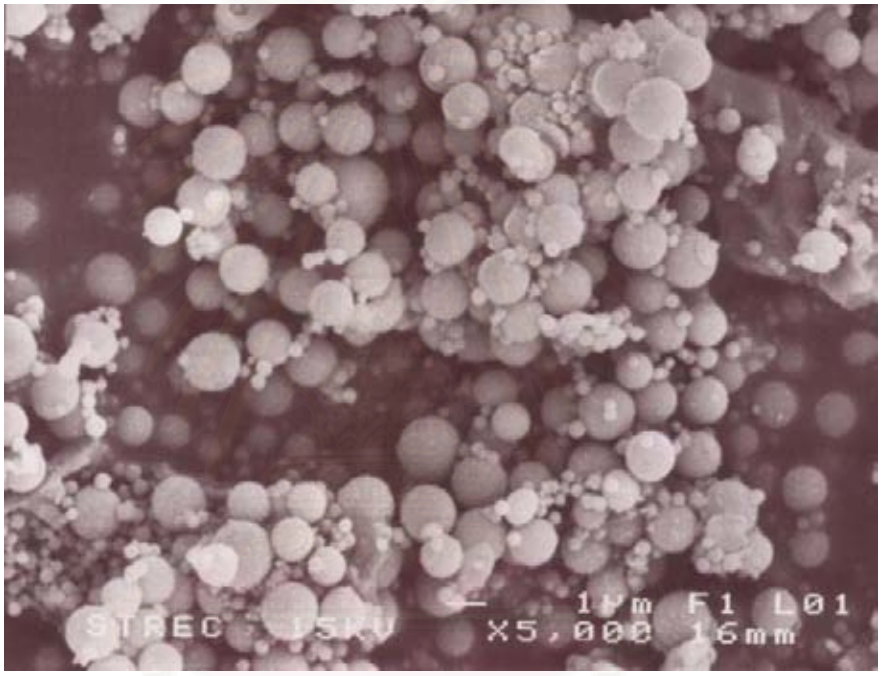

Figure 5.12 (a) SEM micrograph of catalyst granules for Co/ZrO_2-BG-20 (Spent catalyst)

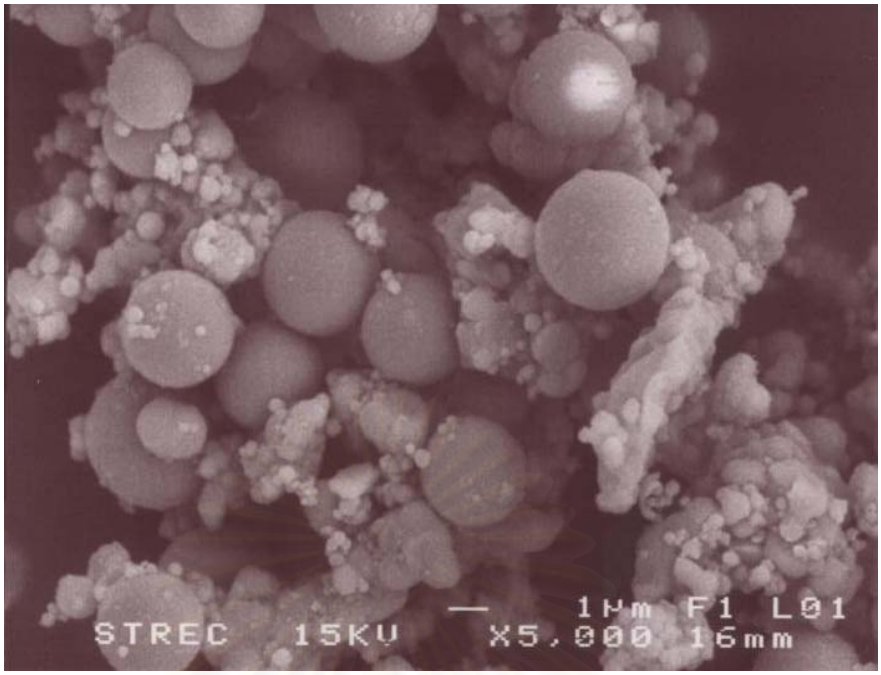

Figure 5.12 (b) SEM micrograph of catalyst granules for Co/ZrO_2-BG-30 (Spent catalyst)

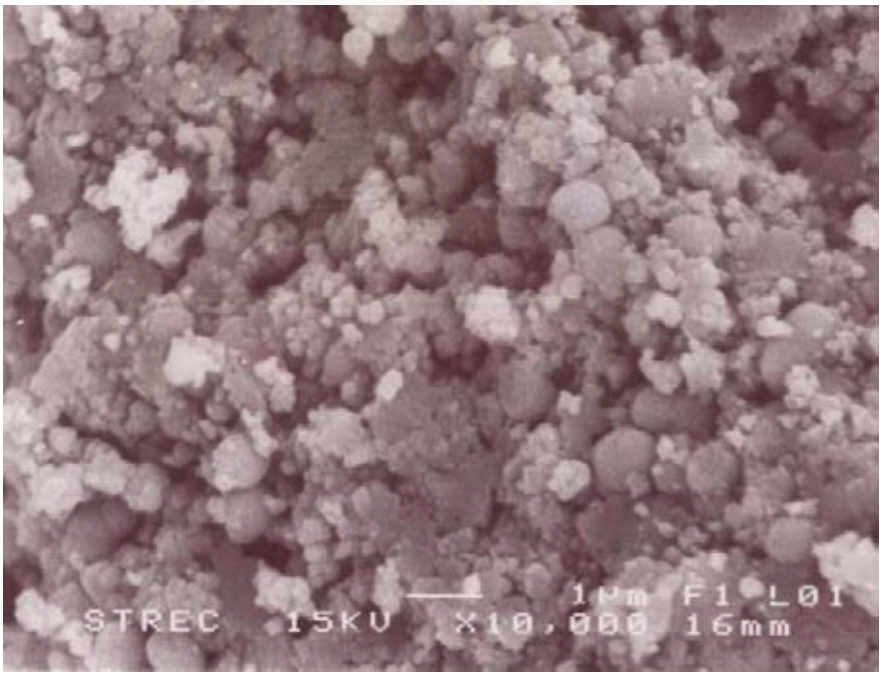

Figure 5.12 (c) SEM micrograph of catalyst granules for Co/ZrO_2-PeG-20 (Spent catalyst)

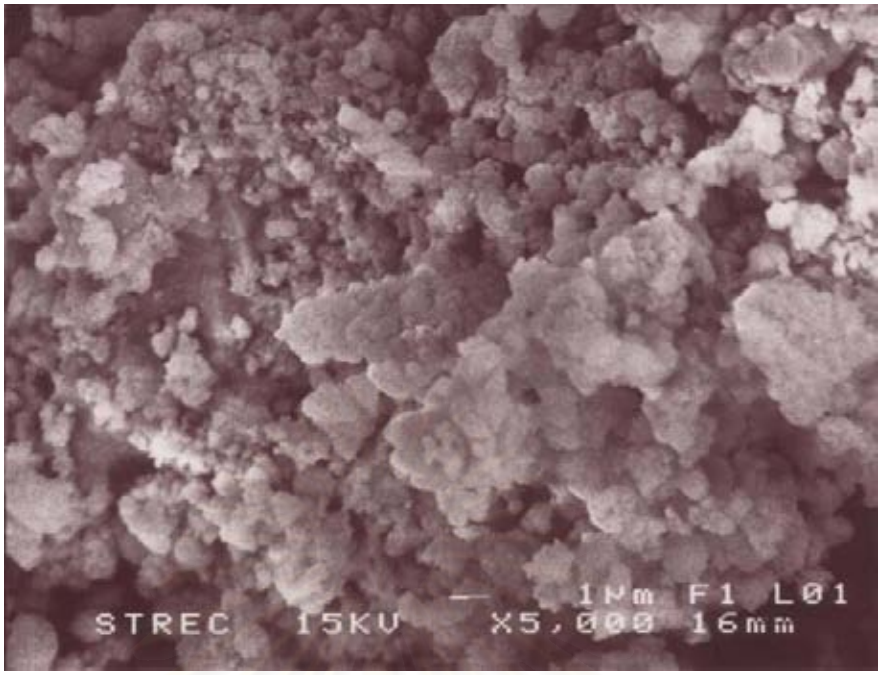

Figure 5.12 (d) SEM micrograph of catalyst granules for Co/ZrO_2-PeG-30 (Spent catalyst)

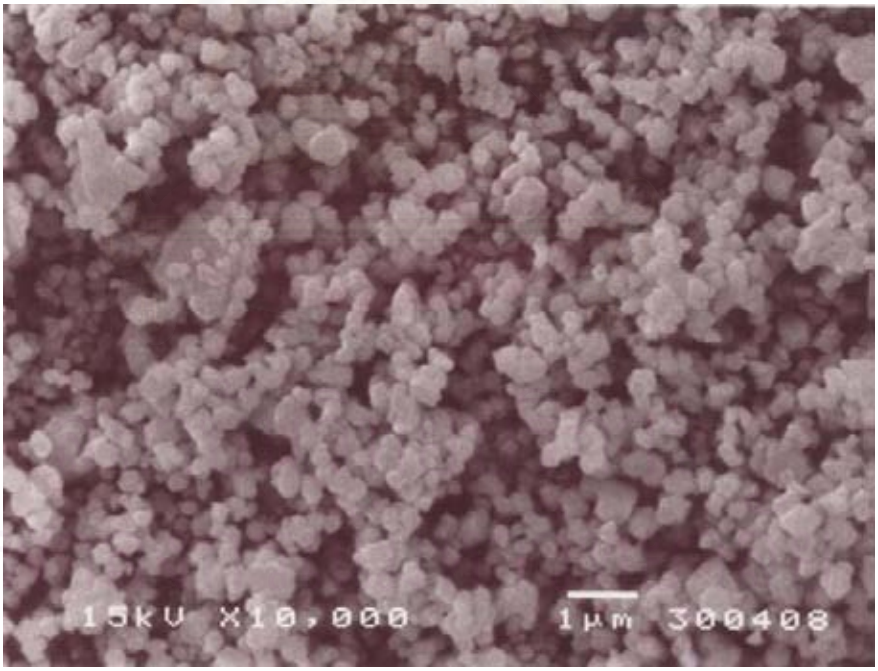

Figure 5.12 (e) SEM micrograph of catalyst granules for Co/ZrO_2-Commercial (Spent catalyst)

5.3 Effect of Si-modified ZrO_2

The effect of silica-modified ZrO_2 on the characteristics and catalytic properties of ZrO_2 supported cobalt catalysts was studied by addition of small percentages of silica (Si/Zr ratio of 0.005-0.02) to the ZrO_2 prepared in 1,4-BG and 1,5-PeG. The ZNP solution with concentration of 20.5% ZrO_2 was used for both cases. The catalysts were characterized by various analysis techniques such as SEM, XRD, TEM, FT-IR, H_2 chemisorption, TPR and CO hydrogenation reaction.

5.3.1 SEM Results of the Si-modified ZrO_2

Figure 5.13 shows the scanning electron micrographs of the ZrO_2 prepared with Si/Zr ratio of 0 and 0.02 in 1,4-BG. The ZrO_2 obtained in 1,4-BG composed of spherical particles. However, the products obtained without addition of TEOS had narrow particle size distribution whereas the particle size distribution of the ZrO_2 products containing silica was wide. It is suggested that when TEOS was added to the reaction, the spherical particles formed agglomerates. Figure 5.14 shows the scanning electron micrographs of the ZrO_2 prepared with Si/Zr ratio of 0 and 0.01 in 1,5-PeG. The products obtained in 1,5-PeG were not significant changed after addition of TEOS.

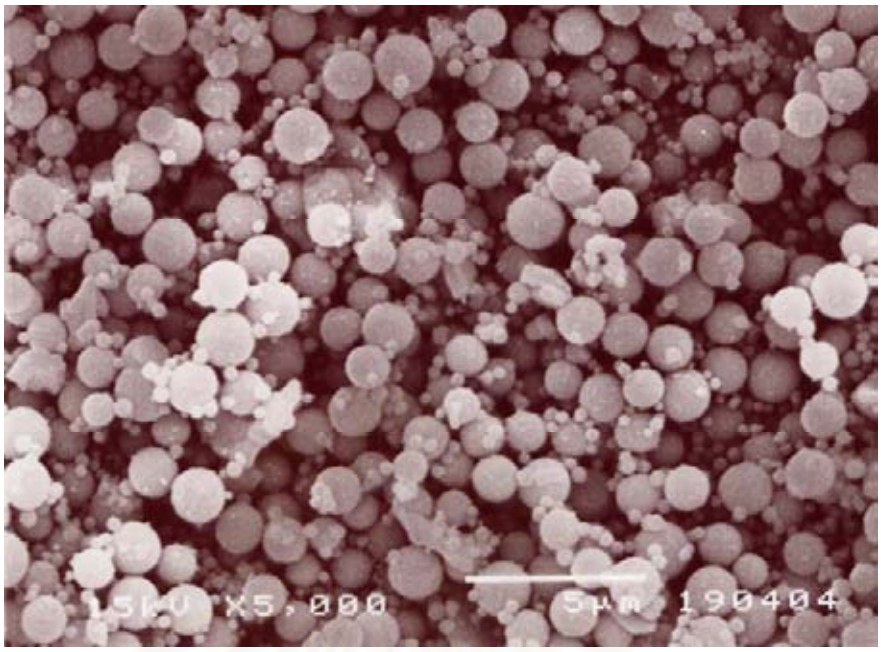

Figure 5.13 (a) SEM micrograph of catalyst granules for ZrO_2-BG-20

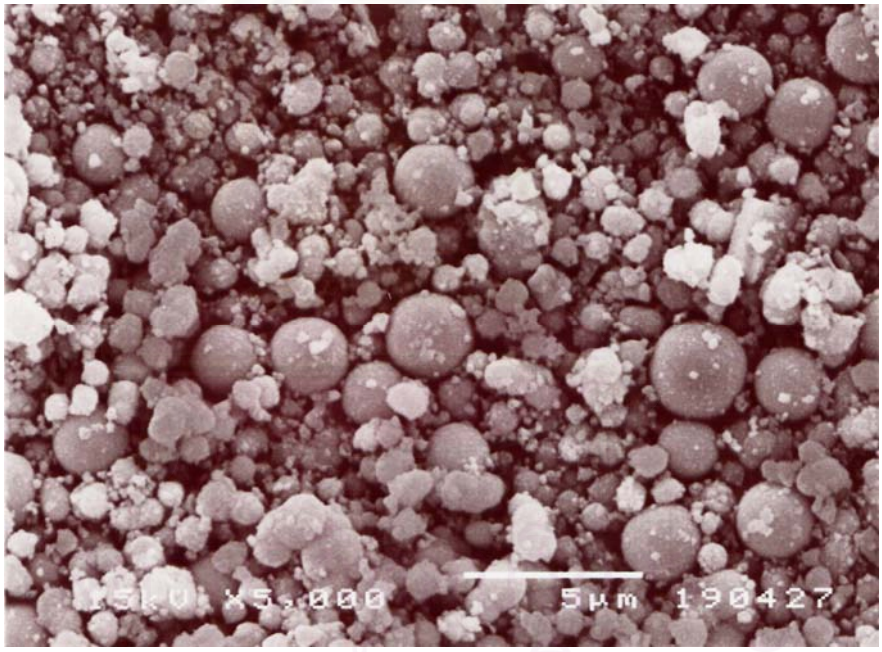

Figure 5.13 (b) SEM micrograph of catalyst granules for ZrO_2-BG-20 (0.02Si)

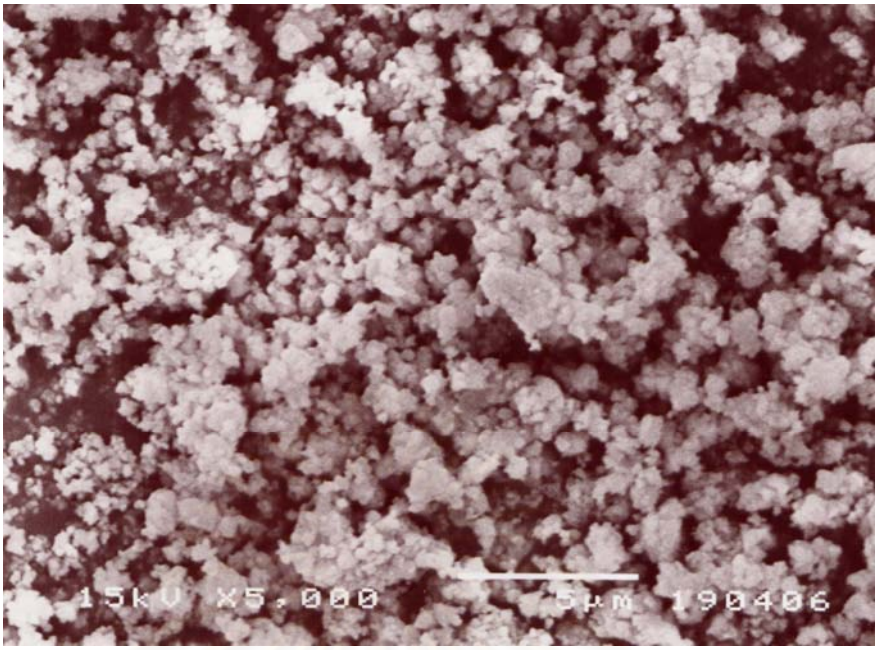

Figure 5.14 (a) SEM micrograph of catalyst granules for ZrO_2-PeG-20

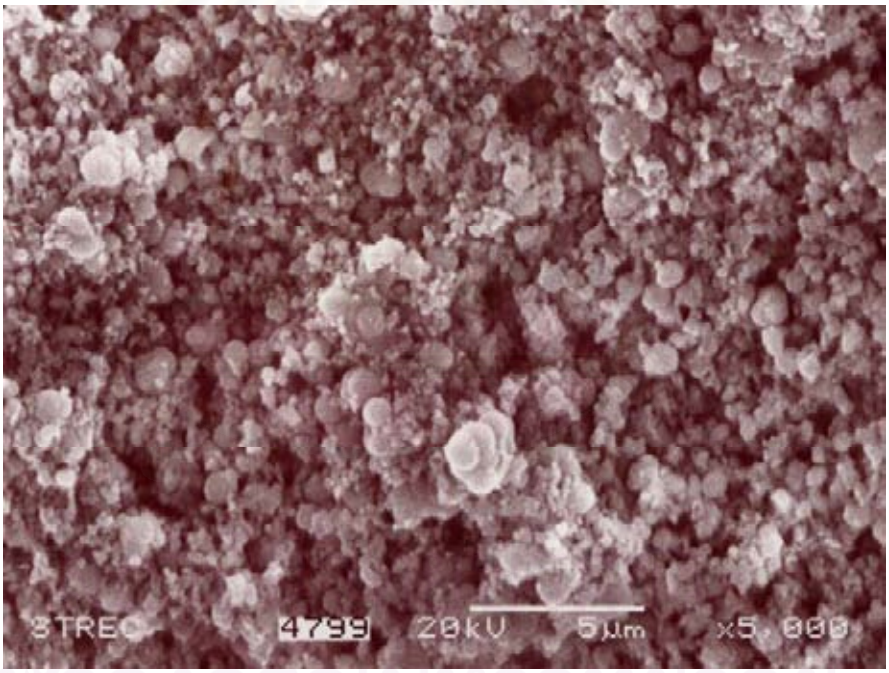

Figure 5.14 (b) SEM micrograph of catalyst granules for ZrO_2-PeG-20 (0.01Si)

5.3.2 XRD Results of the Si-modified ZrO_2

The X-ray diffraction patterns of the different mole fractions of silica modified zirconia prepared in 1,4-BG and 1,5-PeG are shown in Figure 5.15 and Figure 5.16, respectively. It was found that tetragonal zirconia was formed for all the products with the Si/Zr ratio of 0-0.02. Furthermore, the peak intensities were not altered with increasing TEOS content. Thus, the crystallinity of the ZrO_2 prepared by the glycothermal method was not affected by addition of Si. These results are in agreement with the work previously reported by S. Kongwudthiti *et al*., 2002.

The crystallite sizes of all the Si-modified ZrO_2 were in the ranges of 2-3 nm while those of un-modified ones were about 4 nm. The crystallite sizes decreased with increasing Si content. This suggests that the nucleation frequency of ZrO_2 is affected by the TEOS content added to the reaction mixture.

Table 5.10 Phases presented in the Si-modidied ZrO_2 samples and their average crystallite sizes

Catalysts	ZrO_2 Phase	Crystal Size (nm)[a]
ZrO_2-BG-20(0Si)	T	3.9
ZrO_2-BG-20(0.005Si)	T	3.1
ZrO_2-BG-20(0.02Si)	T	2.7
ZrO_2-PeG-20(0Si)	T	3.7
ZrO_2-PeG-20(0.01Si)	T	2.9

[a] Based on XRD line broadening.

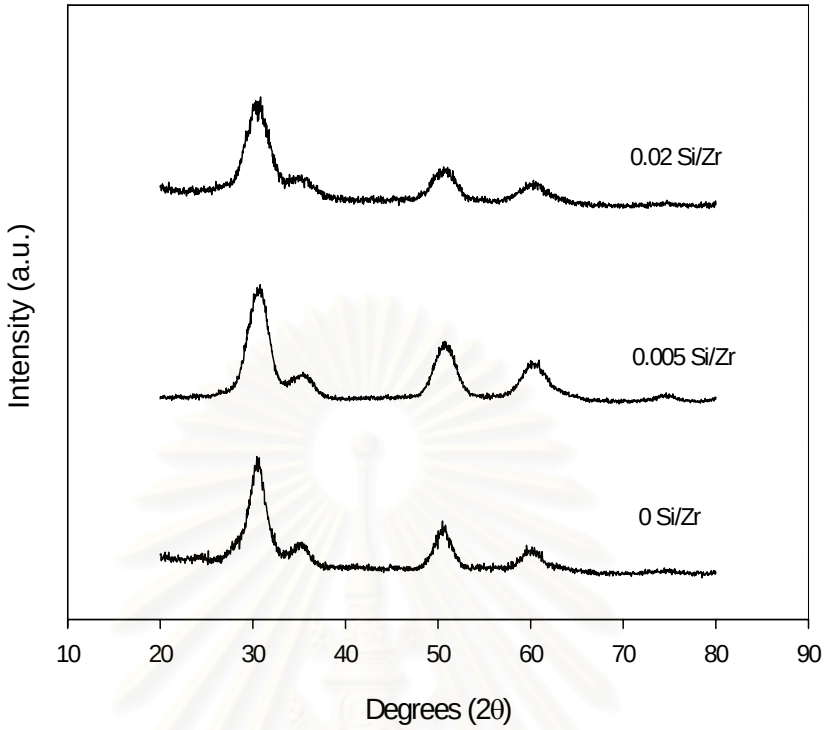

Figure 5.15 XRD patterns of the glycothermal-derived Si modified ZrO_2 in 1,4-BG.

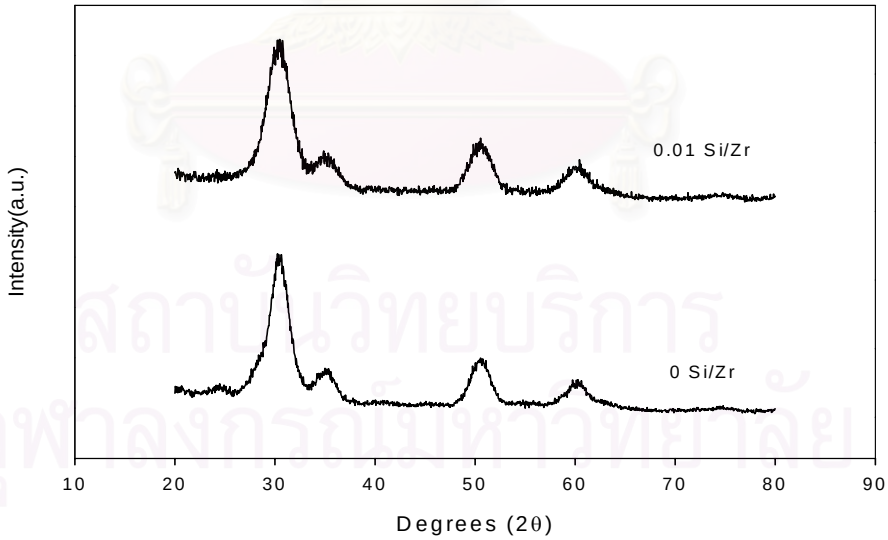

Figure 5.16 XRD patterns of the glycothermal-derived Si modified ZrO_2 in 1,5-PeG.

5.3.3 FT-IR Results of the Si-modified ZrO_2

Figure 5.17 shows the FT-IR spectra of the zirconia prepared in 1,4-BG at the various Si/Zr ratios. The band at 1630 cm^{-1} was attributed to adsorbed water. All the samples exhibit IR bands at around 1560, 1460 and 1420 cm^{-1} which were assigned to the glycol moieties occluded in the sample (S. Kongwudthiti *et al*., 2003).

The bands located around 1047 cm^{-1} are attributed to Si-O-Zr bonds of the samples. The characteristic band for Si-O-Zr bonds shifts to higher frequencies as the silica content increases (S. Kongwudthiti *et al*., 2003). It has been reported that the extent of silica incorporated into the lattice of ZrO_2 depends on the amount of TEOS added to the reaction mixture and the formation of the Si-O-Zr populations occurred in the obtained products.

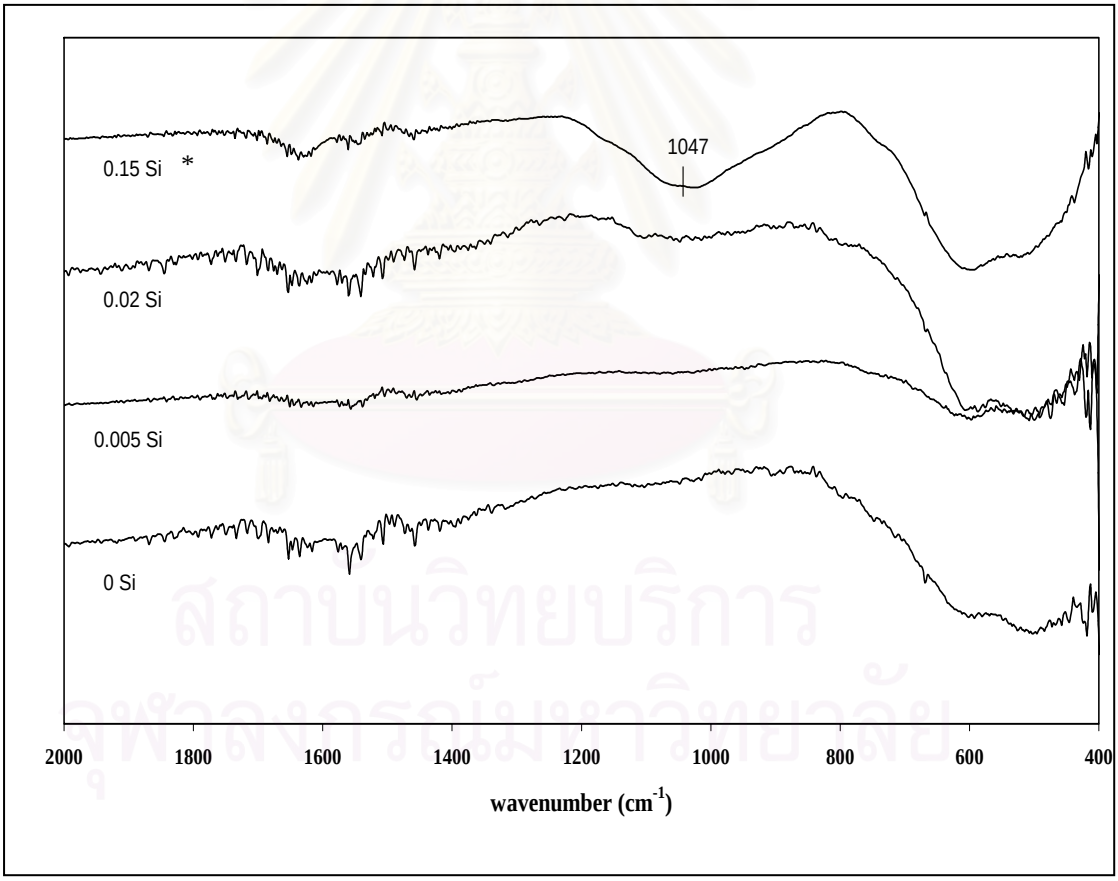

Figure 5.17 IR spectra of the samples at various the Si/Zr ratio.

* From S. Kongwudthiti *et al*., 2003

5.3.4 AAS Results of the Si-modified ZrO_2 Supported Co Catalysts

The amounts of cobalt loading for the Si-modified ZrO_2 supported cobalt catalysts were measured by atomic absorption spectroscopy. The results are given in Table 5.11. Cobalt loadings on the Si-modified ZrO_2 supported Co catalysts decreased slightly from the un-modified ones and were found to decrease with increasing Si content.

Table 5.11 Atomic Absorption Results.

Catalysts	Co (Wt%)
Co/ZrO_2-BG-20(0Si)	8.4
Co/ZrO_2-BG-20(0.005Si)	7.3
Co/ZrO_2-BG-20(0.02Si)	5.1
Co/ZrO_2-PeG-20(0Si)	7.3
Co/ZrO_2-PeG-20(0.01Si)	6.9

5.3.5 XRD Results of the Si-modified ZrO_2 Supported Co Catalysts

The X-ray diffraction patterns of the Si-modified ZrO_2-supported cobalt catalysts are shown in Figure 5.18. It was found that after impregnation cobalt and calcination at 300 ^oC, no XRD peaks for Co_3O_4 were observed for all the Si-modified ZrO_2-supported cobalt catalysts. The results suggested that the crystallite sizes of cobalt oxide formed on the glycothermal-derived Si-modified zirconia were smaller than the detectability limit of XRD.

The crystal sizes and zirconia phase of cobalt supported catalysts are given in Table 5.12. The crystal sizes of ZrO_2 in the Si-modified zirconia-supported cobalt catalysts were found to be 2-3 nm similar to those before Co loading.

Table 5.12 Phases Present in the Samples and the Average Crystallite Size of Co/ZrO_2

Catalysts	ZrO_2 Phase	Crystal size of ZrO_2 [a] (nm)
Co/ZrO_2-BG-20(0.0Si)	T	3.6
Co/ZrO_2-BG-20(0.005Si)	T	3.1
Co/ZrO_2-BG-20(0.02Si)	T	2.8
Co/ZrO_2-PeG-20(0Si)	T	3.2
Co/ZrO_2-PeG-20(0.01Si)	T	3.0

[a] Base on XRD line broadening.

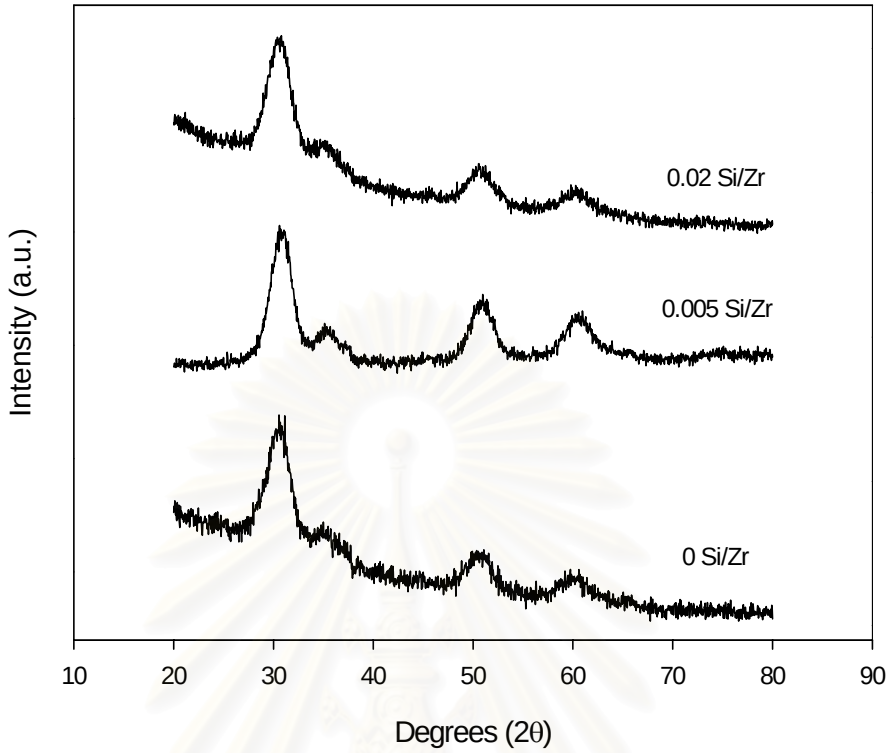

Figure 5.18 (a) XRD patterns of the glycothermal-derived Si-modified ZrO_2 in 1,4-BG supported cobalt catalysts.

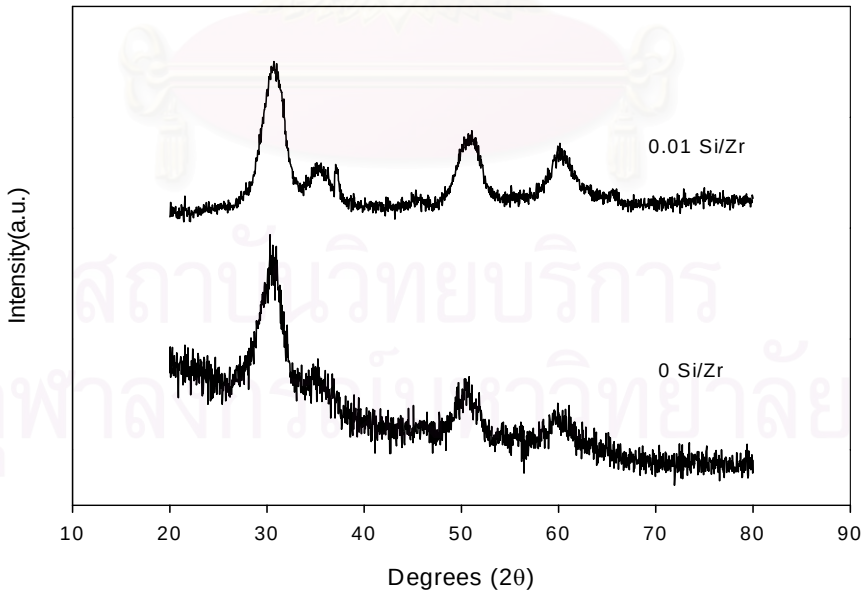

Figure 5.18 (b) XRD patterns of the glycothermal-derived Si-modified ZrO_2 in 1,5-PeG supported cobalt catalysts.

5.3.6 TEM Results of the Si-modified ZrO_2 Supported Co Catalysts

TEM micrographs were taken for all the catalysts in order to physically measure the size of cobalt oxide particles and/or cobalt cluster. Figure 5.19 shows TEM images of the glycothermal-derived Si-modified ZrO_2 prepared in 1,4-BG and 1,5-PeG with the Si/Zr ratio of 0-0.02. The results were found to be in accordance those obtained from XRD that cobalt was supported as very small cobalt clusters with high Co dispersion.

Figure 5.19 (a) TEM micrograph of Co/ZrO_2-BG-20 (0 Si)

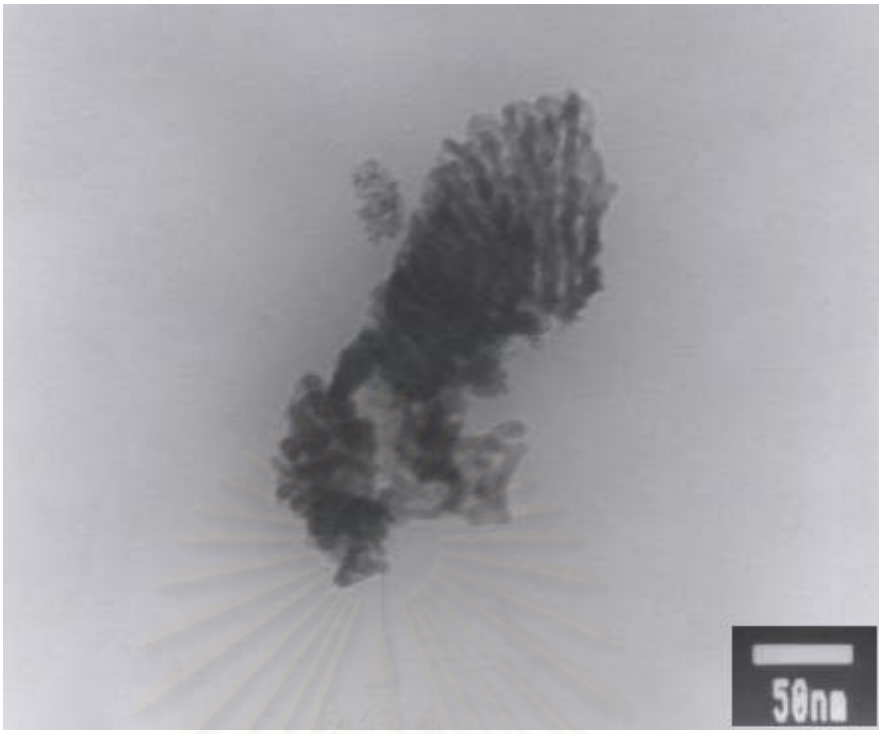

Figure 5.19 (b) TEM micrograph of Co/ZrO_2-BG-20 (0.005Si)

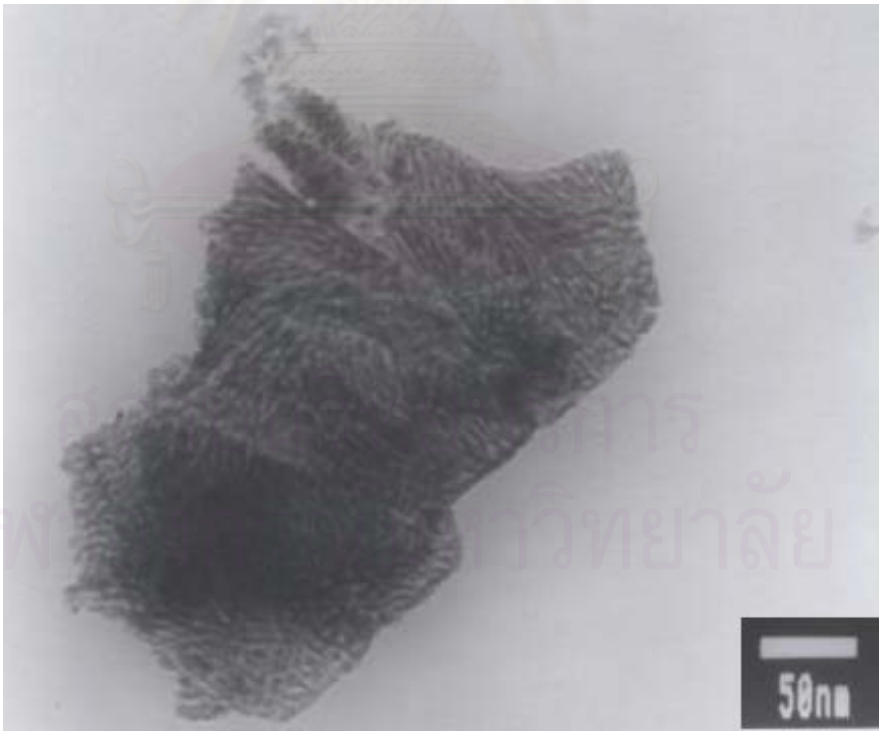

Figure 5.19 (c) TEM micrograph of Co/ZrO_2-BG-20 (0.02Si)

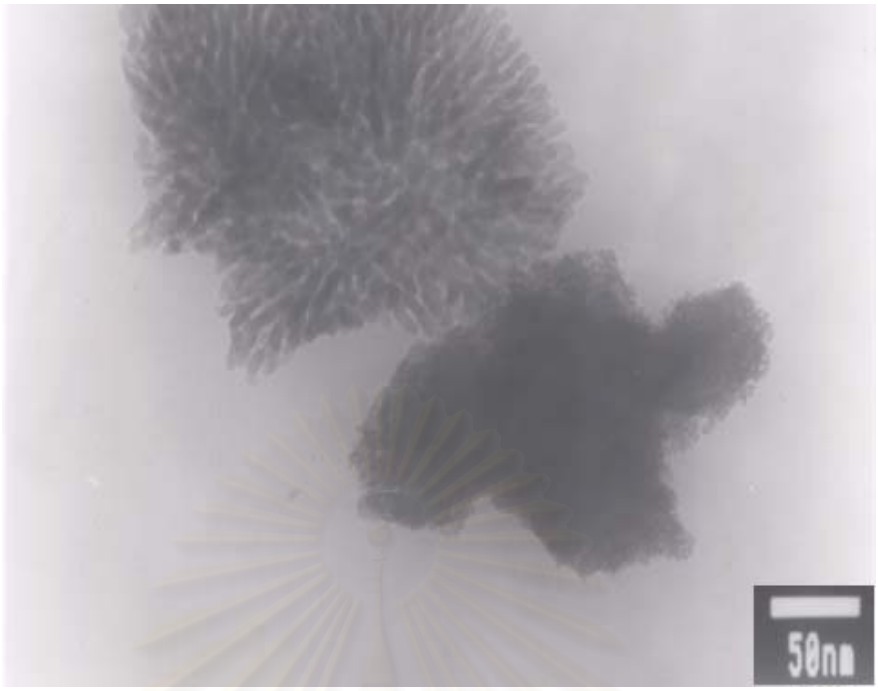

Figure 5.19 (d) TEM micrograph of Co/ZrO_2-PeG-20 (0Si)

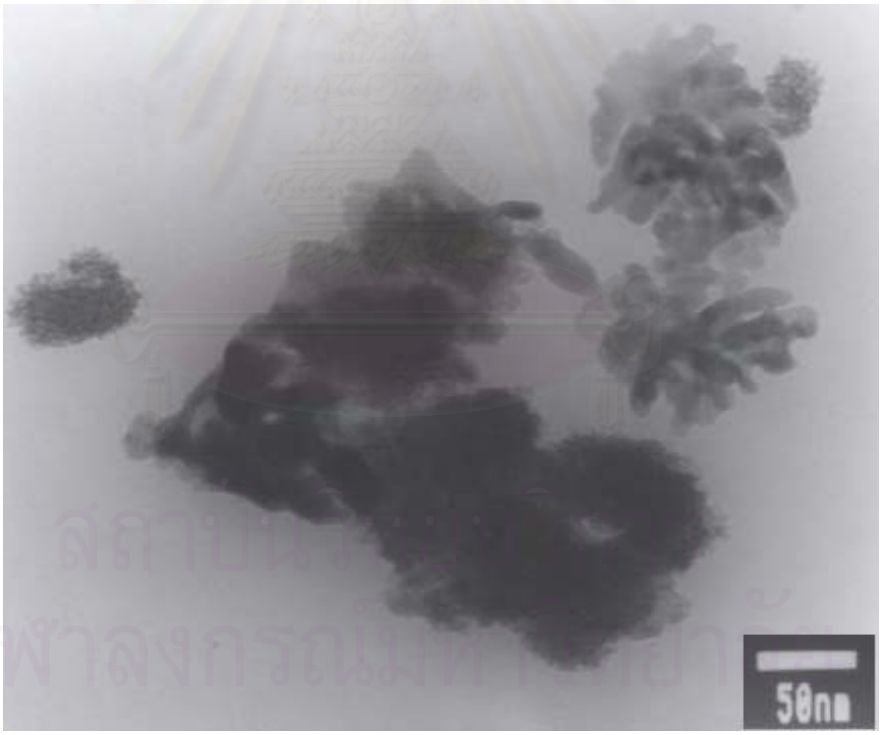

Figure 5.19 (f) TEM micrograph of Co/ZrO_2-PeG-20 (0.01Si)

5.3.7 Hydrogen Chemisorption Result

The total hydrogen uptakes, the percentages of cobalt dispersion and the average cobalt metal size are reported in Table 5.13. Addition of a small amount of Si resulted in lower H_2 chemisorption of the Co catalysts. When Si was added, H_2 chemisorption of Co/ZrO_2-BG-20 decreased by 33.3-26.8 % whereas Co/ZrO_2-PeG-20 decreased by 71.6 %.

The crystallite sizes of cobalt on the Si-modified ZrO_2 were slightly increased from 2-3 nm. to 4.3 nm. Increasing the amount of Si/Zr from 0.05 to 0.02 did not further decrease the H_2 chemisorption ability and %Co dispersion.

Table 5.13 Results from H_2 Chemisorption

Catalysts	Amount H_2 $x10^{19}$ (atom/g Co) [a]	% Co Dispersion [b]	dp Co^o (nm) [c]
Co/ZrO_2-BG-20(0 Si)	15.3	49.7	1.9
Co/ZrO_2-BG-20(0.005Si)	5.1	22.1	4.3
Co/ZrO_2-BG-20(0.02Si)	4.1	22.8	4.2
Co/ZrO_2-PeG-20(0Si)	8.1	30.9	3.1
Co/ZrO_2-PeG-20(0.01Si)	5.8	18.5	4.3

[a] Error of measurement = +/- 5%.

[b] Base on total number of Co atoms in the sample x fraction reduced

[c] dp Co^0 = 96 / (%D) (Moradi *et al*., 2003)

5.3.8 Temperature Programed Reduction (TPR)

TPR profiles of the silica modified zirconia supported cobalt catalysts are shown in Figure 5.20. The TPR spectra was obtained for the calcined catalysts. Which the nitrate precursors have been completely thermally decomposed. For ZrO_2-BG-20, the reduction peaks were shifted to lower temperatures when Si was added to the ZrO_2. However, for ZrO_2-PeG-20 the reduction peaks remained the same.

The reducibilities of the Si-modified ZrO_2 supported Co catalysts during TPR 30-350 ^oC are reported in Table 5.14. The degrees of reduction of the catalysts were calculated based on the areas under the TPR from 30-350 ^oC. Since the standard reduction procedure is at 350 ^oC. The reducibilities during TPR 30-350 ^oC for all catalysts in Table 5.14 were not significantly different, ranging from 31-45 %.

Table 5.14 Results from TPR

Catalysts	% Reducibility during TPR 30 to 350 ^oC
Co/ZrO_2-BG-20(0Si)	35.9
Co/ZrO_2-BG-20(0.005Si)	31.3
Co/ZrO_2-BG-20(0.02Si)	34.6
Co/ZrO_2-PeG-20(0Si)	35.5
Co/ZrO_2-PeG-20(0.01Si)	44.7

[a] From TPR experiments. Correlates to percentage of metal reduce during standard reduction procedure (ramp 1 ^oC/min to 350 ^oC).

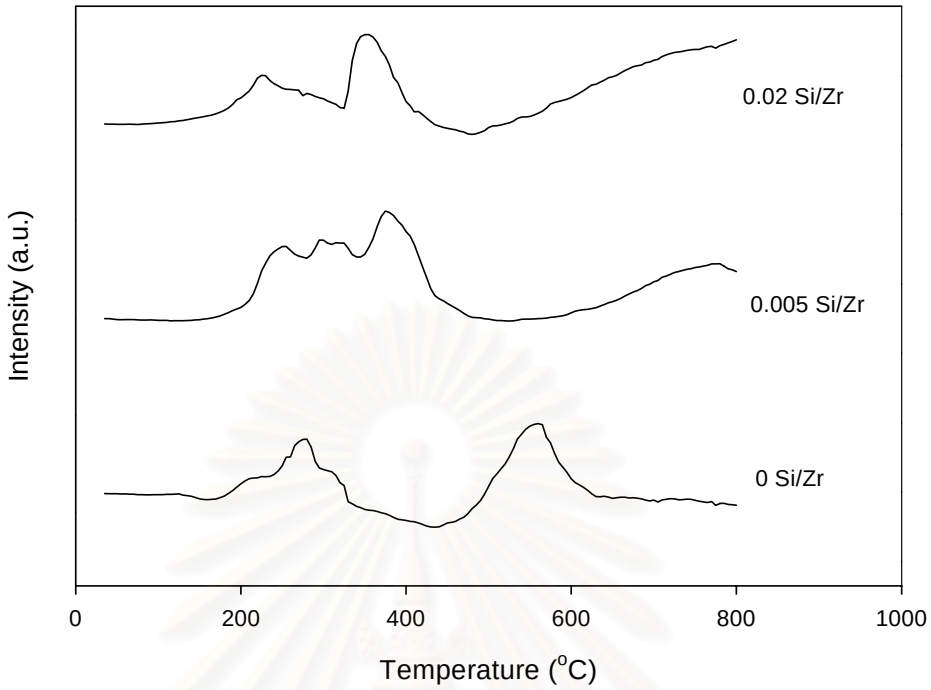

Figure 5.20(a) TPR profiles of cobalt supported on different ZrO_2-BG-20 catalysts

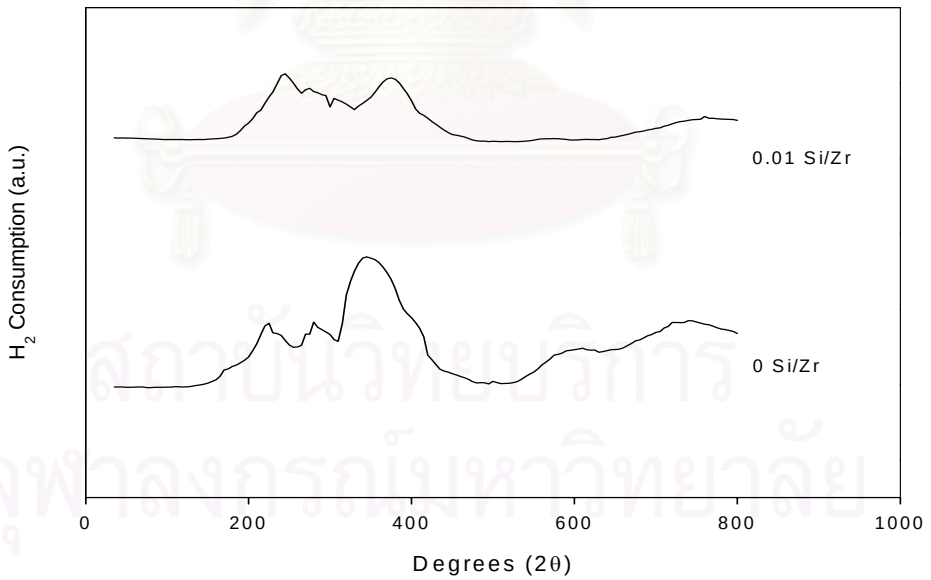

Figure 5.20(b) TPR profiles of cobalt supported on different ZrO_2-PeG-20 catalysts

5.3.9 CO Hydrogenation Activity over Cobalt Catalyst upported on Si-modified ZrO_2

The CO hydrogenation rates, product selectivities and TOFs for silica-modified zirconia supported cabalt catalysts are presented in Table 5.15. It was found that the initial CO hydrogenation rates for the Si-modified ZrO_2-supported catalysts especially the ZrO_2-BG-20, decreased sharply with Si addition. However, the steady state rates of cobalt supported on Si-modified ZrO_2 (BG-20) increased with increasing Si/Zr ratio (0.005-0.02). The results suggest that Si may enhance the stability of cobalt on the ZrO_2-BG-20. Methane selectivity of the catalysts also increased with increasing Si/Zr ratio. On the other hand, there was no significant impact of Si addition to the Co/ZrO_2-PeG-20 catalyst. The turnover frequencies were similar for all the catalysts typical for CO hydrogenation reaction to be structure-insensitive reaction.

Table 5.15 Results of CO Hydrogenation Reaction[a].

Catalysts	CO hydrogenation rate (gCH_2/gCo.h)		Selectivity			TOF
	Initial	Steady- state	C_1	C_2-C_3	C_4+	(s^{-1})
Co/BG-20(0Si)	14.5	1.6	29.5	11.4	59.1	1.1
Co/BG-20(0.005Si)	3.6	2.1	47.5	6.6	45.9	0.8
Co/BG-20(0.02Si)	4.0	3.0	59.4	3.5	37.1	1.1
Co/PeG-20(0Si)	7.7	4.1	73.4	7.5	19.1	1.1
Co/PeG-20(0.01Si)	6.8	4.0	82.2	5.4	12.3	1.3

[a] Reaction conditions were 220 ^oC, 1 atm, and H_2/CO = 10 (H_2/CO/Ar = 40/4/16 cc/min).

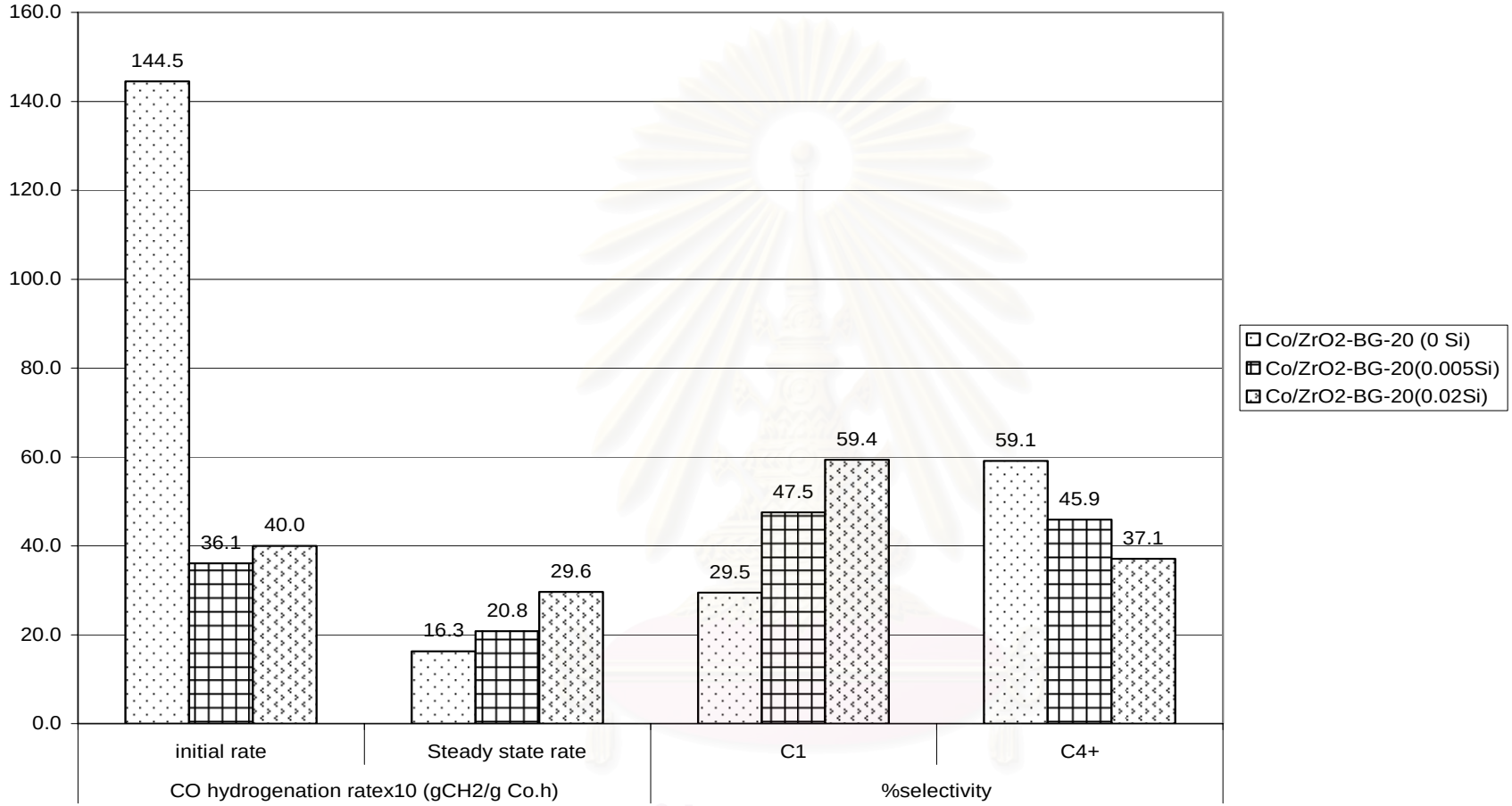

Figure 5.21 (a) Results of CO hydrogenation reaction for Co/ ZrO_2-BG-20 catalysts with various Si/Zr ratios.

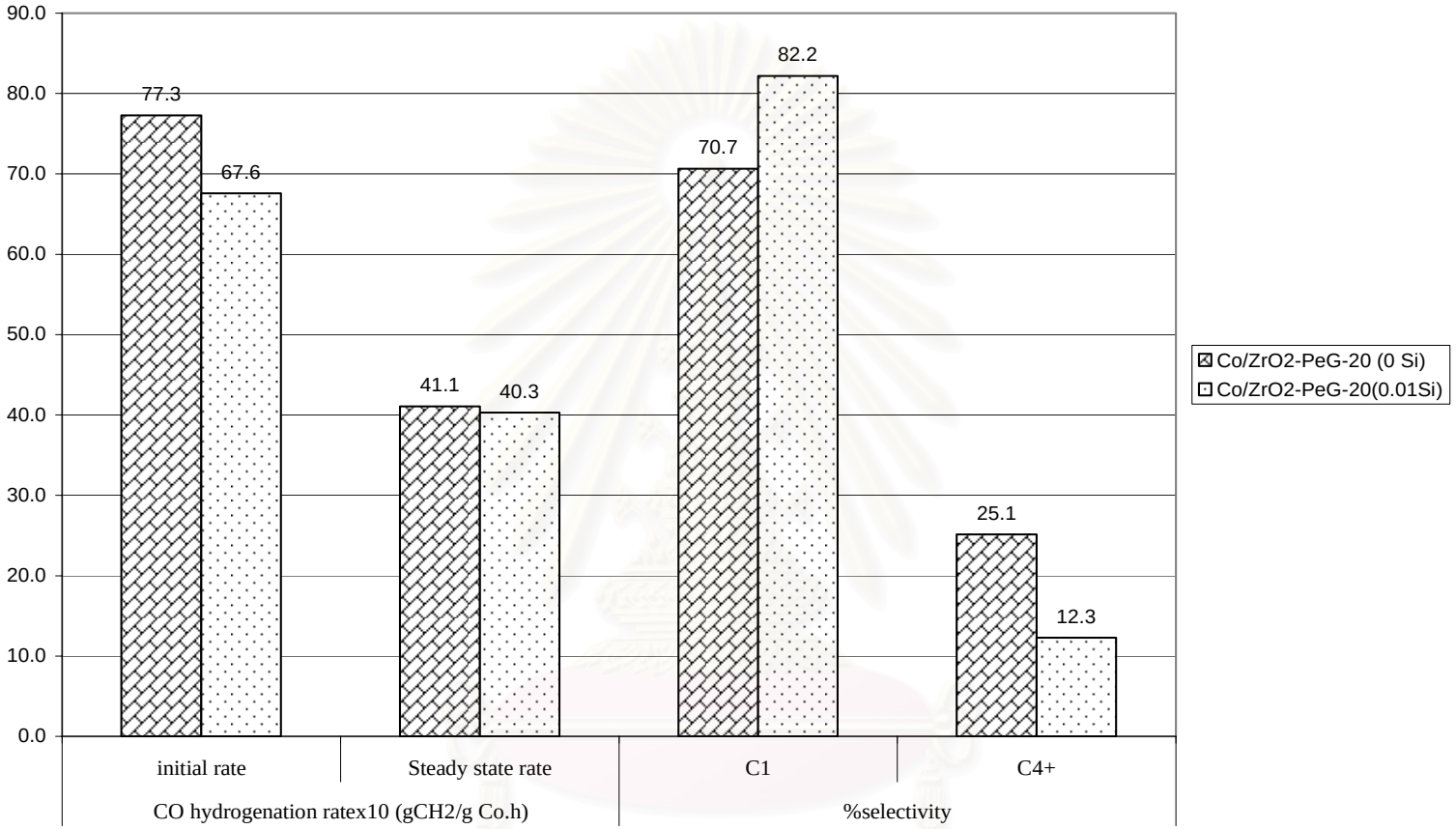

Figure 5.21 (b) Results of CO hydrogenation reaction for Co/ ZrO_2-PeG-20 with and without Si addition.

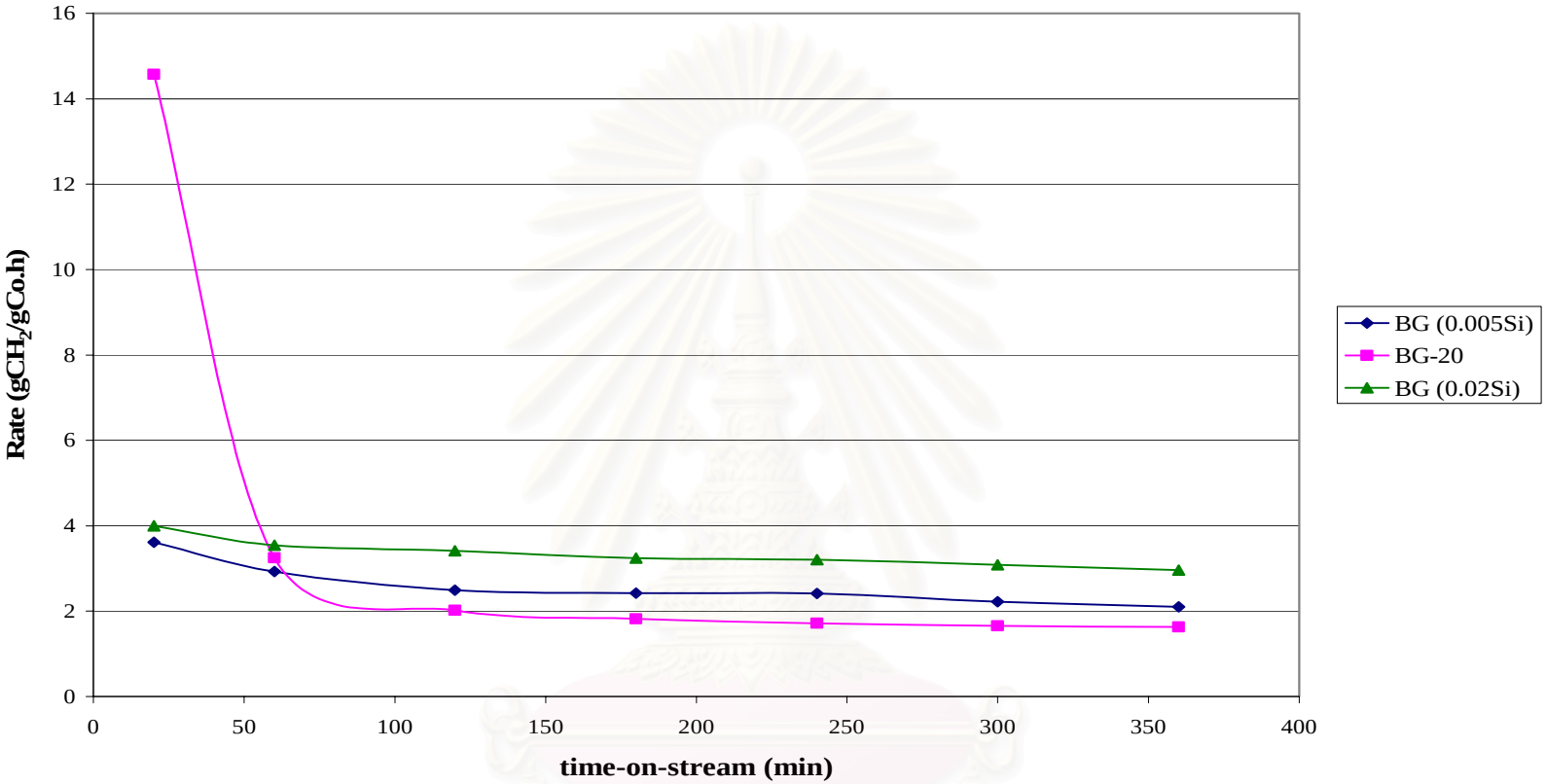

Figure 5.22 (a) CO hydrogenation rate vs time-on-stream.

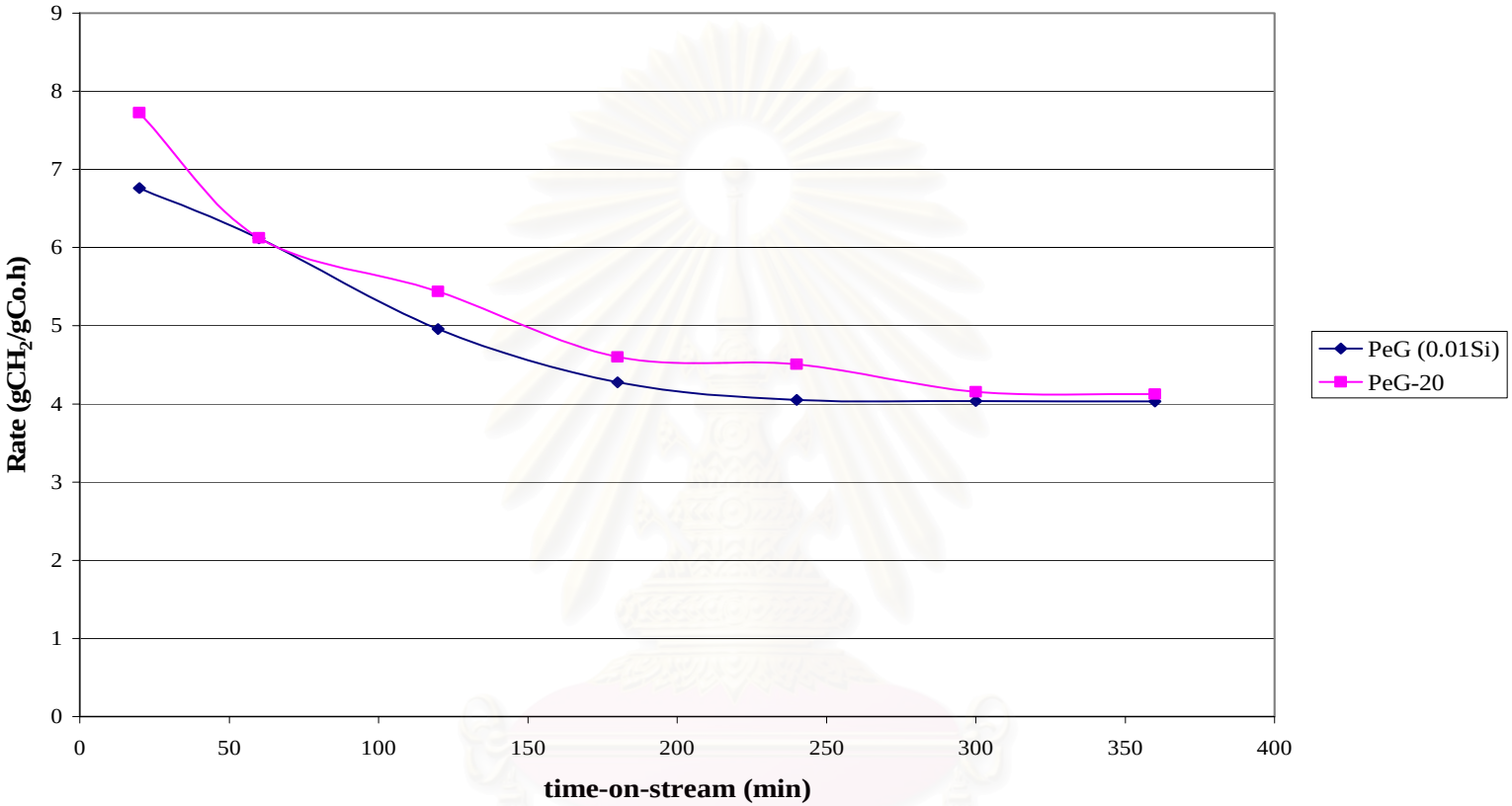

Figure 5.22(b) CO hydrogenation rate vs time-on-stream.

5.4 The Comparative of Cobalt Catalysts Supported on Micron-size ZrO_2 and Nano-size ZrO_2

This section presents a comparative study of cobalt catalysts supported on micron-size ZrO_2 and nano-size ZrO_2 in CO hydrogenation reaction. The characteristics and the catalytic properties of micron-size ZrO_2 and nano-size ZrO_2 supported cobalt catalysts are studied by various analysis techniques such as SEM, XRD, H_2 chemisorption, TPR and CO hydrogenation reaction.

5.4.1 Scanning Electron Microscopy (SEM)

Figure 5.23(a) and Figure 5.24(a) show the scanning electron micrographs of micron-size ZrO_2 and nano-size ZrO_2, respectively. It is clearly seen that the catalyst granule size of the micron-size ZrO_2 was bigger than the nano-size ZrO_2. The cobalt catalysts supported on micron-size ZrO_2 and nano-size ZrO_2 are shown in Figure 5.23(b) and Figure 5.24(b), respectively. In the SEM figures, the white or light spots on the catalyst granules represent a high concentration of cobalt and its compounds. The morphologies of the Co/ZrO_2-micron after cobalt impregnation were not significant changed while the Co/ZrO_2-nano showed some agglomeration of the catalyst granules. Some large cobalt granules were also observed on the Co/ZrO_2-nano.

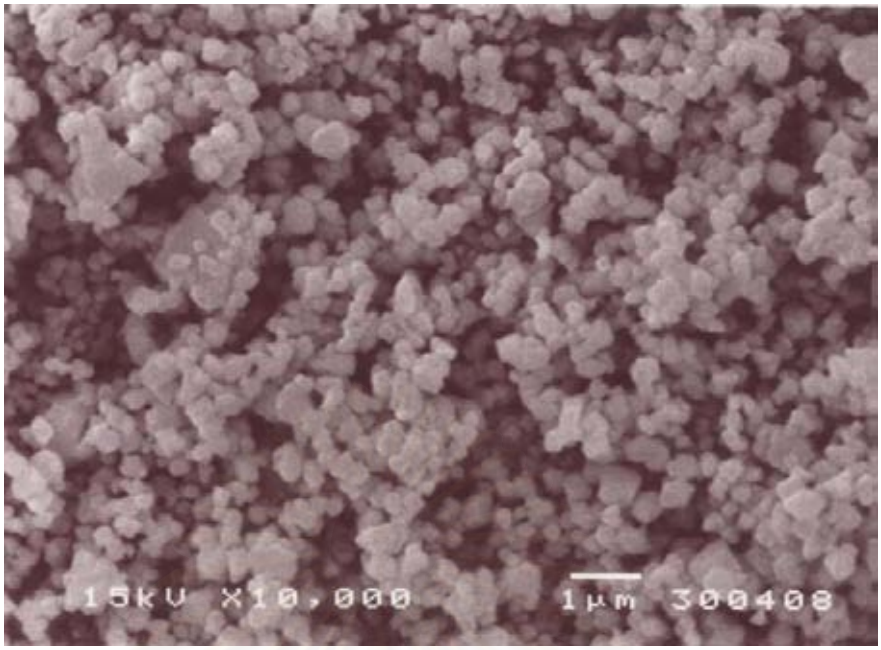

Figure 5.23 (a) SEM micrograph of catalyst granules for ZrO_2-micron

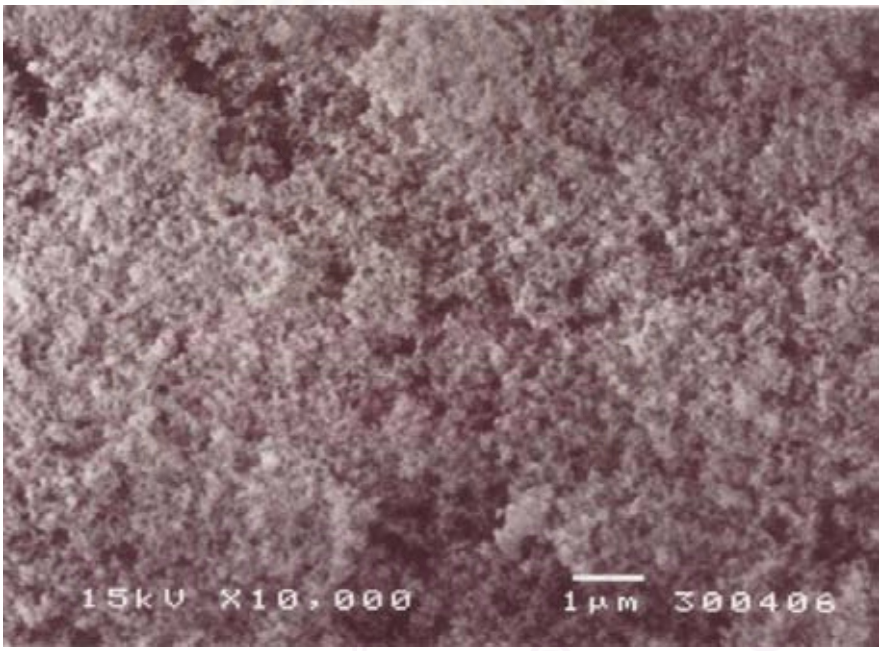

Figure 5.23 (b) SEM micrograph of catalyst granules for ZrO_2-nano

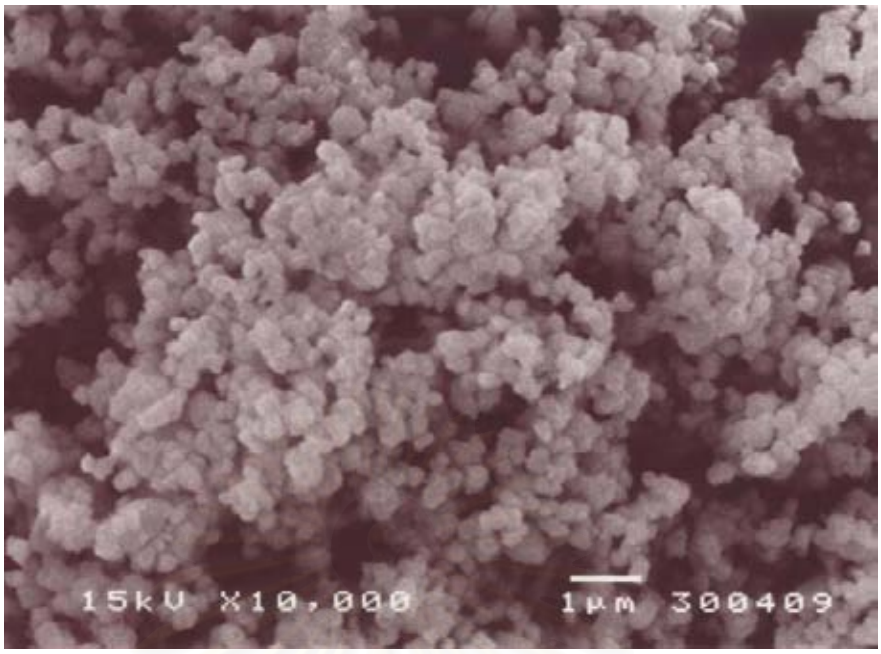

Figure 5.24 (a) SEM micrograph of catalyst granules for Co/ZrO_2-micron

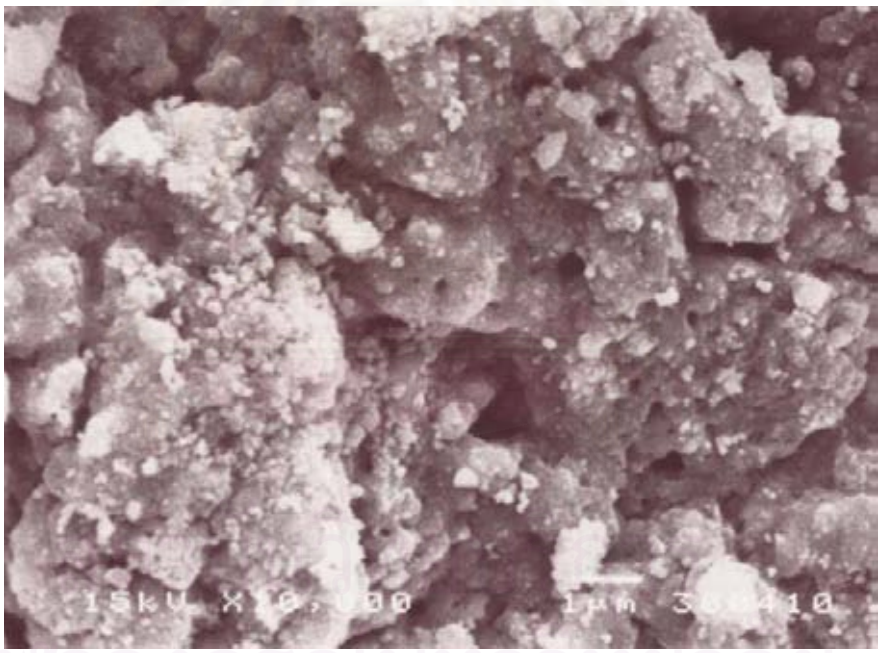

Figure 5.24 (b) SEM micrograph of catalyst granules for Co/ZrO_2-nano

5.4.2 X-ray Diffraction (XRD)

The X-ray diffraction patterns of the micron-size ZrO_2 and nano-size ZrO_2 unsupported and supported cobalt catalyst are shown in Figure 5.25 (a) and (b), respectively. It was found that both commercial ZrO_2 contain tetragonal and monoclinic phase ZrO_2. After impregnation of ca. 8 wt% cobalt and calcination at 300^{o}C, XRD peaks for Co_3O_4 were apparent for all the commercial ZrO_2-supported cobalt catalysts. The crystal sizes and zirconia phase of cobalt supported catalysts are given in Table 5.16.

Table 5.16 Phases Present in the Samples and the Average Crystallite Size of Co/ZrO_2

Catalysts	ZrO_2 Phase	Crystal size of ZrO_2 [a] (nm)		Crystal size of Co_3O_4 (nm)[a]
		unsupported	supported	
ZrO_2-micron	T,M[b]	10.5	8.9	6.9
ZrO_2-nano	T,M	11.5	10.7	7.9

[a] Base on XRD line broadening.

[b] T, tetragonal zirconia; M, monoclinic zirconia.

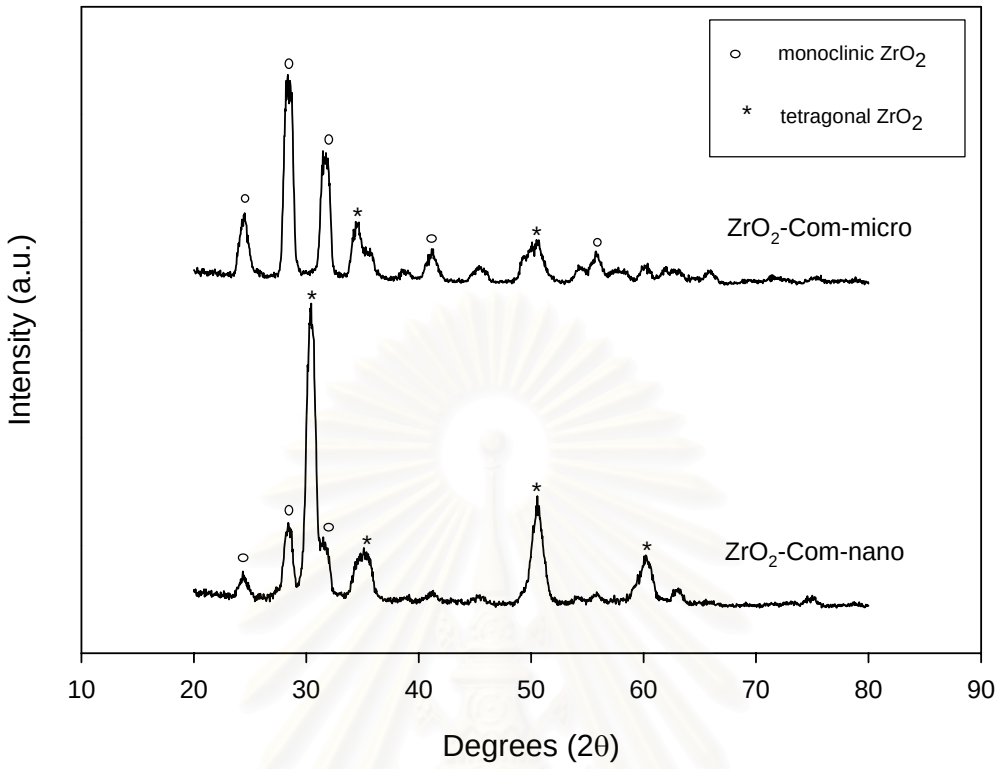

Figure 5.25 (a) XRD patterns of the commercial ZrO_2.

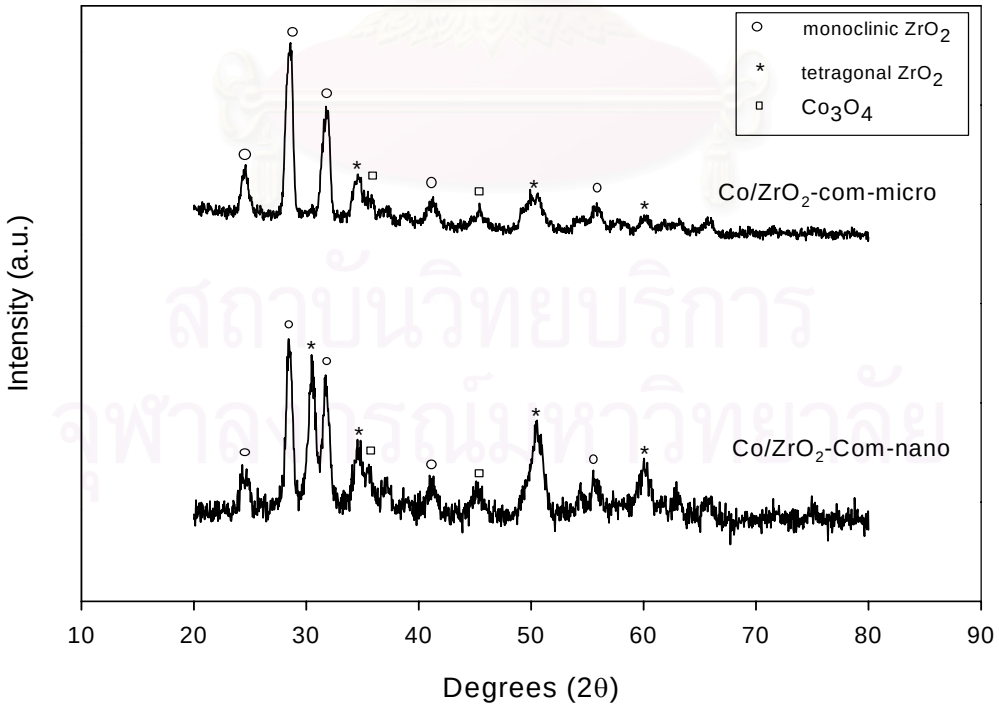

Figure 5.25 (b) XRD patterns of the commercial ZrO_2 supported cobalt catalysts.

5.4.3 Atomic Absorption Spectroscopy (AAS)

The amount of cobalt loading for the micron-size ZrO_2 and nano-size ZrO_2 supported cobalt catalysts were measured by atomic absorption spectroscopy. The results are given in Table 5.17. Cobalt loading on the catalysts was approximately 8 wt% on both ZrO_2 supports.

Table 5.17 Atomic Absorption Results.

Catalysts	Co (Wt%)
Co/ZrO_2-micron	7.9
Co/ZrO_2-nano	8.1

5.4.4 Hydrogen Chemisorption

The total hydrogen uptakes, the percentages of cobalt dispersion and the average cobalt metal size are reported in Table 5.18. It was found that the cobalt supported on nano-size zirconia catalyst exhibited much higher amount of H_2 chemisorption than the micron-size zirconia supported cobalt catalysts.

Table 5.18 Results from H_2 Chemisorption

Catalysts	Amount H_2 $x10^{19}$ (atom/g Co) [a]	% Co Dispersion [b]	dp Co^o (nm) [c]
Co/ZrO_2-micron	3.1	3.8	25.3
Co/ZrO_2-nano	10.1	12.1	7.9

[a] Error of measurement = +/- 5%.

[b] Base on total number of Co atoms in the sample x 100% reduced

[c] dp Co^0 = 96 / (%D) (Moradi *et al*., 2003)

5.4.5 Carbon Monoxide Hydrogenation

The CO hydrogenation rates, product selectivities and TOFs of the micron-size ZrO_2 and nano-size ZrO_2 supported cobalt catalysts were presented in Table 5.19. It was found that under the reaction conditions used, the Co/ZrO_2-nano exhibited much higher CO hydrogenation rates than the Co/ZrO_2-micron catalysts. The results were in accordance with the results from H_2 chemisorption that Co/ZrO_2-nano posseses higher active metal Co sites than Co/ZrO_2-micron.

Table 5.19 Results CO Hydrogenation Reaction at Methanation Conditions[a].

Catalysts	CO hydrogenation rate ($gCH_2/gCo.h$)		Selectivity			TOF (s^{-1})
	Initial	Steady-state	C_1	C_2-C_3	C_4+	
Co/ZrO_2-micron	1.7	1.4	57.8	14.4	17.8	0.6
Co/ZrO_2-nano	3.8	2.2	77.8	8.6	13.5	0.5

[a] Reaction condition were 220 ^oC, 1 atm, and H_2/CO=10 ($H_2/CO/Ar$ = 40/4/16 cc/min).

CHAPTER VI

CONCLUSIONS AND RECOMMENDATIONS

6.1 Conclusions

With careful experimental works, the effects of glycol source and Zr concentration on the physicochemical properties of ZrO_2 prepared by glycothermal method, the characteristics of the corresponding ZrO_2 supported Co catalysts and their catalytic activities for CO hydrogenation were extensively investigated. The following conclusions can be drawn:

1. ZrO_2 prepared by the glycothermal method in two different glycols with various Zr contents in the starting ZNP solution possess similar crystallite sizes of ca. 3-4 nm and high surface areas (195-220 m^2/g).

2. Use of ZrO_2 prepared in 1,4-butanediol as a support for cobalt catalysts resulted in the higher amounts of H_2 chemisorption and initial CO hydrogenation activities than those obtained from cobalt on ZrO_2 prepared in 1,5-pentanediol due probably to lower metal-support interaction of cobalt and the ZrO_2 as shown by lower reduction temperature peaks in the TPR profiles (from 30-350 ^oC).

3. The steady state rates in CO hydrogenation of cobalt supported on Si-modified ZrO_2 prepared in 1,4-butanediol increased with increasing Si/Zr ratio from 0.005 to 0.02. But there was no effect of Si addition for the Co supported on ZrO_2 prepared in 1,5-pentanediol.

4. The cobalt catalyst supported on commercial nano-size ZrO_2 was found to exhibit higher CO hydrogenation activity than that of the one supported on micron-size ZrO_2.

5. Compared to both commercial ZrO_2 supported Co catalysts (nano and micron size), the cobalt catalysts supported on ZrO_2 prepared by the glycothermal method exhibited much higher CO hydrogenation activities. Thus the ZrO_2 prepared by glycothermal method are suitable for cobalt catalyst supports, however, the type of

the glycol and Zr concentration must be carefully chosen in order to obtain the highest activity of Co/ZrO_2 catalysts.

6.2 Recommendations

1. Use of the ZrO_2 prepared in 1,4-butanediol as cobalt catalyst showed the highest initial CO hydrogenation activities but the cobalt seemed to be unstable resulting in low activities at the steady-state. The stability of cobalt on such support should be further investigated.
2. The ways to improve steady-state rates of Co/ZrO_2-BG-20 should be tried, for example, addition of a second metal (i.e., Rh, Ru) as a promoter.
3. Addition of other elements (i.e., alumina titania) during ZrO_2 preparation by glycothermal method should be investigated since it may modify the properties of the ZrO_2.
4. The reaction study under commercial Fischer-Tropsch synthesis conditions using Co/ZrO_2 catalysts is also recommended.

REFERENCES

Aguilar, D. H., et al. A study of the crystallization of ZrO_2 in the sol-gel system: ZrO_2-SiO_2. J. Solid State Chem. 158 (2001): 349-357.

Amenomiya, Y. Methanol syntheses from CO_2+H_2. 2. copper-based binary and ternary catalysts. Appl. Catal. 30 (1987): 57-68.

Anderson, R. B. The Fischer-Tropsch Synthesis, Academic Press, San Diego, 1984.

Bitter, J. H.; Sechan K.; and Lercher, J. A. The state of zirconia supported platinum catalysts for CO_2/CH_4 reforming. J. Catal. 171 (1997): 279-286.

Bruce, L.; and Mathews, J. F. The Fischer-Tropsch activity of nickel-zirconia. Appl. Catal. 4 (1982): 353-369.

Chuah, G. K.; and Pong, B. K. The preparation of high-surface-area zirconia II: Influence of precipitating agent and digestion on the morphology and microstructure of hydrous zirconia. J. Catal. 175 (1998): 80-92.

Chuah, G. K. An investigation into the preparation of high surface area zirconia. Catal. Today. 49 (1999): 131-139.

Dow, W. P.; and Huang, T. J. Effect of oxygen vacancy of yttria-stabilized zirconia support on carbon monoxide oxidation over copper catalyst. J. Catal. 147 (1994): 322-332.

Enache, D. I.; et al. In SituXRD Study of the Influence of Thermal Treatment on the Characteristics and the Catalytic Properties of Cobalt-Based Fischer-Tropsch Catalysts. J. Catal. 205, (2002): 346-353.

Enache, D. I.; et al. Differences in the characteristics and catalytic properties of cobalt-based Fischer–Tropsch catalysts supported on zirconia and alumina. Appl. Catal. A: General 268 (2004): 51-60.

Farrauto, R. J.; and Bartholomew, C. H.. Fundamentals of Industrial Catalytic Processes (1997).

Feller, A.; Claeys, M.; and Steen, E.V. Cobalt Cluster Effects in Zirconium Promoted Co/SiO_2 Fischer–Tropsch Catalysts. J. Catal. 185 (1999); 120-130.

Fujii, H.; Mizuno, N.; and Misono, M. Pronounced catalytic activity of LA_1-$XSRXCOO_3$ highly dispersed on ZrO_2 for complete oxidation of propane. Chem. Lett. 11 (1987): 2147-2150.

Gavalas, G. R.; Phichitkul, C.; and Voecks, G. E. Structure and activity of NiO alpha-Al_2O_3 and NiO/ZrO_2 calcined at high-temperatures.1. structure. J. Catal. 88 (1984): 54-64.

He, M. Y.; and Ekerdt, J. G. Infrared studies of the adsorption of synthesis gas on zirconium dioxide. J. Catal. 87 (1984): 381-388.

Heuer, A. H. Transformation Toughening in ZrO_2-containing Ceramics. J. Am. Ceram. Soc. 70 (1987): 689-98.

Iglesia, E.; Soled, S. L.; and Fiato, R. A. Fischer-Tropsch Synthesis on Cobalt and Ruthenium: Metal Dispersion and Support Effects on Reaction Rate and Selectivity. J. Catal. 137 (1992): 212-224.

Inoue, M.; Kominami, H.; and Inui, T. Novel synthetic method for the catalytic use of thermally stable zirconia- thermal-decomposition of zirconium alkoxides in organic media. Appl. Catal. A: General 97 (1993): L25-L30.

Inoue, M.; et al. Glycothermal synthesis of zirconia-rare earth oxide solid solutions. Cat. Lett. 65 (2000): 79-83.

Jacobs, G.; et al. Fischer–Tropsch synthesis: support, loading, and promoter effects on the reducibility of cobalt catalysts. Appl. Catal. A: General 233 (2002): 263-281.

Jongsomjit, B.; Panpranot, J.; and Goodwin, J.G. Effect of zirconia-modified alumina on the properties of Co/γ –Al2O3 catalysts. J. of Catal. 215 (2003): 66-77.

Kongwudthiti, R. Crystallization Mechanism of Zirconia under the Glycothermal Condition and the Effect of Silica on the Thermal Stability and Surface Area of Modified Zirconia. Doctor's Thesis, Department of Chemical Engineering, Engineering, Chulalongkorn University, 2002.

Kongwudthiti, R.; et al. Synthesis of large-surface area silica-modified zirconia by the glycothermal method. J. of Meter. Sci. Lett. 21 (2002): 1461-1464.

Kongwudthiti, R.; et al. Infuence of synthesis conditions on the preparation of zirconia powder by the glycothermal method. Ceram. Inter. 29 (2003): 807–814.

Kongwudthiti, R.; et al. The influence of Si-O-Zr bonds on the crystal-growth inhibition of zirconia prepared by the glycothermal method. J. Mater. Pro. Tech. 136 (2003): 186-189.

Kraum, M.; and Baerns, M. Fischer–Tropsch synthesis: the influence of various cobalt compounds applied in the preparation of supported cobalt catalysts on their performance. App. Catal. 186 (1999): 189-200.

Lapidus, A.; et al. Preparation and characterization of Fischer–Tropsch active Co/SiO_2 catalysts. Appl. Catal. A. 186 (1999): 145-168.

Lapidus, A.; et al. Hydrocarbon synthesis from carbon monoxide and hydrogen on impregnated cobalt catalysts Part I. Physico-chemical properties of 10% cobalt/alumina and 10% cobalt/silica. Appl. Catal. A. 73 (1991): 65-83.

Livage, J.; Doi, K.; and Mazieres, C. Nature and thermal evolution of amorphous hydrated zirconium oxide. J. Am. Ceram. Soc. 51 (1968): 349-53.

Maruya, K.; et al. Active sites on ZrO for the formation of isobutene from 2CO and H_2. J. of Mol. Catal. A: Chemical 159 (2000): 97-102.

Monte, F. D.; Larsen, W.; and Mackenzie, J. D. Stabilization of tetragonal ZrO_2 in ZrO_2-SiO_2 binary oxides. J. Am. Ceram. Soc., 83 (2000): 628-634.

Moradi, G. R.; et al. Promotion of Co/SiO_2 Fischer–Tropsch catalysts with zirconium. Catal. Comm. 4 (2003): 27-32.

Nakano, Y.; Yamaguchi, T.; and Tanabe, K. Hydrogenation of conjugated dienes over ZrO_2 by H_2 and cyclohexadiene. J. Catal. 80 (1983): 307-312.

Osendi, M. I.; et al. Metastability of tetragonal zirconia powders. J. Am. Ceram. Soc. 68 (1985): 135-39.

Oukaci, R.; et al. Comparison of patented Co F–T catalysts using fixed-bed and slurry bubble column reactors. Appl. Catal. A: General 186 (1999): 129-144.

Panpranot, J., et al. Synthesis and characteristics of MCM-41 supported CoRu catalysts. Catal. Today. 77 (2002): 269-284.

Prokhorenko, E. V.; Pavlenko, N. V.; and Golodets, G. I. Effect of the nature of the support on the catalytic properties of cobalt and nickel-catalysis in the reaction of hydrogenation of carbon-monoxide. Kinet. Catal. (English Trans). 29 (1988): 702-706.

Reuel, R. C., and Bartholomew, C.H. Effects of Support and Dispersion on the CO Hydrogenation Activity/Selectivity Properties of Cobalt. J. Catal. 85 (1984): 78-88.

Reuel, R. C.; and Bartholomew, C. H. The Stoichiometries of H_2 and CO Adsorption on cobalt : Effect of Support and Preparation. J. Catal. 85 (1984): 63-77.

Rohra, F.; et al. Fischer–Tropsch synthesis over cobalt catalysts supported on zirconia-modified alumina. Catal. Today 58 (2000): 247-254.

Schanke, D.; et al. Study of Pt-Promoted Cobalt CO Hydrogenation Catalysts. J. Catal. 156 (1995): 85-95.

Shinoda, M.; et al. New bimodal pore catalysts for Fischer–Tropsch synthesis. Fuel Pro. Tech.(2004).

Tanabe, K. Surface and catalytic properties of ZrO_2. Mater Chem. Phys. 13 (1985): 347-364.

Tani, E.; Yoshimura, M.; and Somiya, S. Formation of Ultrafine tetragonal ZrO_2 powder under hydrothermal conditions. J. Am. Ceram. Soc. 66 (1982): 11-14.

West, A. R.; Solid State Chemistry and its Application, John Wiley&Sons, Brisbane, 1997.

Yoshimura, M.; and Somiya, S. Hydrothermal synthesis of crystallized nano-particles of rare earth-doped zirconia and hafnia. Master. Chem. Phys. 61 (1999):1-8.

Zhang, Y., et al. Effect of Water Vapor on the Reduction of Ru-Promoted Co/Al_2O_3. J. Catal. 188 (1999): 281-290.

Zhaoa, Q.; et al. The effect of curing on the thermal stability of Si-doped ZrO_2 powders. Appl.Catal. A: General. 262 (2004): 215–221.

APPENDICES

APPENDIX A

CALCULATION OF THE AMOUNT OF THE REAGENT REQUIRED FOR THE REACTION

In this study, silica-modified zirconia with various molar ratios were prepared using 1,4-butanediol as the solvent, and therefore detailed calculation procedure is given here.

Calculation of the amount of TEOS for silica-modified zirconia preparation

Zirconium tetra *n*-propoxide (ZNP) and tetraethyl orthosilicate (TEOS) are used as the reactants to prepare silica-modified zirconia.

1. Zirconium *n*-propoxide [$Zr(OC_3H_7)_4$] has a molecular weight of 327.57 g/mol.

   Zirconium, Zr, has an atomic weight of 91.22 g/mol.
2. Tetraethyl orthosilicate [$(C_2H_5O)_4Si$] has a molecular weight of 208.33 g/mol

   Silicon, Si, has an atomic weight of 28.0855 g/mol.

Example: Calculation of preparation of silica-modified zirconia with the molar ratio Si/Zr of 0.02 are as follows:

Fifteen gram of zirconium *n*-propoxide was used for the preparation of silica-modified zirconia with a molar ratio Si/Zr of 0.02.

Zirconium *n*-propoxide 15 g was consisted of zirconium equal to:

Zirconium = 15/327.57 = 0.0458 mol

To get the product with molar ratio Si/Zr of 0.02;

Silicon = 0.02 x 0.0458 mol = 0.00091 mol

Tetraethyl orthosilicate reqired is equal to: 208.33 x 0.00091 = 0.1908 g

APPENDIX B

CALCULATION FOR CATALYST PREPARATION

Preparation of 10%Co/ZrO_2 catalysts by the incipient wetness impregnation method are shown as follows:

Reagent: - Cobalt (II) nitrate hexahydrate [$Co(NO_3)_2 \cdot 6H_2O$]

Molecular weight = 291.03 g

- Support: ZrO_2

Example Calculation for the preparation of 10% Co/ZrO_2 catalyst with $Co(NO_3)_2 \cdot 6H_2O$ as Co precursor (Co/ZrO_2)

Based on 100 g of catalyst used, the composition of the catalyst will be as follows:

Cobalt = 10 g

ZrO_2 = 100-10 = 90 g

For 1 g of catalyst

Cobalt required = 1×(10/100) = 0.1 g

Cobalt 0.1 g was prepared from $Co(NO_3)_2 \cdot 6H_2O$ and molecular weight of Co is 58.93

$$\text{the } Co(NO_3)_2 \cdot 6H_2O \text{ content} = \frac{\text{MW of } Co(NO_3)_2 \cdot 6H_2O \times \text{cobalt required}}{\text{MW of Co}}$$

$$= (291.03/58.93) \times 0.1 = 0.49 \text{ g}$$

Since the pore volume of the pure silica support is 0.402 ml/g for ZrO_2. Thus, the total volume of impregnation solution which must be used is 0.803 ml for ZrO_2 by the requirement of incipient wetness impregnation method, the de-ionised water is added until equal pore volume for dissolve Cobalt (II) nitrate hexahydrate.

APPENDIX C

CALCULATION OF THE CRYSTALLITE SIZE

Calculation of the crystallite size by Debye-Scherrer equation

The crystallite size was calculated from the half-height width of the diffraction peak of XRD pattern using the Debye-Scherrer equation.

From Scherrer equation:

$$D = \frac{K\lambda}{\beta \cos \theta} \qquad (C.1)$$

where D = Crystallite size, Å

K = Crystallite-shape factor = 0.9

λ = X-ray wavelength, 1.5418 Å for CuKα

θ = Observed peak angle, degree

β = X-ray diffraction broadening, radian

The X-ray diffraction broadening (β) is the pure width of a powder diffraction free from all broadening due to the experimental equipment. α-Alumina is used as a standard sample to observe the instrumental broadening since its crystallite size is larger than 2000 Å. The X-ray diffraction broadening (β) can be obtained by using Warren's formula.

From Warren's formula:

$$\beta = \sqrt{B_M^2 - B_S^2} \qquad (C.2)$$

Where B_M = The measured peak width in radians at half peak height.

B_S = The corresponding width of the standard material.

Example: Calculation of the crystallite size of zirconia

The half-height width of 111 diffraction peak = 1.83^o (from the figure C.1)

= $(2\pi x180)/360$

= 0.0319 radian

The corresponding half-height width of peak of α-alumina (from the Bs value at the 2θ of 30.3^o in figure C.2) = 0.0043 radian

The pure width, $\beta = \sqrt{B_M^2 - B_S^2}$

$= \sqrt{0.0319^2 - 0.0043^2}$

= 0.0316 radian

B = 0.0316 radian

2θ = 30.3^o

θ = 15.15^o

λ = 1.5418 Å

The crystallite size = $\frac{0.9x\,1.5418}{0.0316\,\cos 15.15}$ = 45.49 Å

= 4.5 nm

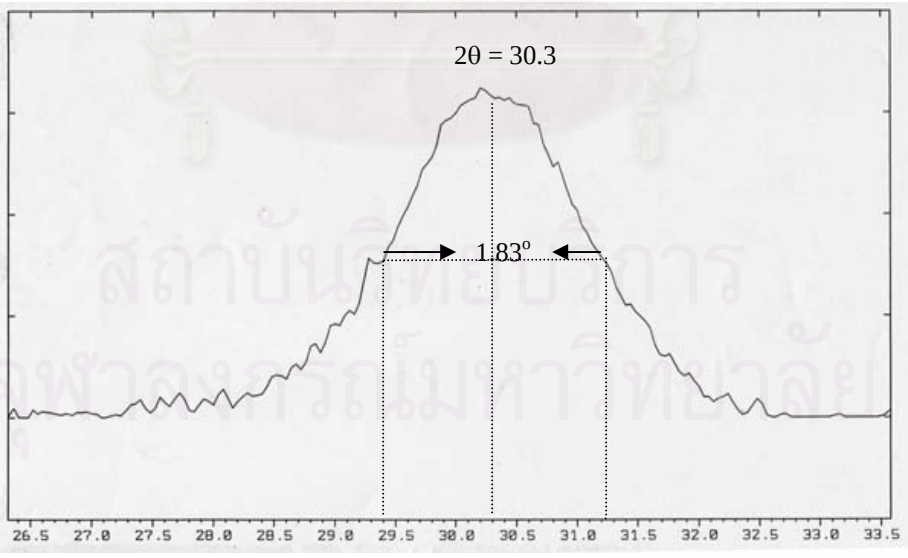

Figure C.1 The 111 diffraction peak of zirconia for calculation of the crystallite size

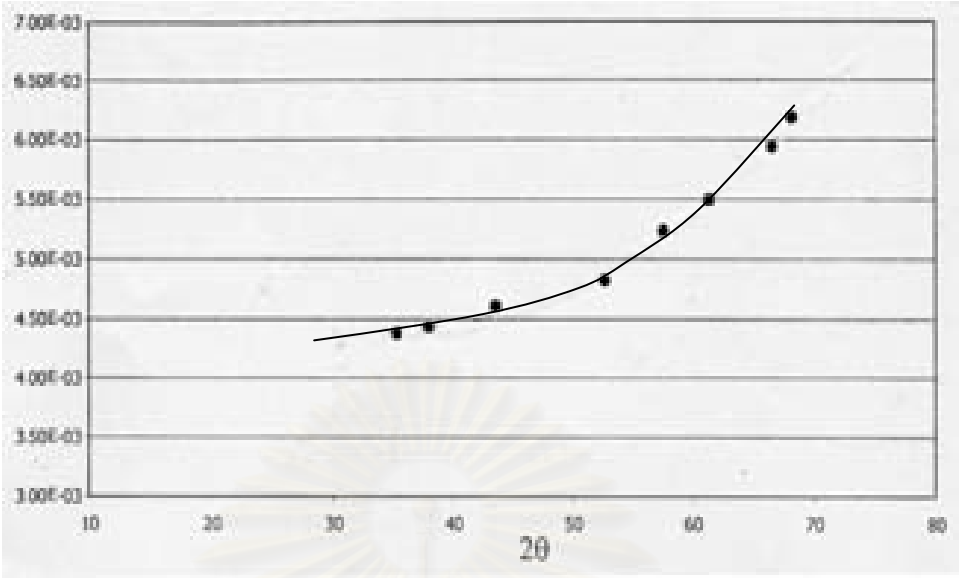

B_s

Figure C.2 The plot indicating the value of line broadening due to the equipment. The data were obtained by using α-alumina as a standard

APPENDIX D

CALCULATION OF BET SURFACE AREA BY THE SINGLE POINT METHOD

From Brunauer-Emmett-Teller (BET) equation:

$$\frac{X}{V(1-X)} = \frac{1}{VmC} + \frac{(C-1)X}{VmC} \qquad (D.1)$$

Where: X = relative partial pressure of N_2, P/P_o

P_o = saturated vapor pressure of N_2 (or adsorbed gas) at the experimental temperature

P = equilibrium vapor pressure of N_2

V = volume of gas adsorbed at a pressure P; ml at the NTP/ g of sample

V_m = volume of gas adsorbed at monolayer, ml. at the NTP / g of sample

C = constant

Assume $C \rightarrow \infty$, then

$$\frac{X}{V(1-X)} = \frac{X}{Vm} \qquad (D.2)$$

$$Vm = V(1-P/P_o)$$

From the gas law,

$$\frac{P_bV}{273} = \frac{P_tV}{T} \qquad (D.3)$$

Where: V = constant volume

P_b = pressure at 0 ^oC

P_t = pressure at t ^oC

T = 273.15 + t, K

P_t = 1 atm and thus, P_b = (273.15 / T)

Partial pressure of Nitrogen:

$$P = \frac{[\text{Flow of } (He+N_2) - \text{Flow of } He]}{\text{Flow of } (He+N_2)} \quad (D.4)$$

$$= 0.3 \text{ atm}$$

N_2 saturated vapor pressure, P_o = 1.1 atm

$$p = P / P_o = P / 1.1 = 0.3/1.1 = 0.2727$$

How to measure V

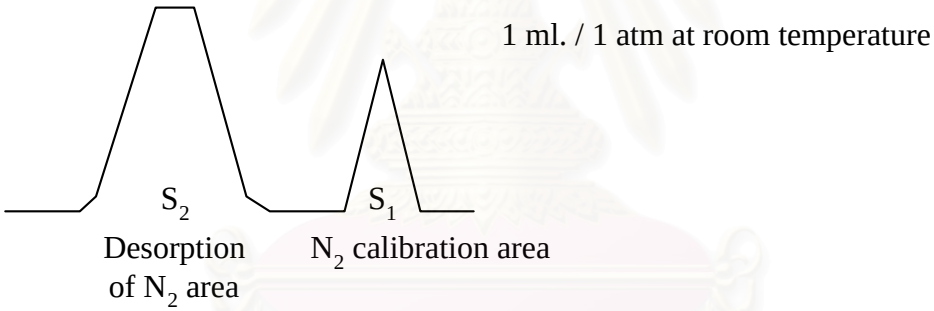

$$V = \frac{S_2}{S_1} \times \frac{1}{W} \times \frac{273.15}{T} \text{ ml. / g of catalyst} \quad (D.5)$$

Where, S_1 = Nitrogen 1 ml/1 atm of room temperature area

S_2 = Desorption of nitrogen area

W = Weight of the sample (g)

T = Room temperature (K)

Therefore,

$$Vm = \frac{S_2}{S_1} \times \frac{1}{W} \times \frac{273.15}{T} \quad X\ (1\text{-}p)$$

$$Vm = \frac{S_2}{S_1} \times \frac{1}{W} \times \frac{273.15}{T} \quad X\ 0.7273 \qquad (D.6)$$

Surface area of catalyst:

$$S = \frac{N\sigma V_m}{M}$$

Where, N = Avogadro number = 6.02×10^{23}

σ = area occupied by one molecule of adsorbed nitrogen = 16.2×10^{-20}

M = volume of one mole nitrogen = 22410 cm^3/mol

Then,

$$S = 4.352\ Vm$$

$$S = \frac{S_2}{S_1} \times \frac{1}{W} \times \frac{273.15}{T} \quad x\ 0.7273\ x\ 4.352$$

$$S = \frac{S_2}{S_1} \times \frac{1}{W} \times \frac{273.15}{T} \quad x\ 3.1582 \qquad (D.7)$$

APPENDIX E

CALCULATION FOR TOTAL H_2 CHEMISORPTION AND DISPERSION

Calculation of the total H_2 chemisorption and metal dispersion of the catalyst, a stoischiometry of H/Co = 1, measured by H_2 chemisorption is as follows:

Let the weight of catalyst used	=	W	g
Integral area of H_2 peak after adsorption	=	A	unit
Integral area of 45 μl of standard H_2 peak	=	B	unit
Amounts of H_2 adsorbed on catalyst	=	B-A	unit
Concentration of Co (by AAS)	=	C	% wt
% reducibility (TPR)	=	D	%
Volume of H_2 adsorbed on catalyst	=	45×[(B-A)/B]	μl
Volume of 1 mole of H_2 at 100^{o}C	=	28.038	μl
Mole of H_2 adsorbed on catalyst	=	[(B-A)/B]×[45/28.038]	μmole

Total hydrogen chemisorption = [(B-A)/B]×[45/28.038]×[1/W] μmole /g of catalyst

= N μmole /g of catalyst

Total hydrogen chemisorption = [Nx100]/C = M μmole /g of cobalt

Molecular weight of cobalt = 58.93

Amount hydrogen chemisorption = [2 x M x 58.93]/[C/100] μatom /g of cobalt

$$\text{Metal dispersion (\%)} = \frac{2 \times H_{2\ tot}/\text{g of cobalt x } 58.93}{(\text{concentration of Co}/100) \times (\%\text{reducibility}/100)}$$

$$= \frac{2 \times M \times 58.93}{(C/100) \times (D/100)}$$

APPENDIX F

CALCULATION FOR REDUCIBILITY

For supported cobalt catalyst, it can be assumed that the major species of calcined Co catalysts is Co_3O_4. H_2 consumption of Co_3O_4 is calculated as follows:

Molecular weight of Co = 58.93

Molecular weight of Co_3O_4 = 240.79

Calculation of the calibration of H_2 consumption using cobalt oxide (Co_3O_4)

Let the weight of Co_3O_4 used = 0.01 g

= 4.153×10^{-5} mole

From equation of Co_3O_4 reduction;

$$Co_3O_4 + 4H_2 \rightarrow 3Co + 4H_2O \qquad \textbf{(F.1)}$$

H_2 = 4 Co_3O_4

= $4\times4.153\times10^{-5}$ = 1.661×10^{-4} mole

Integral area of Co_3O_4 after reduction = 396572.5 unit

Thus, the amount of H_2 that can be consumed at 100 % reducibility is 1.661×10^{-4} mole which related to the integral area of Co_3O_4 after reduction 396572.5 unit.

Calculation of reducibility of supported cobalt catalyst

Integral area of the calcined catalyst	=	X	unit
The amount of H_2 consumption	=	$[1.661\times10^{-4}\times(X)/396572.5]$	mole
Let the weight of calcined catalyst used	=	W	g
Concentration of Co (by AAS)	=	Y	% wt
Mole of Co	=	$[(W\times Y)/58.93]$	mole
Mole of Co_3O_4	=	$[(W\times Y)/3\times58.93]$	mole
Mole of H_2 can be consumed	=	$[(W\times Y)\times4/3\times58.93]$	mole

$$\text{Reducibility (\%) of supported Co catalyst} = \frac{[1.661\times10^{-4}\times(X)/396572.5]\times100}{[(W\times Y)\times4/3\times58.93]}$$

APPENDIX G

CALIBRATION CURVES

This appendix shows the calibration curves for calculation of composition of reactant and products in CO hydrogenation reaction. The reactant is CO and the main product is methane. The other products are linear hydrocarbons of heavier molecular weight that are C_2-C_4 such as ethane, ethylene, propane, propylene and butane. Mol of reagent in y-axis and area reported by gas chromatography in x-axis are shown in the curves.

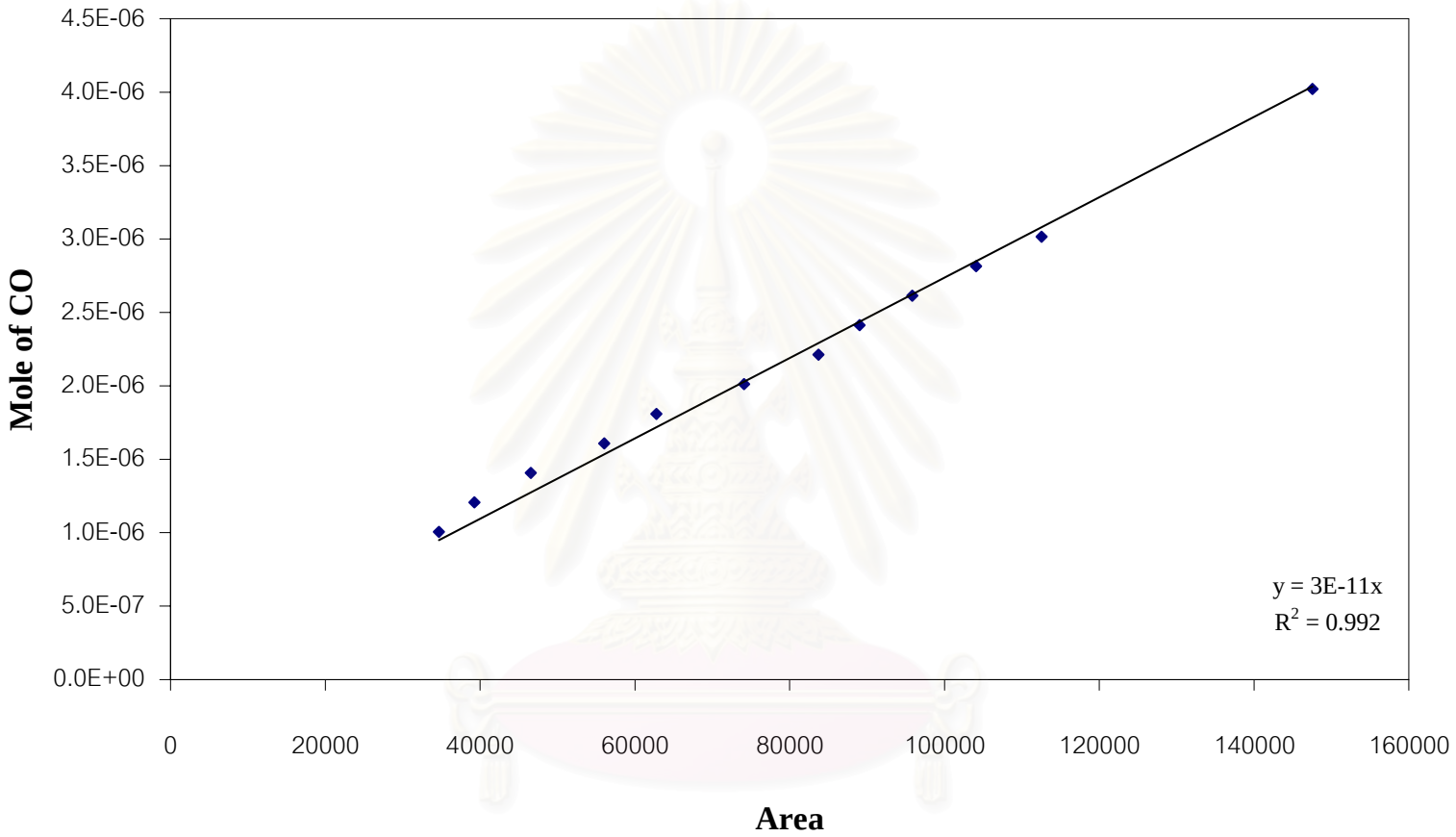

Figure G.1 Calibration curve of CO

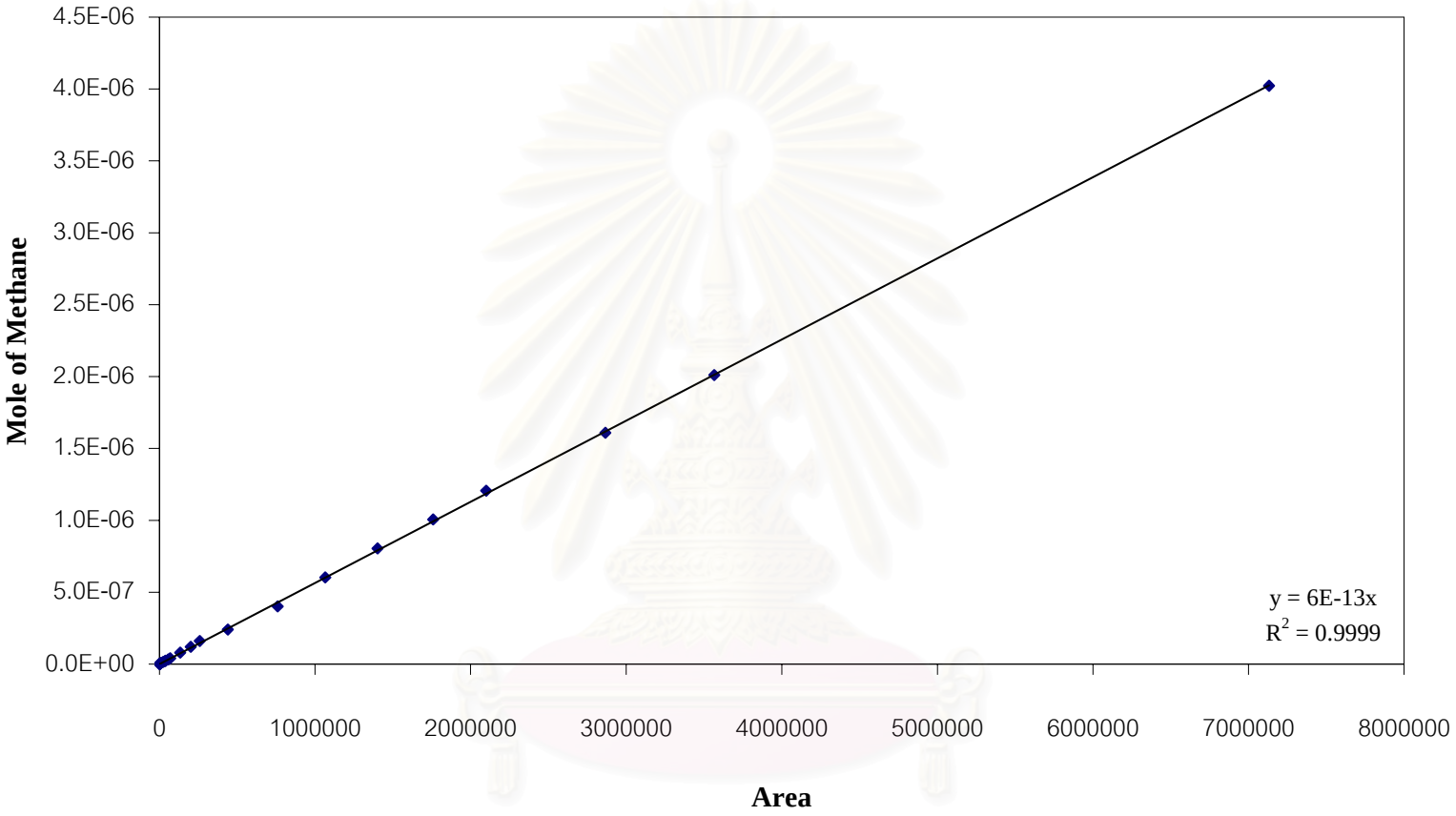

Figure G.2 Calibration curve of methane

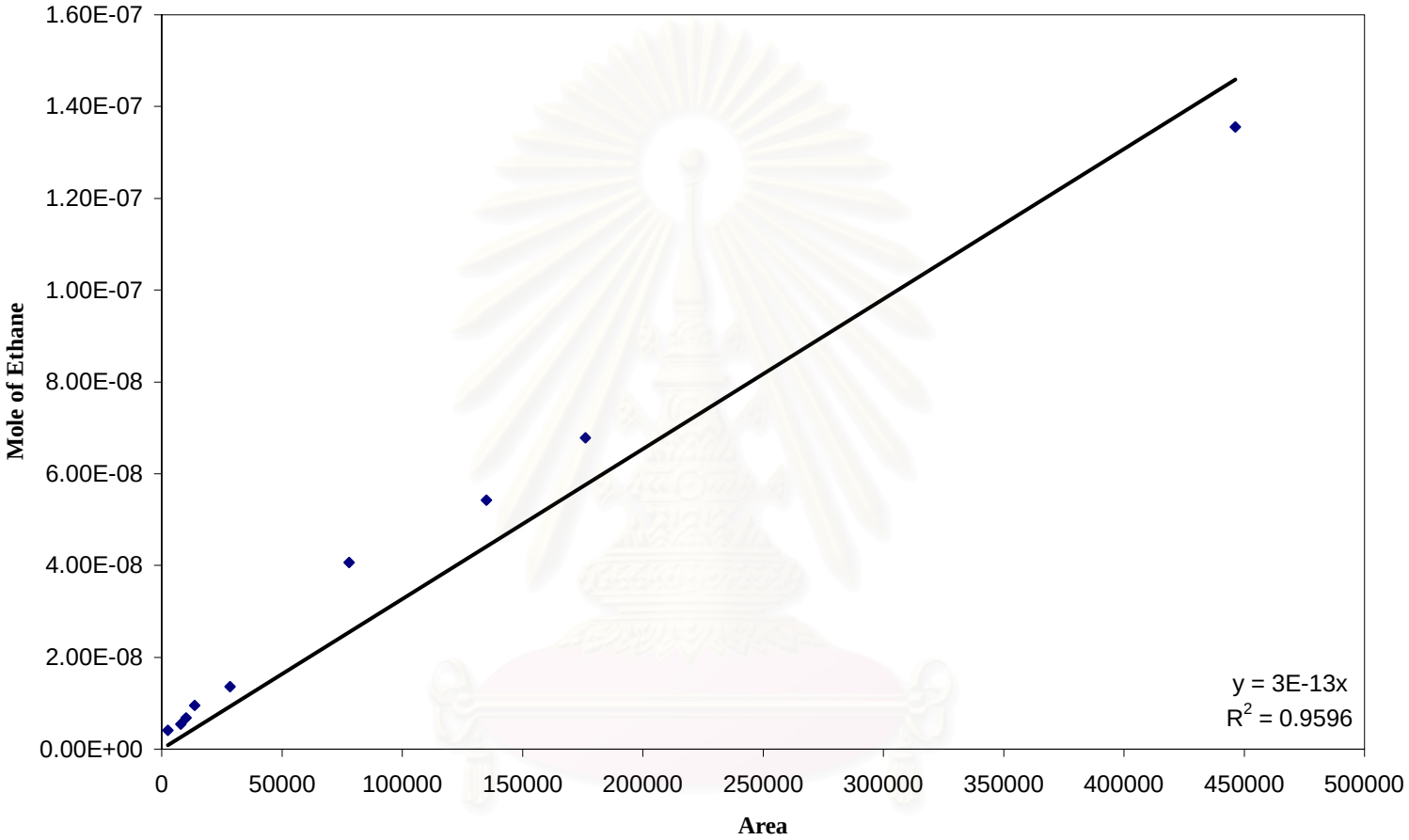

Figure G.3 Calibration curve of ethane

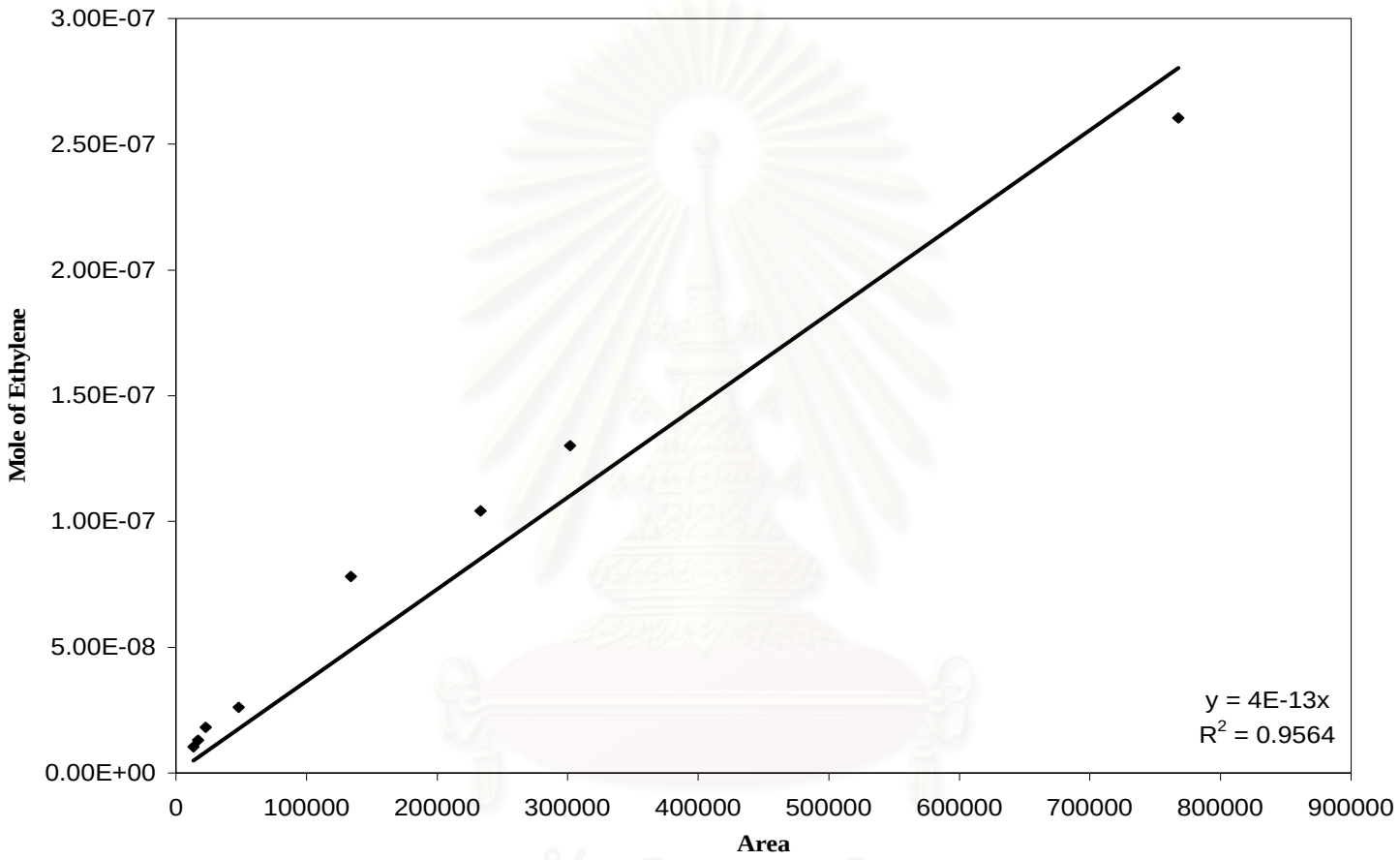

Figure G.4 Calibration curve of ethylene

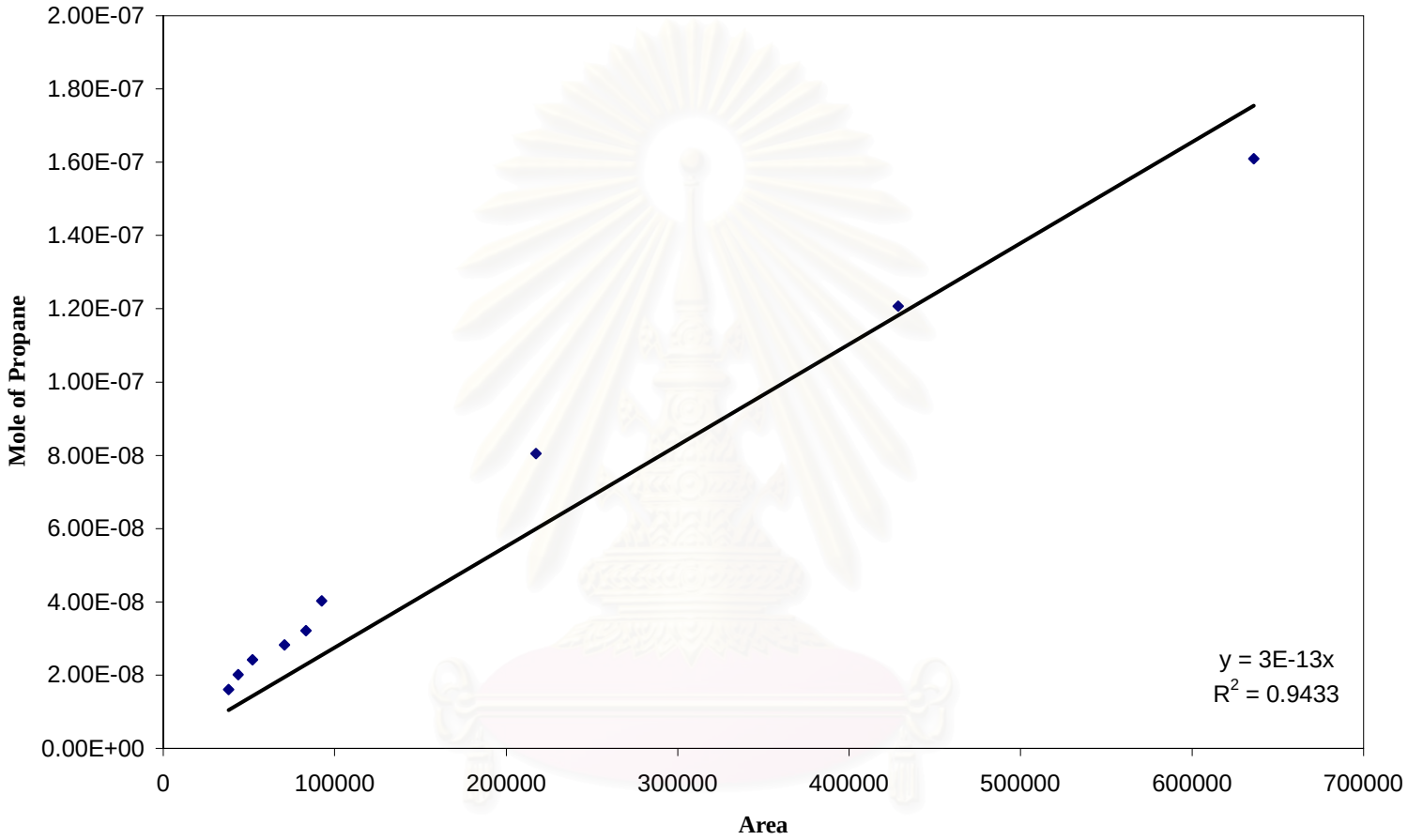

Figure G.5 Calibration curve of propane

APPENDIX H

CALCULATION OF CO CONVERSION, REACTION RATE AND SELECTIVITY

The catalyst performance for the CO hydrogenation was evaluated in terms of activity for CO conversion reaction rate and selectivity.

Activity of the catalyst performed in term of carbon monoxide conversion and reaction rate. Carbon monoxide conversion is defined as moles of CO converted with respect to CO in feed:

$$\text{CO conversion (\%)} = \frac{100 \times [\text{mole of CO in feed} - \text{mole of CO in product}]}{\text{mole of CO in feed}} \quad \text{(i)}$$

where mole of CO in feed can be measured employing the calibration curve of CO in Figure G.1, Appendix G., i.e.,

mole of CO in feed = (area of CO peak from integrator plot on GC-8A)$\times 3 \times 10^{-11}$

mole of CO in product = mole of C(balance) in product from GC-14B

Reaction rate was calculated from CO conversion that is as follows:

Let the weight of catalyst used	=	W	g
Flow rate of CO	=	4	ml/min
Reaction time	=	60	min
Weight of CH_2	=	14	g
Volume of 1 mole of gas at 1 atm	=	22400	ml
Concentration of Co (by AAS)	=	C	% wt

$$\text{Reaction rate (g } CH_2\text{/g of catalyst/h)} = \frac{[\text{\% conversion of CO}/100]\times 60\times 14\times 4}{W\times 22400} \quad \text{(ii)}$$

$$= A \quad (\text{g } CH_2\text{/g of catalyst/h})$$

$$\text{Reaction rate (g } CH_2\text{/g of cobalt/h)} = \frac{A \times 100}{C} \quad (\text{g } CH_2\text{/g of cobalt/h})$$

Selectivity of product is defined as mole of product (B) form with respect to mole of CO converted:

$$\text{Selectivity of D (\%)} = 100 \times [\text{mole of D form/mole of CO converted}] \quad \text{(iii)}$$

Or;

$$\text{Selectivity of D (\%)} = 100 \times \frac{\text{mole of D form}}{\text{mole of CO converted}} \times \frac{\text{no. of C atom of B}}{\text{no. of C atom of CO}} \quad \text{(iv)}$$

Where D is product, mole of D can be measured employing the calibration curve of products such as methane, ethane, ethylene, propane, propylene and butane

$$\text{mole of } CH_4 = (\text{area of } CH_4 \text{ peak from integrator plot on GC-14B}) \times 6 \times 10^{-13} \quad \text{(v)}$$

APPENDIX I

LIST OF PUBLICATION

1. Nuttakarn Taochaiyaphum, Joongjai Panpranot, and Piyasan Praserthdam, “Characteristics of Cobalt Catalysts Supported on Zirconia Nanoparticles Prepared by Glycothermal Method”, Proceedings of the Regional Symposium on Chemical Engineering 2004, Bangkok, Thailand, Dec. 1-3, 2004, Ref. No. NS-013.
2. Joongjai Panpranot, Nuttakarn Taochaiyaphum and Piyasan Praserthdam “Glycothermal Synthesis of Nanocrystalline Zirconia and their Applications as Cobalt Catalyst Supports”, Materials Chemistry and Physics, 2005 (In Press).

VITA

Miss Nuttakarn Taochaiyaphum was born in July 16th, 1980 in Chaiyaphum, Thailand. She finished high school from Satree Chaiyaphum School, Chaiyaphum in 1999, and received bachelor's degree in Chemical Engineering from the department of Chemical Engineering, Faculty of Engineering, King Mongkut's Institute of Technology Ladkrabang, Bangkok, Thailand in 2003.